

# Optimization of the Fading MIMO Broadcast Channel: Capacity and Fairness Perspectives

Timothy William King

A Thesis Submitted in Partial Fulfillment  
of the Requirements for the Degree of

Doctor of Philosophy

in

Electrical and Electronic Engineering

University of Canterbury

Christchurch, New Zealand

November 26, 2009



# Abstract

Multiple input multiple output (MIMO) systems are now a proven area in current and future telecommunications research. MIMO wireless channels, in which both the transmitter and receiver have multiple antennas, have been shown to provide high bandwidth efficiency. In this thesis, we cover MIMO communications technology with a focus on cellular systems and the MIMO broadcast channel (MIMO-BC).

Our development of techniques and analysis for the MIMO-BC starts with a study of single user MIMO systems. One such single user technique is that of antenna selection. In this thesis, we discuss various flavours of antenna selection, with the focus on powerful, yet straightforward, norm-based algorithms. These algorithms are analyzed and the results of this analysis produce a powerful and flexible power scaling factor. This power scaling factor can be used to model the gains of norm-based antenna selection via a single signal-to-noise ratio (SNR)-based parameter. This provides a powerful tool for engineers interested in quickly seeing the effects of antenna selection on their systems. A novel low complexity power allocation scheme follows on from the selection algorithms. Named “Poor Man’s Waterfilling” (PMWF), this scheme can provide significant gains in low SNR systems with very little extra complexity compared to selection alone.

We then compare a variety of algorithms for the MIMO-BC, ranging from selection to beamforming, to the optimal, yet complex, iterative waterfilling (ITWF) solution. In this thesis we show that certain algorithms perform better

in different scenarios, based on whether there is shadow fading or not. A power scaling factor analysis is also performed on these systems. In the cases where the user's link gains are widely varying, such as when shadowing and distance effects are present, user fairness is impaired when optimal and near optimal throughput occurs.

This leads to a key problem in the MIMO-BC, the balance between user fairness and throughput performance. In an attempt to find a suitable balance between these two factors, we modify the ITWF algorithm by both introducing extra constraints and also by using a novel utility function approach. Both these methods prove to increase user fairness with only minor loss in throughput over the optimal systems.

The introduction of MIMO systems to the cellular domain has been hampered by the effects of interference between the cells. In this thesis we move MIMO to the cellular domain, addressing the interference using two different methods. We first use power control, where the transmit power of the base station is controlled to optimize the overall system throughput. This leads to promising results using low complexity methods. Our second method is a novel method of collaboration between base stations. This collaboration transforms neighbouring cell sectors into macro-cells and this results in substantial increases in performance.

# Acknowledgments

I would like to thank those who have helped me throughout my PhD. research.

I owe a large debt to Associate Professor Peter Smith for his guidance throughout my time as a postgraduate at the University of Canterbury. As my supervisor he has provided a large amount of support both assisting me with technical details, and I especially appreciate the large amount of hours he spent proof reading my papers and this thesis.

I would also like to thank Dr. Lee Garth and Dr. Mansoor Shafi for their guidance throughout my research. Also, I would like to thank the members of the Communications group and especially Professor Des Taylor and Dr. Philippa Martin for helping me prepare for conferences. I would also like to thank Professor Jim Cavers and Dr. Stephen Hanly for ideas and inspiration. Also, I would like to thank my roommates in E338B who have provided help, friendship and large amounts of conversation.

I would finally like to thank my friends and family who have helped support me through these years of study. Many thanks goes out to Bronwyn for her love and support and to Deborah for her patience, love and kindness over the last year. Also, I would like to thank Mimo the kitten for his cuteness and company during my final weeks, even though he does bite!



# List of Original Papers

The majority of the material presented in this thesis is based on the following original papers:

- L. M. Garth, T. W. King, P. J. Smith, and M. Dohler, “An analysis of low complexity algorithms for MIMO antenna selection,” in *Proc. IEEE International Conference on Communications*, Istanbul, Turkey, June 11-15 2006, pp. 1380-1385.
- P. J. Smith, T. W. King, and L. M. Garth “Capacity and fairness of MIMO broadcast algorithms in shadow fading environments,” in *Proc. IEEE Global Telecommunications Conference*, Washington D.C., USA, November 26-30 2007, pp. 3617-3622.
- P. J. Smith, T. W. King, L. M. Garth, and M. Dohler, “A power scaling analysis of norm-based antenna selection techniques,” *IEEE Transactions on Wireless Communications*, vol. 7, no. 8, pp. 3140-3149, August 2008.
- T. W. King, and P. J. Smith, “Transmit power control in MIMO cellular systems,” *accepted for publication in Australian Communications Theory Workshop*, Sydney, Australia, Feb. 4-7 2009.
- P. J. Smith, T. W. King, L. M. Garth, and M. Shafi, “MIMO-BC algorithms in shadow fading environments: Capacity and fairness aspects,” *submitted to IEEE Transactions on Wireless Communications*, Feb. 2009.

- T. W. King, and P. J. Smith, “Modified waterfilling algorithms to increase MIMO-BC system fairness,” *submitted to EURASIP Journal on Wireless Communications and Networking*, Feb. 2009.

# List of Abbreviations

ASA	arbitrary selection algorithm
AWGN	additive white Gaussian noise
BC	broadcast channel
BF	beamforming
bps	bits per second
BS	base station
CDF	cumulative distribution function
CSI	channel state information
dB	decibels
EPIUT	equal-power independent uncorrelated transmission
FDMA	frequency division multiple-access
i.i.d.	independent and identically distributed
ITWF	iterative waterfilling
KKT	Karush-Kuhn-Tucker (conditions)
LOS	line-of-sight
MAC	multiple-access channel
MIMO	multiple-input multiple-output
MS	mobile station
MU	multiple user
NSA	norm-based selection algorithm
OFDM	orthogonal frequency division multiplexing
OSA	optimal selection algorithm

PA	power allocation
PDF	probability density function
PMWF	poor man's waterfilling
PS	power scaling
RF	radio frequency
RX	receiver
SC	semi-correlated
SNR	signal-to-noise ratio
SU	single user
SVD	singular value decomposition
TX	transmitter
WNSA	worst-case norm-based selection algorithm
WSA	worst-case selection algorithm

# List of Symbols

$r$	number of receive antennas
$t$	number of transmit antennas
$m$	number of pre-selected receive antennas
$n$	number of pre-selected transmit antennas
$r_i$	number of receive antennas for user $i$
$(\cdot)^*$	an optimal point
$(\cdot)^\dagger$	Hermitian conjugate transpose
$\mathbf{Q}$	single user or MAC transmit covariance matrix
$\Sigma$	BC transmit covariance matrix
$C$	capacity
$E(\cdot)$	expectation operator
$\log$	logarithm
$ \cdot $	matrix determinant
$\text{adj}(\cdot)$	matrix adjugate
$\zeta, \nu$	Lagrange multipliers
$\text{dom}f$	domain of function $f$
$\mathbf{H}$	channel matrix
$\mathbf{S}$	selected channel matrix
$K$	number of users
$P$	transmit power



# Contents

<b>1</b>	<b>Introduction</b>	<b>1</b>
1.1	Overview of MIMO systems . . . . .	1
1.2	Research Framework . . . . .	5
1.2.1	Motivations and Contributions . . . . .	5
1.2.2	Specific Contributions . . . . .	7
1.3	Thesis Outline . . . . .	9
<b>2</b>	<b>Background &amp; Assumptions</b>	<b>11</b>
2.1	Single User MIMO Link . . . . .	11
2.1.1	Capacity for the Single User MIMO Link . . . . .	12
2.2	Singular Value Decomposition . . . . .	13
2.3	Multiuser-MIMO Systems . . . . .	13
2.3.1	Multiple-Access Channel . . . . .	14
2.3.2	Broadcast Channel . . . . .	15
2.3.3	Duality . . . . .	15
2.3.4	Fairness . . . . .	17
2.4	Selection . . . . .	18
2.5	Beamforming . . . . .	18
2.5.1	Broadcast Channel . . . . .	18
2.5.2	Multiple Access Channel . . . . .	20
2.6	Channels . . . . .	21
2.6.1	Rayleigh Flat-Fading Channel . . . . .	21

2.6.2	Ricean Channel . . . . .	21
2.6.3	Partial Spatial Correlation . . . . .	22
2.7	Channel State Information . . . . .	22
2.8	Fading . . . . .	23
2.8.1	Shadow Fading . . . . .	24
2.8.2	Path Loss . . . . .	24
2.9	Analytical Mean Capacity . . . . .	25
2.10	Order Statistics . . . . .	26
2.10.1	Concomitants . . . . .	27
2.11	Optimization . . . . .	27
2.11.1	The Lagrangian . . . . .	28
2.11.2	Karush-Kuhn-Tucker Conditions . . . . .	28
2.11.3	Convexity . . . . .	29
2.11.4	Waterfilling . . . . .	30
2.11.5	Iterative Waterfilling . . . . .	33
2.12	Cellular Layouts and Modelling . . . . .	34
2.12.1	Single Cell ‘Bagel’ Model . . . . .	34
2.13	Summary . . . . .	36
<b>3</b>	<b>Single User MIMO: Selection Methods and Analysis</b>	<b>39</b>
3.1	Selection Algorithms . . . . .	41
3.1.1	Transmit Selection Algorithms . . . . .	41
3.1.2	Algorithms for Transmitter-Receiver Selection . . . . .	45
3.1.3	Poor Man’s Waterfilling . . . . .	47
3.2	Algorithm Analysis . . . . .	49
3.2.1	NSA Analysis . . . . .	49
3.2.2	Rayleigh Flat Fading Channels . . . . .	51
3.2.3	Semi-Correlated Rayleigh Channels . . . . .	55
3.2.4	Ricean Channels . . . . .	59
3.2.5	Transmitter-Receiver Antenna Selection . . . . .	60

3.2.6	Poor Man's Waterfilling . . . . .	60
3.3	Effects of Imperfect Channel State Information . . . . .	64
3.4	Algorithm Complexity . . . . .	67
3.5	System Size . . . . .	68
3.6	Summary . . . . .	71
<b>4</b>	<b>Multuser MIMO: Broadcast Channel Capacity</b>	<b>73</b>
4.1	Performance Metrics and Algorithms . . . . .	75
4.1.1	Iterative Waterfilling . . . . .	75
4.1.2	Equal Power Independent Uncorrelated Transmission . . . . .	76
4.1.3	Beamforming Techniques . . . . .	76
4.1.4	Selection Techniques . . . . .	77
4.2	Equivalent Single-user System Analysis . . . . .	78
4.2.1	Equal Power Independent Uncorrelated Transmission . . . . .	78
4.2.2	Beamforming Techniques . . . . .	79
4.2.3	Selection Techniques . . . . .	80
4.2.4	System Comparison . . . . .	81
4.3	MAC Design . . . . .	83
4.4	Complexity Analysis . . . . .	86
4.5	Simulation Results . . . . .	86
4.5.1	Results Overview . . . . .	100
4.5.2	Performance vs. Fairness . . . . .	100
4.5.3	Proportional Power . . . . .	102
4.6	Summary . . . . .	103
<b>5</b>	<b>Multuser MIMO: Broadcast Channel Capacity and Modifica-</b>	
	<b>tions to the Waterfilling Algorithm</b>	<b>105</b>
5.1	Constraint Modification . . . . .	107
5.1.1	Minimum Power Constraints . . . . .	107
5.1.2	Maximum Power Constraints . . . . .	108
5.1.3	Dual Constraints and Practical Implementation . . . . .	110

5.1.4	Perturbation and Sensitivity Analysis . . . . .	110
5.2	Utility Functions . . . . .	112
5.2.1	Nonlinear Utility Functions . . . . .	113
5.2.2	Linear Utility Functions . . . . .	116
5.2.3	Utility Function Example . . . . .	116
5.2.4	Concavity Preservation . . . . .	117
5.3	Multiuser Applications . . . . .	119
5.3.1	Convergence Analysis . . . . .	119
5.4	Simulation Results . . . . .	121
5.5	Summary . . . . .	127
<b>6</b>	<b>Collaborative MIMO: Broadcast Channel Capacity</b>	<b>129</b>
6.1	System Model and Capacity Results . . . . .	131
6.1.1	Cell Clusters . . . . .	131
6.2	Optimization . . . . .	132
6.3	Practical Algorithm . . . . .	135
6.4	Power Allocation to One Dominant User . . . . .	136
6.5	Three Cell Collaboration . . . . .	137
6.6	Simulation Results . . . . .	139
6.6.1	Power Control . . . . .	141
6.6.2	Three Cell Collaboration . . . . .	144
6.7	Summary . . . . .	146
<b>7</b>	<b>Conclusions and Future Work</b>	<b>149</b>
7.1	Conclusions . . . . .	149
7.2	Suggestions for Future Work . . . . .	151
<b>A</b>	<b>Finding the Cumulative Distribution Function of the Ratio of Two Shadow Fading Link Gains</b>	<b>153</b>
<b>B</b>	<b>Isotropic Analysis of Largest Column Density</b>	<b>161</b>

# List of Figures

2.1	MIMO multiuser channels: broadcast channel (left) and multiple-access channel (right). . . . .	14
2.2	An illustration of the multipath phenomenon. . . . .	23
2.3	Visual interpretation of the waterfilling algorithm. . . . .	32
2.4	CDF of the ratio $\Gamma_1/\Gamma_2$ for different values of $R$ and $R_0$ . . . . .	37
3.1	Comparison of selection schemes for a $(N, N + 2)$ choose $(N, N)$ system (SNR = 0dB). . . . .	43
3.2	Comparison of selection schemes for a $(N, N + 2)$ choose $(N, N)$ system (SNR = 10dB). . . . .	44
3.3	Comparison of selection schemes for a $(N, N + 2)$ choose $(N, N)$ system (SNR = 20dB). . . . .	44
3.4	Comparison of selection schemes for a $(N, N + K)$ choose $(N, N)$ system with variable $K$ (SNR = 10dB). . . . .	45
3.5	Comparison of TX-RX selection schemes for a $(N + 2, N + 2)$ choose $(N, N)$ system (SNR = 10dB). . . . .	46
3.6	Comparison of TX-RX selection schemes for a $(N, N)$ choose $(2, 2)$ system (SNR = 10dB). . . . .	47
3.7	Comparison of selection schemes and PMWF for a $(N, N + 2)$ choose $(N, N)$ system (SNR = 0dB). . . . .	48
3.8	Comparison of selection schemes and PMWF for a $(N, N + 2)$ choose $(N, N)$ system (SNR = 10dB). . . . .	48

3.9	Comparison of NSA and approximations for a $(N, N+2)$ choose $(N, N)$ system (SNR = 0dB). . . . .	51
3.10	Comparison of NSA and approximations for a $(N, N+2)$ choose $(N, N)$ system (SNR = 10dB). . . . .	52
3.11	Comparison of selection algorithms over different channels for a $(N, N+2)$ choose $(N, N)$ system (SNR = 0dB). . . . .	58
3.12	Comparison of selection algorithms over different channels for a $(N, N+2)$ choose $(N, N)$ system (SNR = 10dB). . . . .	58
3.13	Comparison of NSA and approximations using PMWF for a $(N, N+2)$ choose $(N, N)$ system (SNR = 0dB). . . . .	64
3.14	Comparison of NSA and approximations using PMWF for a $(N, N+2)$ choose $(N, N)$ system (SNR = 10dB). . . . .	65
3.15	Percentage capacity improvement of PMWF, NSA and OSA relative to each other in a $(2, 4)$ choose $(2, 2)$ system for an i.i.d. Rayleigh channel. . . . .	65
3.16	Comparison of selection algorithms and PS approximations under imperfect CSI (SNR = 0dB). . . . .	67
3.17	Comparison of selection algorithms under correlation with a variable width and a $(N, N+2)$ choose $(N, N)$ system (SNR = 10dB). . . . .	70
3.18	Comparison of selection algorithms under correlation with a fixed width (1 wavelength) and a $(N, N+2)$ choose $(N, N)$ system (SNR = 10dB). . . . .	70
4.1	Comparison between simulation (Sim) and equivalent SNR approximation (Aprx) for BF2 and S2 algorithms (SNR <sub>av</sub> = 10dB, $(2,4)$ three user system with shadow fading effects). . . . .	83
4.2	Comparison between simulation (Sim) and equivalent SNR approximation (Aprx) for BF2 and S2 algorithms (SNR <sub>av</sub> = 10dB, $(4,4)$ three user system with shadow fading effects). . . . .	84

4.3	CDF of the ratio $\Gamma_1/\Gamma_2$ for different values of $R$ and $R_0$ . . . . .	89
4.4	Algorithm comparison for a (2,4) two user system ( $\text{SNR}_{\text{av}} = 10\text{dB}$ , no shadow fading effects). . . . .	89
4.5	Algorithm comparison for a (2,4) two user system ( $\text{SNR}_{\text{av}} = 10\text{dB}$ , shadow fading effects). . . . .	90
4.6	Algorithm comparison for a (2,4) two user system ( $\text{SNR}_{\text{av}} = 0\text{dB}$ , shadow fading effects). . . . .	90
4.7	Algorithm comparison for a (2,4) two user system for varying ratios of link gain ( $\text{SNR}_{\text{av}} = 10\text{dB}$ ). . . . .	91
4.8	Algorithm comparison for a (2,4) two user system for varying ratios of link gain ( $\text{SNR}_{\text{av}} = 10\text{dB}$ ). . . . .	91
4.9	Algorithm comparison for a (2,4) two user system for varying ratios of link gain ( $\text{SNR}_{\text{av}} = 0\text{dB}$ ). . . . .	92
4.10	Proportion power allocation algorithm comparison for a (2,4) two user system for varying ratios of link gain ( $\text{SNR}_{\text{av}} = 10\text{dB}$ ). . . . .	92
4.11	Algorithm comparison for a (2,4) three user system ( $\text{SNR}_{\text{av}} = 10\text{dB}$ , no shadow fading effects). . . . .	93
4.12	Algorithm comparison for a (2,4) three user system ( $\text{SNR}_{\text{av}} = 10\text{dB}$ , shadow fading effects). . . . .	94
4.13	Algorithm comparison for a (2,4) three user system ( $\text{SNR}_{\text{av}} = 0\text{dB}$ , shadow fading effects). . . . .	94
4.14	Algorithm comparison for a (2,4) six user system ( $\text{SNR}_{\text{av}} = 10\text{dB}$ , no shadow fading effects). . . . .	95
4.15	Algorithm comparison for a (2,4) six user system ( $\text{SNR}_{\text{av}} = 10\text{dB}$ , shadow fading effects). . . . .	95
4.16	Algorithm comparison for a (2,4) six user system ( $\text{SNR}_{\text{av}} = 0\text{dB}$ , shadow fading effects). . . . .	96
4.17	Algorithm comparison for a (2,8) three user system ( $\text{SNR}_{\text{av}} = 10\text{dB}$ , no shadow fading effects). . . . .	96

4.18	Algorithm comparison for a (2,8) three user system ( $\text{SNR}_{\text{av}} = 10\text{dB}$ , shadow fading effects).	97
4.19	Algorithm comparison for a (2,8) three user system ( $\text{SNR}_{\text{av}} = 0\text{dB}$ , shadow fading effects).	97
4.20	Algorithm comparison for a (4,4) three user system ( $\text{SNR}_{\text{av}} = 10\text{dB}$ , no shadow fading effects).	98
4.21	Algorithm comparison for a (4,4) three user system ( $\text{SNR}_{\text{av}} = 10\text{dB}$ , shadow fading effects).	98
4.22	Algorithm comparison for a (4,4) three user system ( $\text{SNR}_{\text{av}} = 0\text{dB}$ , shadow fading effects).	99
4.23	Percentage of spatial channels open and active users for ITWF in a (2,4) three user system for variable $\text{SNR}_{\text{av}}$ .	102
4.24	Gains of proportional power allocation over fixed power allocation for a (2,4) three user system (shadow fading effects).	103
5.1	Perturbation analysis for a $12 \times 12$ MIMO system with constraint-modified waterfilling.	112
5.2	Capacity comparisons for a three user (2,4) MIMO-BC system.	121
5.3	Comparison of the number of active subchannels for a three user (2,4) MIMO-BC system.	122
5.4	Percentage power in the dominant subchannel (DS) for a three user (2,4) MIMO-BC system.	122
5.5	Percentage power in the dominant subchannel (DS) for ITWF with a per-channel maximum power constraint for a three user (2,4) MIMO-BC system.	123
5.6	Capacity comparisons for ITWF with a per-channel maximum power constraint for a three user (2,4) MIMO-BC system.	124
5.7	Capacity comparisons for ITWF with dual constraints for a three user (2,4) MIMO-BC system.	124

5.8	Percentage of ITWF capacity acheived in a two user (2,4) MIMO-BC system for varying values of the link gains, $\Gamma_i$ . . . . .	125
5.9	Percentage power in the dominant subchannel (DS) for SNR-adjusted ITWF for a three user (2,4) MIMO-BC system. . . . .	126
5.10	Comparison of the number of active subchannels for SNR-adjusted ITWF for a three user (2,4) MIMO-BC system. . . . .	126
5.11	Percentage gain over EPIUT for SNR-adjusted ITWF (standard ITWF = 100%) for a three user (2,4) MIMO-BC system. . . . .	127
6.1	Layouts of both 3-cell (left) and 7-cell (right) cellular systems. . . . .	131
6.2	Original three cell system. . . . .	139
6.3	Three sector collaboration and equivalent macro-cell. . . . .	140
6.4	Three cell collaboration system comparison (solid lines refer to desired signals and dashed lines refer to interfering signals). . . . .	140
6.5	Comparison of mean sum-rates for Algorithm 6.1 with the optimal ON/OFF solution. . . . .	142
6.6	Comparison of mean sum-rates for 3-cell and 7-cell systems with various allocation policies. . . . .	143
6.7	Distribution of active cells for a 3-cell system (number of active cells is labeled). . . . .	144
6.8	Comparison of different FDMA reuse factors. . . . .	145



# List of Tables

3.1	$P_{av}$ Values for Various $n$ and $t$ ( $m = 2$ ) . . . . .	53
3.2	$P_{av}$ Values for Various $n$ and $t$ ( $m = 3$ ) . . . . .	54
3.3	$P_{av}$ Values for Various $n$ and $t$ ( $m = 4$ ) . . . . .	54
4.1	Equivalent MIMO Systems . . . . .	82
4.2	Number of Active Users (AU) and Open Subchannels (OS) Available to Various Algorithms for Simulated (2,4) Three User Systems . . . . .	101
6.1	Percentage of the Optimal Capacity Achieved by a 2-cell ON/OFF Selection System . . . . .	142
6.2	Sum-Rates (in bps/Hz) for Different Levels of 3-cell Collabora- tion ( $\text{SNR}_{av} = 14.7\text{dB}$ ) . . . . .	146



# Chapter 1

## Introduction

The radio and wireless systems have revolutionized the modern era ever since the invention of the radio telegraph by Guglielmo Marconi in 1895 [1]. Over 110 years later, wireless technology is still a broad area of ongoing research. In this modern era researchers are trying to improve on the current systems due to high consumer demand, both military and civilian, for faster transmission speeds and higher throughput. One area of current research that promises vast improvements over legacy systems is the use of multiple antennas. A particularly effective form of multiple antenna system is when multiple antennas are employed at both the transmitter and receiver. Such a system is referred to as a multiple-input multiple-output (MIMO) system and is the focus of this thesis.

### 1.1 Overview of MIMO systems

Wireless services have found their niche in mobile devices due to the inherent lack of availability of traditional wireline services in these devices. Mobile devices can range from vehicular radio to smaller handheld devices, such as cellphones and PDAs. In the past the computing power required for technologies such as MIMO was not available in these small devices. However, in the last decade, there have been advances in two key areas: VLSI electronics and nanotechnology, and computing and digital signal processing. These advances

now allow complex algorithms and coding schemes, vital for modern mobile communication, to be viable in small devices. This technological growth has led to rapid market growth of wireless systems and equipment on a global scale. Today there are increasing demands for faster wireless speed and greater bandwidth as companies, such as cellular network providers, try to get an edge on their competitors. Now and in the near future the drivers behind increased performance requirements are multimedia applications such as streamed audio and high-quality video. To achieve the network capacity needed for the future, higher spectral efficiency is required. Not surprisingly, this field of wireless research is a very hot topic in the field of communications engineering and is now part of a wide range of present and future standards [2]. However, researchers must overcome the many challenges of the wireless environment, including limited bandwidth, multi-path propagation, interference and signal fading.

Claude E. Shannon first postulated the term channel capacity as the highest rate possible for error-free communication [3]. In [3], Shannon derived the classic formula, based on information theory ideals such as mutual information, which gave capacity as a function of both signal-to-noise-ratio (SNR) and bandwidth. This naturally leads to increasing either or both of these two factors as a direct means of improving capacity. However, in today's market, increasing these factors is impractical. Firstly, modern mobile devices are power-limited due to battery size and lifetime. Also, regulations can place a limit on transmit power in many circumstances. Secondly, similar regulatory restrictions on spectrum usage prevent the modern engineer from increasing system bandwidth to gain increases in capacity. Due to these factors, designers must now increase spectral efficiency, defined as the bit rate per unit of bandwidth, through techniques such as advanced modulation and coding. Another, now tremendously popular technique, is utilizing the spatial degrees of freedom of multi-antenna systems. This is now regarded as one of the most promising techniques for next generation wireless communications [4]. In particular,

MIMO systems, where multiple antennas occur at both the transmitter and receiver, have been shown to increase coverage and reliability without the use of extra power or bandwidth [5], [6].

In general, multiple antenna systems can be split into two types<sup>1</sup>. The first is a diversity system, where multiple copies of the same signal are sent out from the transmitter and then combined at the receiver [8]. The purpose of diversity is to reduce the error rate in the system and thus the system reliability. Signal combination at the receiver can be done by simply taking the signal with the highest SNR or by using maximal ratio combining, where the signals are weighted by their SNRs and then summed together. Certain coding techniques also use the spatial degrees of freedom of multiple antenna systems to increase diversity. These include space-time trellis codes [9] and space-time block codes [10].

The second type of multiple antenna system is one which employs spatial multiplexing. The aim of spatial multiplexing is to send different signals from each transmitter in order to increase system throughput. An example of a spatial multiplexing system is BLAST<sup>2</sup> coding [11]. Spatial multiplexing systems are the focus of this thesis.

Modern MIMO systems fall into four distinct categories: Single-User Single-Cell, Multiple-User Single-Cell, Single-User (per Cell) Multiple-Cell and Multiple-User (per Cell) Multiple-Cell. These categories are discussed as follows:

- Single-User Single-Cell: This is the generic point-to-point MIMO link. A single transmitter (TX) communicates with a single receiver (RX) using multiple antennas. Work in this category is covered in Chapter 3 of this thesis, which covers antenna selection. Benchmark work on the single-user (SU) MIMO link can be found in Winters [12], Foschini and Gans [13] and Teletar [14]. A good tutorial paper on MIMO in general

---

<sup>1</sup>However, there are some systems which exploit both diversity and multiplexing gains. An example of such a system is given in [7].

<sup>2</sup>Bell Laboratories Layered Space-Time.

is given by Gesbert *et al.* [15].

- **Multiple-User Single-Cell:** This is a point-to-multipoint MIMO link. In this case a single transmitter, usually called a base station (BS), transmits over multiple antennas to a number of receivers, called mobile stations<sup>3</sup> (MS), each equipped with multiple receive antennas. There are two major systems for this case: the Broadcast Channel (BC), which is a model for the TX-RX downlink, and the Multiple-Access Channel (MAC), which models the uplink from the RXs to the single TX. This category is covered in depth in Chapters 4 and 5. In Chapter 4 we study the MIMO-BC and provide a detailed set of results on performance and fairness in a shadowing environment. In Chapter 5 we derive modifications to the benchmark Iterative Waterfilling (ITWF) algorithm [16, 17]. Another benchmark paper for this category is by Goldsmith *et al.* on the duality between the BC and MAC channels [18]. Other work in this category includes [19–22].
- **Single-User (per Cell) Multiple-Cell:** This is a collection of single-user MIMO links which are in close proximity to one another. This causes interference between cells which is detrimental to communication. In certain cases, collaboration between transmitters can be achieved and this case can be modeled as a Multiple-User (MU) Single-Cell system. This category and the next category are the heart of modern cellular communications. In Chapter 6 we discuss BS power control in an attempt to mitigate this interference. A good summary of methods to combat the effects of other cell interference is given in [23]. Other work in the literature on this category includes [24–27].
- **Multiple-User (per Cell) Multiple-Cell:** This is a collection of multiple-user MIMO links which are in close proximity to one another. Although

---

<sup>3</sup>Also referred to as mobile terminals.

not explicitly discussed within this thesis, certain cases can be modeled as Multiple-User Single-Cell by accounting for cell positions and base station collaboration in the modeling. Although not directly addressed in this thesis, this category relates closely to the others and work from any of the chapters can be relevant here. Examples of work in this category include [23, 28–31].

## 1.2 Research Framework

In this section we describe the main objectives and motivations of this thesis. Also presented is a summary of the contributions.

### 1.2.1 Motivations and Contributions

Since the advent of MIMO systems, antenna selection for these systems has become a hot topic [32–38]. One of the more notable antenna selection methods is based on the column or row norms of the channel matrix. However, this algorithm has yet to be analyzed in depth. In this thesis we carry out an in depth analysis of this algorithm and other simple algorithms and provides a powerful equivalent SNR model for the gains of these algorithms. Also, we extend the norm-based approach to a proportional power approach, which shows considerable promise in low-SNR regions.

Recent work on the MIMO broadcast channel (MIMO-BC) has mainly focussed on achieving maximum throughput [18, 39] and algorithms to achieve this [17], [16]. Other work has been focussed on achieving user fairness, as in the work by Jindal *et al.* [40]. Only a small amount of work has looked into the balance between these two important yet competing factors. In this thesis we add to the work in this area by looking at the MIMO-BC and its dual, the MIMO multiple access channel (MIMO-MAC) [19], and considering the balance between fairness and throughput over a variety of algorithms.

A large amount of work on the MIMO-BC has focussed on achieving optimality without any restrictions on the complexity of the algorithms required. However, in real-world systems, processing power may be limited and other less complex methods may need to be used. In this thesis, we cover a number of less complex methods which are shown to approach the optimal throughput in certain cases and at certain SNRs.

Recent work on the MIMO-BC has generally assumed a Rayleigh flat-fading channel [16–22]. However, in practical systems, the effects of shadowing and the mobile user’s position are extremely important. Some research has considered the impact of shadowing [41, 42]. However, the joint effects of both shadowing and path loss do not appear to have been evaluated before in the context of the MIMO-BC. Hence, we develop a model for user position within a cell and takes into account both distance attenuation and shadowing effects. The effects of these phenomena on factors such as throughput and fairness are covered in detail within the thesis.

In an attempt to provide user fairness, researchers have proposed suboptimal algorithms which provide fairness at the expense of throughput [40]. The effect of such techniques on capacity can appear to be slight in the Rayleigh fading case. When shadow fading and distance effects are included, it is shown in this thesis that to achieve the desired fairness levels, the drop in throughput in these systems will be quite significant. In an attempt to balance fairness with throughput, we develop algorithms based on modifying the optimization problem from which the common waterfilling algorithm is derived [14]. Some similar modifications have been investigated in the literature. For example, waterfilling with a minimum rate constraint appears in [16, 17], however not in the MIMO multiuser (MIMO-MU) domain. In this thesis we provide minimum power and novel maximum power constraint modifications which have a variety of applications from MIMO-MU to orthogonal division frequency multiplexing (OFDM) systems. We also include an analysis of these methods

which indicates that the loss in throughput over the optimal waterfilling systems is based on two factors. The first is the amount of gain in fairness levels and the second is the (un)fairness of the original system. As a result, these methods have shortcomings in shadowing environments where the variation between link gains is severe. In an attempt to address this problem we develop a novel utility function approach which provides a different balance between fairness and throughput.

One of the main target uses for MIMO technology is in cellular environments [2, 23]. However, placing MIMO systems in adjacent cells without frequency reuse creates a large amount of intercell interference [24, 26, 27]. In an attempt to remedy this, researchers have proposed base station collaboration to effectively turn a cellular system into a giant MIMO-BC [28–31]. The drawback with this approach is the large amount of feedback required to ensure every BS has full network channel state information (CSI). Thus, in this thesis we focus on varying the power at the BS in order to mitigate the intercell interference which requires far less network CSI. The concept of power control in cellular systems is well-known [43, 44], but the majority of this work has been based on single antenna links. Here we consider power allocation in the MIMO case and for the MIMO-BC in particular. Our approach to the power control problem is built upon the twin single antenna link optimization in [45]. This twin single antenna link refers to two separate single-input single-output systems that interfere with each other. Note that this optimization leads to the simplified solution of turning base stations on or off. Also, we derive a practical algorithm to effectively perform the optimization.

### 1.2.2 Specific Contributions

The main contributions of this thesis are as follows:

- **An in-depth analysis of the use of norm-based algorithms for antenna selection:** We look at various antenna selection algorithms for

single user MIMO systems. We analyze these algorithms and develop a powerful equivalent SNR model for the gains of these algorithms.

- **Analysis and results for the effects of shadowing and distance attenuation in a multiuser MIMO environment:** We examine the effects of large variations in link gains caused by shadowing and distance attenuation effects on the MIMO-BC. We derive an equivalent SNR model for a variety of suboptimal algorithms, including selection and beamforming. The thesis also contains a large number of results comparing a range of suboptimal and optimal (ITWF) algorithms. We then discuss these results and analyze them focussing on the balance of performance versus fairness and the use of proportional power allocation in suboptimal algorithms.
- **Modifications to the waterfilling algorithm to promote fairness:** We consider modifications to the waterfilling algorithm based on adjusting the constraints of the optimization problem. We include both minimum power and maximum power constraints and provides a brief analysis of the effects of these constraints on system throughput. We develop a novel utility function based approach to modifying the waterfilling algorithm to promote fairness, providing a powerful and flexible method to increase system fairness with very little reduction in throughput.
- **Optimization of transmitter power control in MIMO cellular environments:** We look at the problem of transmitter power control in MIMO cellular environments and provide a detailed development of a near-optimal method for controlling transmitter power to mitigate inter cell interference. We demonstrate that the resulting algorithm provides gains over interference limited systems with very little overhead.
- **Three cell collaboration in MIMO cellular environments:** We develop a model of three collaborating sectorized cells. In this model,

neighbouring sectors are transformed into a macro-cell structure and the resulting system mitigates interference and increases throughput.

## 1.3 Thesis Outline

The rest of this thesis is organized as follows:

We begin Chapter 2 with a discussion of the single-user MIMO link. We define the MIMO capacity and give a brief overview of mobile propagation and fading and statistical channel models. We then discuss the effects of imperfect channel state information and the singular value decomposition. Next, we cover Multiple-user MIMO systems, considering both the multiple-access and broadcast channels. We then discuss the duality between these channels as well as the use of beamforming in both domains. We also cover the topic of fairness amongst users. Next, we discuss the different types of selection, along with some straightforward results on order statistics. We also highlight a formula for the mean capacity of a multiuser system. Next, we cover optimization, especially the waterfilling algorithm and its multiuser form, iterative waterfilling. We conclude the chapter with a brief discussion on the models used in describing the cellular environment.

We start Chapter 3 with a discussion of various antenna selection algorithms for the single-user MIMO link. Next, we analyze these algorithms and express them in terms of a single power-scaling factor. We cover the effects of imperfect channel state information on selection and also discuss of the complexity of the algorithms. We conclude the chapter with a discussion of the effects of small system dimension on the algorithms.

We begin Chapter 4 by introducing various performance metrics relevant to the broadcast channel. Next, we cover a variety of algorithms and then create single user equivalent systems for these algorithms. Then, we analyze these algorithms. Following this, we discuss algorithm design in the BC and MAC domains and analyze the complexity of various algorithms. We finalize

with results and a summary of the chapter.

We begin Chapter 5 by looking at modifications to the constraints of the optimization problem that the waterfilling algorithm stems from. We discuss both minimum power and maximum power constraints. Next, we cover the use of utility functions in the same optimization problem, with examples. We then introduce power constraints and utility functions to the multiuser domain using iterative waterfilling techniques. We conclude the chapter with results from the algorithms and comparisons to the optimal values.

We start Chapter 6 with a discussion of multiple cell cluster models and then follow with the optimization of the sum capacity of those systems by using power control. We continue by explaining a practical algorithm for implementing this optimization. We give an example of full collaboration between three adjacent cells and then conclude the chapter with results.

In Chapter 7 we provide a conclusion to the thesis and also include a discussion of possible options for future work on topics relating to the thesis.

## Chapter 2

# Background and Assumptions

In this chapter we outline some required background information. Firstly, we examine different aspects of the single-user MIMO link. Next, we discuss the properties of the MIMO channel matrix and the SVD. Then we discuss MIMO multiuser systems, including both broadcast and multiple-access systems. Next, we describe selection and beamforming as well as different statistical channel models and the phenomenon of fading both in the small and large scale. We follow with some basic results on order statistics. Next, we discuss optimization, including the powerful waterfilling algorithm. Finally, we summarize the cellular layouts and modelling used within the thesis.

### 2.1 Single User MIMO Link

Consider the single-user MIMO link consisting of a transmitter with  $t \geq 1$  transmit antennas and a receiver with  $r \geq 1$  receive antennas (denoted  $(r \times t)$ ) spaced a distance  $d$  metres apart. In this link the transmitter sends symbols from a complex symbol alphabet. These symbols are firstly encoded, then modulated, up-converted and finally transmitted over the radio link. The receiver, upon receiving these signals, firstly mixes them down to baseband, samples them and finally passes the samples on to a decoder to extract the original message. In this thesis, we assume that the channel response is frequency independent and all received symbols are perfectly synchronized. This

results in no inter-symbol interference. To model this, the channel between the transmitter and receiver is concisely expressed by an  $r \times t$  complex channel matrix,  $\mathbf{H}$ . Note that it is assumed, without loss of generality, that  $t \geq r$  unless stated. The relationship between the received signal vector,  $\mathbf{r}$  ( $r \times 1$ ), and the transmitted signal vector,  $\mathbf{s}$  ( $t \times 1$ ), is given by

$$\mathbf{r} = \sqrt{\Gamma}\mathbf{H}\mathbf{s} + \mathbf{v}, \quad (2.1)$$

where  $\Gamma$  is the link gain and  $\mathbf{v}$  is the  $t \times 1$  additive white Gaussian noise (AWGN) vector. Note that the elements of  $\mathbf{v}$  are complex Gaussian with variance  $\sigma^2$ , such that  $\text{E}\{\mathbf{v}\mathbf{v}^\dagger\} = \sigma^2\mathbf{I}$ . From (2.1), the signal-to-noise ratio for the system is defined as  $\text{SNR} = \frac{\text{E}\{\mathbf{s}^\dagger\mathbf{s}\}}{\text{E}\{\mathbf{v}^\dagger\mathbf{v}\}}$ . Without loss of generality, it will be assumed that the noise variance  $\sigma^2 = 1$  unless explicitly stated otherwise.

### 2.1.1 Capacity for the Single User MIMO Link

For the single-user MIMO link the instantaneous capacity of the system is given by [14]

$$C = \log_2 |\mathbf{I}_t + \Gamma\mathbf{H}^\dagger\mathbf{Q}\mathbf{H}| \quad \text{bps/Hz}, \quad (2.2)$$

where  $\mathbf{Q}$  is the Hermitian covariance matrix of the transmit vector and  $\Gamma$  is the SNR of the link (also referred to as the link gain). For the most part, in the single-user case it is assumed that the transmitter does not have access to the CSI. Therefore, the best strategy is equal power across the transmit antennas [1, 14]. This leads to  $\mathbf{Q} = \mathbf{I}/t$ . If waterfilling is used (see Sec. 2.11) then the optimum or waterfilling capacity is obtained, where  $\mathbf{Q} = \mathbf{Q}_{WF}$  and the resulting capacity is given by

$$C_{WF} = \log_2 |\mathbf{I}_t + \Gamma\mathbf{H}^\dagger\mathbf{Q}_{WF}\mathbf{H}| \quad \text{bps/Hz}. \quad (2.3)$$

## 2.2 Singular Value Decomposition

One of the most powerful tools in the analysis of MIMO systems is the Singular Value Decomposition (SVD) [1, p. 43]. Consider the single-user MIMO link with  $m \times n$  channel matrix  $\mathbf{H}$ . Using the SVD,  $\mathbf{H}$  can now be expressed as

$$\mathbf{H} = \mathbf{U}\mathbf{D}\mathbf{V}^\dagger, \quad (2.4)$$

where  $\mathbf{U} \in \mathbb{C}^{n \times n}$  and  $\mathbf{V} \in \mathbb{C}^{m \times m}$  are unitary matrices and  $\mathbf{D}$  is a diagonal matrix whose diagonal elements  $(d_1, d_2, \dots, d_\ell, 0, \dots, 0)$  are the singular values of  $\mathbf{H}$  and  $\ell = \min\{m, n\}$ . Note that the non-diagonal entries of  $\mathbf{D}$  are 0 and its rank is  $\ell$ . From the SVD the eigenvalues of the instantaneous channel matrix  $\mathbf{H}\mathbf{H}^\dagger$  can be found. Note that

$$\mathbf{H}\mathbf{H}^\dagger = \mathbf{U}\mathbf{D}\mathbf{D}^\dagger\mathbf{U}^\dagger, \quad (2.5)$$

where  $\mathbf{D}\mathbf{D}^\dagger$  is a diagonal matrix containing the eigenvalues of  $\mathbf{H}\mathbf{H}^\dagger$ ,  $(d_1^2, d_2^2, \dots, d_\ell^2, 0, \dots, 0)$  and the columns of  $\mathbf{U}$  are the eigenvectors of  $\mathbf{H}\mathbf{H}^\dagger$ . We define  $\lambda_i = d_i^2$ . It follows that the columns of  $\mathbf{V}$  are the eigenvectors of  $\mathbf{H}^\dagger\mathbf{H}$ .

## 2.3 Multiuser-MIMO Systems

There are two key types of multiuser-MIMO systems. The first is the Multiple-Access Channel (MIMO-MAC) which can model the upstream between the mobile users and the base station [16–18]. The second is the Broadcast Channel (MIMO-BC) which can model the downstream between the base station and the mobile users [17, 18, 21, 22].

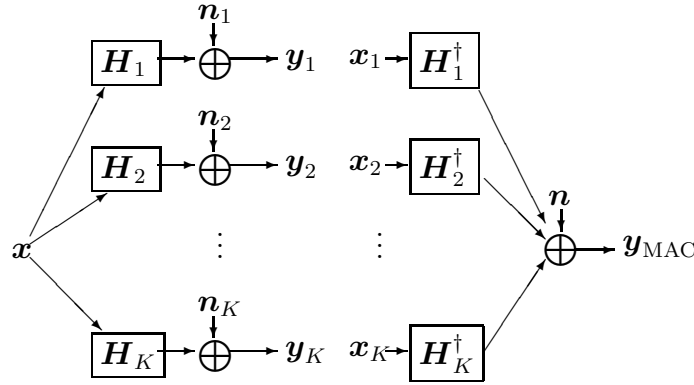


Figure 2.1: MIMO multiuser channels: broadcast channel (left) and multiple-access channel (right).

### 2.3.1 Multiple-Access Channel

The MIMO-MAC<sup>1</sup> is the uplink in a wireless system, where multiple uncoordinated transmitters send their information to a common receiver. It is shown in Fig. 2.1 [19]. The MAC system equation is for a system with  $t$  base station antennas and  $r_i$  mobile antennas at user  $i$ :

$$\mathbf{y}_{\text{MAC}} = \sum_{i=1}^K \mathbf{H}_i^\dagger \mathbf{x}_i + \mathbf{n} \quad (2.6)$$

where  $K$  is the number of users,  $\mathbf{y}_{\text{MAC}}$  is the  $t \times 1$  received signal vector,  $\mathbf{n}$  is an AWGN vector with elements with zero-mean and variance  $\sigma^2$ ,  $\mathbf{x}_i$  is the  $r_i \times 1$  transmit vector from user  $i$  and  $\mathbf{H}_i^\dagger$  is the  $t \times r_i$  channel matrix for the link between the base station and user  $i$ . It follows that the capacity of the MAC is [16–18, 20]

$$C_{\text{MAC}} = \log_2 \left| \mathbf{I}_t + \sum_{i=1}^K \mathbf{H}_i^\dagger \mathbf{Q}_i \mathbf{H}_i \right| \text{ bps/Hz}, \quad (2.7)$$

<sup>1</sup>Note also that MAC does not refer to the media access control layer in the network stack but signal processing technique in the physical layer.

where  $\mathbf{Q}_i$  is the  $r_i \times r_i$  covariance matrix associated with user  $i$ .

### 2.3.2 Broadcast Channel

The MIMO-BC is the downlink in a wireless system. It is shown in Fig. 2.1 [19]. Given  $t$  base station antennas and  $r_i$  mobile antennas at user  $i$ , the MIMO-BC system equation is given by:

$$\mathbf{y}_i = \mathbf{H}_i \mathbf{x} + \mathbf{n}_i, \quad (2.8)$$

where

$$\mathbf{x} = \sum_{i=1}^K \mathbf{x}_i$$

is a superposition of the signals intended for the  $K$  users and  $\mathbf{y}_i$  is the  $r_i \times 1$  received signal vector at user  $i$ ,  $\mathbf{n}_i$  is the AWGN noise vector (at user  $i$ ) with elements with zero-mean and variance  $\sigma^2$ ,  $\mathbf{x}_i$  is the  $t \times 1$  downlink transmitted signal vector for user  $i$  and  $\mathbf{H}_i$  is the  $r_i \times t$  channel matrix for the link between the base station and user  $i$ . For a system with  $K$  users the capacity is defined as follows [17, 18, 21, 22]

$$\begin{aligned} C_{BC} = & \log_2 \left| \mathbf{I}_r + \mathbf{H}_1 \mathbf{\Sigma}_1 \mathbf{H}_1^\dagger \right| + \log_2 \frac{\left| \mathbf{I}_r + \mathbf{H}_2 (\mathbf{\Sigma}_1 + \mathbf{\Sigma}_2) \mathbf{H}_2^\dagger \right|}{\left| \mathbf{I}_r + \mathbf{H}_2 \mathbf{\Sigma}_1 \mathbf{H}_2^\dagger \right|} + \dots \\ & + \log_2 \frac{\left| \mathbf{I}_r + \mathbf{H}_K \left( \sum_{i=1}^K \mathbf{\Sigma}_i \right) \mathbf{H}_K^\dagger \right|}{\left| \mathbf{I}_r + \mathbf{H}_K \left( \sum_{i=1}^{K-1} \mathbf{\Sigma}_i \right) \mathbf{H}_K^\dagger \right|} \text{ bps/Hz}, \end{aligned} \quad (2.9)$$

where  $\mathbf{\Sigma}_i$  is the  $t \times t$  transmit covariance matrix associated with user  $i$ .

### 2.3.3 Duality

Vishwanath *et al.* [19] showed that the MIMO-BC and MIMO-MAC are duals of each other. This is a very important result and it states that if there

exists an achievable rate  $R_{MAC}$  for a set of  $\mathbf{H}_i$  and  $\mathbf{Q}_i$  matrices then there exists an equivalent set of BC covariance matrices  $\mathbf{\Sigma}_i$  such that  $R_{BC} = R_{MAC}$ . This works in both directions. The key application of this result is that the achievable rates in the MIMO-MAC domain can be computed more easily and then converted to the MIMO-BC domain.

### MAC to BC Conversion

To convert a set of MAC covariance matrices,  $\mathbf{Q}_i$ , to their BC equivalents,  $\mathbf{\Sigma}_i$ , the following steps are required [19]. First let

$$\mathbf{A}_j \triangleq \left( \mathbf{I} + \mathbf{H}_j \left( \sum_{l=1}^{j-1} \mathbf{\Sigma}_l \right) \mathbf{H}_j^\dagger \right) \quad (2.10)$$

and

$$\mathbf{B}_j \triangleq \left( \mathbf{I} + \sum_{l=j+1}^K \mathbf{K} \mathbf{H}_l^\dagger \mathbf{Q}_l \mathbf{H}_l \right) \quad (2.11)$$

where user 1 is decoded first followed by user 2 etc. Taking the SVD of  $\mathbf{B}_j^{-1/2} \mathbf{H}_j^\dagger \mathbf{A}_j^{-1/2} = \mathbf{F}_j \mathbf{\Lambda}_j \mathbf{G}_j^\dagger$ , where  $\mathbf{\Lambda}_j$  is square and diagonal, gives:

$$\mathbf{\Sigma}_j = \mathbf{B}_j^{-1/2} \mathbf{F}_j \mathbf{G}_j^\dagger \mathbf{A}_j^{1/2} \mathbf{Q}_j \mathbf{A}_j^{1/2} \mathbf{G}_j \mathbf{F}_j^\dagger \mathbf{B}_j^{-1/2}. \quad (2.12)$$

Note that (2.12) must be used in an iterative process with  $\mathbf{\Sigma}_1$  being calculated first, followed by  $\mathbf{\Sigma}_2$ , etc.

### BC to MAC Conversion

To convert a set of BC covariance matrices,  $\mathbf{\Sigma}_i$ , to their MAC equivalents,  $\mathbf{Q}_i$ , the same procedure as above is required except that the SVD is over  $\mathbf{A}_j^{-1/2} \mathbf{H}_j \mathbf{B}_j^{-1/2} = \mathbf{F}_j \mathbf{\Lambda}_j \mathbf{G}_j^\dagger$  [19]. Noting that  $\mathbf{\Lambda}_j$  is still square and diagonal, the conversion equation is as follows:

$$\mathbf{Q}_j = \mathbf{A}_j^{-1/2} \mathbf{F}_j \mathbf{G}_j^\dagger \mathbf{B}_j^{1/2} \mathbf{\Sigma}_j \mathbf{B}_j^{1/2} \mathbf{G}_j \mathbf{F}_j^\dagger \mathbf{A}_j^{-1/2}. \quad (2.13)$$

### 2.3.4 Fairness

So far the achievable sum-rates in (2.7) and (2.9) have been the metrics discussed. However, in practical systems the system fairness must also be considered. A system's fairness can be loosely defined by whether every user has a satisfactory link or not. Fairness is a subjective issue and a variety of different metrics are available to attempt to measure the fairness of a system. Note here that a complete study of fairness would involve media access control layer design [46, 47], but in this thesis we focus only on the physical layer. Some of the metrics we use in this thesis are listed below.

1. **Number of Active Users:** An active user is defined as one whose rate is above a designated lower-bound. This gives baseline results on what percentage of users are currently active and equivalently, the percentage of users that are inactive or in shutout.
2. **Percentage of Spatial Channels Open:** A multiuser system has  $K \min(m, n)$  spatial channels (eigenchannels) available for transmission. The percentage of these that are used (open) is a good measure of the spread of power throughout the system. This is also referred to in [41] as the degrees of freedom of a system.
3. **Minimum Rate:** We define this as the lowest rate of an individual user. This is a measure of the transmission quality available to the weakest user. This can also be taken as the minimum *non-zero* rate, which is the lowest rate to an active user.
4. **Power Allocated to the Dominant User:** This indicates whether the allocation is one-sided or not. In some cases algorithms allocate the majority of power to a single user, as it may have higher link-quality than the other users.

## 2.4 Selection

Selection is the process where a subset of the system or channel resources is chosen to be utilized in an attempt to optimize the system with limited resources. We consider two types of selection in this thesis:

1. **Antenna Selection:** A subset of the antennas are used. The antennas can be either at the receive or transmit end, and a variety of methods can be used to select them.
2. **User Selection:** In a multiuser system, a subset of users are chosen to transmit to/receive from. The rates to/from the unselected users are zero.

## 2.5 Beamforming

### 2.5.1 Broadcast Channel

In beamforming<sup>2</sup> (BF) for the MIMO-BC, a covariance matrix,  $\Sigma_i$ , is chosen to beamform to the  $i^{\text{th}}$  user using  $\mathbf{H}_i^\dagger \mathbf{H}_i$ . Let  $\mathbf{w}_k^{(i)}$  be the eigenvector corresponding to the  $k^{\text{th}}$  eigenvalue of  $\mathbf{H}_i^\dagger \mathbf{H}_i$  (i.e. for the  $i^{\text{th}}$  user) and  $\mathbf{s}_i$  be the  $t \times 1$  desired data vector to be sent to user  $i$ . Note that the elements of  $\mathbf{s}_i$  have unit magnitude. Thus, if we beamform across  $k$  eigenchannels, then the signal to be sent,  $\mathbf{x}$  (see Sec. 2.3.2), is given by

$$\mathbf{x} = \sum_{i=1}^K \mathbf{x}_i \tag{2.14}$$

---

<sup>2</sup>Note this is eigenbeamforming not antenna beamforming.

where

$$\begin{aligned} \mathbf{x}_i &= \sqrt{\beta} \sum_{j=1}^k \mathbf{w}_j^{(i)} s_{ij} \\ &= \sqrt{\beta} \begin{bmatrix} \mathbf{w}_1^{(i)} & \mathbf{w}_2^{(i)} & \dots & \mathbf{w}_k^{(i)} \end{bmatrix} \begin{bmatrix} s_{i1} \\ s_{i2} \\ \vdots \\ s_{ik} \end{bmatrix} \end{aligned} \quad (2.15)$$

where  $s_{ib}$  is the  $b^{\text{th}}$  element of the vector  $\mathbf{s}_i$ . Note that  $k \leq n$ . This results in the following covariance matrices for these signals

$$\begin{aligned} \boldsymbol{\Sigma}_i &= \mathbb{E} \left( \mathbf{x}_i \mathbf{x}_i^\dagger \right) \\ &= \beta \begin{bmatrix} \mathbf{w}_1^{(i)} & \mathbf{w}_2^{(i)} & \dots & \mathbf{w}_k^{(i)} \end{bmatrix} \begin{bmatrix} \mathbf{w}_1^{(i)\dagger} \\ \mathbf{w}_2^{(i)\dagger} \\ \vdots \\ \mathbf{w}_k^{(i)\dagger} \end{bmatrix} \end{aligned} \quad (2.16)$$

where scaling factor  $\beta$  is chosen to ensure  $\sum_{i=1}^K \text{Tr}(\boldsymbol{\Sigma}_i) \leq P$ . Note that this assumes the same power for each user and for each eigenchannel. We can easily extend the formulation to unequal power allocations by replacing the power scaling factor,  $\beta$ , with a diagonal power loading matrix,  $\mathbf{P}_{L, i}$ , as shown in (2.17).

$$\boldsymbol{\Sigma}_i = \begin{bmatrix} \mathbf{w}_1^{(i)} & \mathbf{w}_2^{(i)} & \dots & \mathbf{w}_k^{(i)} \end{bmatrix} \mathbf{P}_{L, i} \begin{bmatrix} \mathbf{w}_1^{(i)\dagger} \\ \mathbf{w}_2^{(i)\dagger} \\ \vdots \\ \mathbf{w}_k^{(i)\dagger} \end{bmatrix}. \quad (2.17)$$

## 2.5.2 Multiple Access Channel

In beamforming for the MIMO-MAC, a covariance matrix,  $\mathbf{Q}_i$ , is chosen to beamform  $\mathbf{H}_i \mathbf{H}_i^\dagger$ . Let  $\mathbf{v}_k^{(i)}$  be the eigenvector corresponding to the  $k^{\text{th}}$  eigenvalue of  $\mathbf{H}_i \mathbf{H}_i^\dagger$  (i.e. for the  $i^{\text{th}}$  user) and  $\mathbf{s}_i$  be the  $r_i \times 1$  desired data vector to be sent from user  $i$ . Note that the elements of  $\mathbf{s}_i$  have unit magnitude. Thus, if we beamform across  $k$  eigenchannels, then the signal to be sent from user  $i$ ,  $\mathbf{x}_i$  (see Sec. 2.3.1), is given by

$$\begin{aligned} \mathbf{x}_i &= \sqrt{\beta} \sum_{j=1}^k \mathbf{v}_j^{(i)} s_{ij} \\ &= \sqrt{\beta} \begin{bmatrix} \mathbf{v}_1^{(i)} & \mathbf{v}_2^{(i)} & \dots & \mathbf{v}_k^{(i)} \end{bmatrix} \begin{bmatrix} s_{i1} \\ s_{i2} \\ \vdots \\ s_{ik} \end{bmatrix} \end{aligned} \quad (2.18)$$

where  $s_{ib}$  is the  $b^{\text{th}}$  element of the vector  $\mathbf{s}_i$ . Note that  $k \leq \min(r_i)$ . This results in the following covariance matrices for these signals

$$\begin{aligned} \mathbf{Q}_i &= \mathbb{E} \left( \mathbf{x}_i \mathbf{x}_i^\dagger \right) \\ &= \beta \begin{bmatrix} \mathbf{v}_1^{(i)} & \mathbf{v}_2^{(i)} & \dots & \mathbf{v}_k^{(i)} \end{bmatrix} \begin{bmatrix} \mathbf{v}_1^{(i)\dagger} \\ \mathbf{v}_2^{(i)\dagger} \\ \vdots \\ \mathbf{v}_k^{(i)\dagger} \end{bmatrix} \end{aligned} \quad (2.19)$$

where scaling factor  $\beta$  is chosen to ensure  $\sum_{i=1}^K \text{Tr}(\mathbf{Q}_i) \leq P$ .

Note that beamforming in either domain is not equivalent to beamforming in the other. In the results, we perform beamforming in the MAC domain and the resultant system is equivalent to its BC dual, which is not necessarily the same as beamforming in the BC domain. We do this on the grounds of simplicity. See Sec. 4.3 for more discussion on MAC design.

## 2.6 Channels

### 2.6.1 Rayleigh Flat-Fading Channel

The Rayleigh flat-fading channel has been studied extensively in the literature and is considered as a baseline scenario for the majority of systems. For that reason it is our focus in this thesis. The standard model for a Rayleigh flat-fading channel is a channel matrix  $\mathbf{H}$  with elements that are independent, identically distributed (i.i.d.) circularly symmetric complex Gaussian random variables. In this thesis, we assume that the elements of  $\mathbf{H}$  have mean zero and variance one.

For this model to be an accurate representation of a channel, the following conditions need to be met. Firstly, the received signal should be a combination of many multipath components, usually due to large numbers of scatterers in the environments around both the receiver and transmitter. Secondly, the antenna arrays need to be well spaced at each end to ensure no correlation between the channel responses. Finally, we assume that no line-of-sight (LOS) component is present. Extensions to the model, including correlated Rayleigh fading and Ricean fading, are described below.

### 2.6.2 Ricean Channel

When a LOS component exists in a Rayleigh flat-fading channel it can be modeled by the Ricean channel model [48]. This can be expressed as:

$$\mathbf{H}_{\text{rice}} = a \mathbf{H}_{\text{LOS}} + b \mathbf{H} \quad (2.20)$$

where  $a^2 + b^2 = 1$ , the entries of  $\mathbf{H}_{\text{LOS}}$  are constants with unit magnitude and  $\mathbf{H}$  is a Rayleigh matrix. Assuming the common model of a unit rank  $\mathbf{H}_{\text{LOS}}$  matrix, then we can assume without loss of generality that all the elements of  $\mathbf{H}_{\text{LOS}}$  are unity. The parameters  $a$  and  $b$  can also be expressed in terms of the

Ricean  $K$  factor [1, p. 41], where

$$a = \sqrt{\frac{K}{1+K}},$$

and

$$b = \sqrt{\frac{1}{1+K}}.$$

### 2.6.3 Partial Spatial Correlation

If spatial correlation exists either at the transmitter between the transmitting antennas or at the receiver between the receiver antennas, the channel is now correlated. If we assume that the channel is Rayleigh to begin with (see Sec. 2.6.1), the new channel matrix,  $\mathbf{H}_{\text{sc}}$  can be defined as follows:

$$\mathbf{H}_{\text{sc}} = \mathbf{R}^{1/2} \mathbf{H} \mathbf{T}^{1/2}. \quad (2.21)$$

In (2.21),  $\mathbf{H}$  is an i.i.d. Rayleigh channel matrix and  $\mathbf{R}$  and  $\mathbf{T}$  are matrices representing spatial correlation at the receiver and transmitter respectively. Note that this Kronecher model [1, p. 40], [49] is only one of many possibilities for spatially correlated channels.

## 2.7 Channel State Information

In a real world system, knowledge of the channel matrix  $\mathbf{H}$  at the receiver or transmitter is never perfect. This may be due to many factors including incorrect equalization, delays in transmitting the receiver channel information from the receiver to the transmitter and feedback channel limitations. To model the estimated channel,  $\widehat{\mathbf{H}}$ , when imperfect CSI is assumed, we use the well-known model [50]

$$\mathbf{H} = \rho \widehat{\mathbf{H}} + \sqrt{1-\rho^2} \mathbf{E}, \quad (2.22)$$

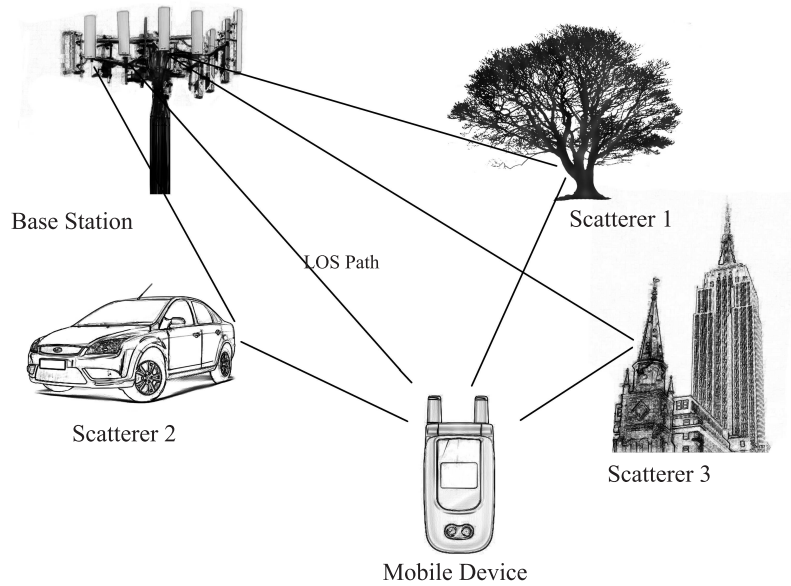


Figure 2.2: An illustration of the multipath phenomenon.

where the correlation,  $\rho$ , is given by  $\rho = \text{corr}(h_{ij}, \hat{h}_{ij})$ ,  $0 \leq \rho \leq 1$  and  $\mathbf{E}$  is an error matrix which is statistically identical to  $\mathbf{H}$ . Note that in some systems the CSI is completely unknown to the transmitter.

## 2.8 Fading

In this thesis, we consider both small scale fading (i.e. multipath effects) and large scale fading (i.e. shadowing). In the mobile environment, small scale fading causes multiple copies of the signal to arrive at the receiver with different delays and phases. Although the motion of the mobile unit causes Doppler shifts on the multipath components, leading to temporally correlated fading, for simplicity these effects are not considered in this thesis. Nonetheless, the received signal fluctuates severely, as multipath components can combine destructively and constructively due to their different phases. Multipath propagation is illustrated in Fig. 2.2.

### 2.8.1 Shadow Fading

Also referred to in the literature as macroscopic fading or just shadowing, shadow fading is due to the shadowing effects of large objects such as buildings or large natural features. Shadow fading is generally slowly changing and is the local mean of a fast fading signal. The distribution of signal power in shadow fading was observed [1, 51] to be well modeled by a log-normal. The corresponding normal probability distribution function (PDF) is given as,

$$f(x) = \frac{1}{\sigma\sqrt{2\pi}} \exp\left(-\frac{(x - \mu)^2}{2\sigma^2}\right), \quad (2.23)$$

where  $\mu$  and  $\sigma$  are the mean and standard deviation of  $x$ . Note that  $x$ ,  $\mu$  and  $\sigma$  are all in dBm units. The mean  $\mu$  is equal to the distance dependent path loss as studied in Sec. 2.8.2. The standard deviation  $\sigma$  can be variable due to the nature of the shadowers, and we use the typical value of 8 dB throughout the thesis. Other values of  $\sigma$  were studied and we concluded that minor variations of  $\sigma$  did not have a significant impact on the results.

### 2.8.2 Path Loss

In free-space, the power loss is inversely proportional to the link distance, squared. This is expressed by [1]

$$P_r = P_t \left(\frac{\lambda_c}{4\pi d}\right)^2 G_t G_r, \quad (2.24)$$

where  $\lambda_c$  is the wavelength,  $P_r$  and  $P_t$  are the received and transmit powers respectively,  $G_r$  and  $G_t$  are the receiver and transmitter antenna gains respectively, and  $d$  is the distance between the receiver and transmitter. However, in real cellular environments, there may be an interfering wave reflected from the surface which accompanies the main wave [1]. This results in the following

approximation to the received power:

$$P_r = P_t \left( \frac{h_t h_r}{d^2} \right)^2 G_t G_r, \quad (2.25)$$

where  $h_r$ ,  $h_t$  are the effective heights of the receive and transmit antennas respectively and we have made the assumption that  $d^2 \gg h_t h_r$ . This inverse fourth power law is an approximation, and in real environments it depends on foliage and terrain and can vary between 2.5 and 6. In this thesis, we also use the inverse third power ( $d^{-3}$ ) as an approximation when we ignore the effects of antenna heights. Values other than  $-3$  were considered but we concluded that minor variations did not have a significant impact on the results. Furthermore, we assume  $G_r = G_t = 1$  for simplicity.

## 2.9 Analytical Mean Capacity

In a MIMO system where both slow and fast fading are present, the mean capacity averaged over the fast fading is given by Chiani and Win in [52]. They consider a single-user MIMO system in Rayleigh fading with a transmit covariance matrix,  $\mathbf{\Phi}$ . The capacity of this single-user system,  $\mathcal{C}$  is given by

$$\mathcal{C}(n_t, n_r, \mathbf{\Phi}) = K_n \sum_{k=1}^{n_r} \left| \mathbf{R}^{(k)} \right|, \quad (2.26)$$

where  $n_t$  and  $n_r$  are the number of transmit and receive antennas respectively. In (2.26) the normalization constant,  $K_n$ , is

$$K_n = \frac{(-1)^{n_r(n_t - n_r)} \prod_{i=1}^L \mu_{(i)}^{m_i n_r}}{\Gamma_{(n_r)}(n_r) \prod_{i < j} (\mu_{(i)} - \mu_{(j)})^{m_i m_j} \prod_{i=1}^L \Gamma_{(m_i)}(m_i)}, \quad (2.27)$$

where  $\mu_{(1)} > \mu_{(2)} > \dots > \mu_{(L)}$  are the  $L$  distinct eigenvalues of  $\mathbf{\Phi}^{-1}$ , with associated multiplicities  $m_1, \dots, m_L$  such that  $\sum_{i=1}^L m_i = n_t$ , and  $\Gamma_{(m)}(a) =$

$\prod_{i=1}^m (a-i)!$ . The  $n_t \times n_t$  matrix  $\mathbf{R}^{(k)}$  has elements:

$$r_{i,j}^{(k)} = \begin{cases} (-1)^{d(i)} (j+d(i)-1)! / \mu_{(e(i))}^{j+d(i)} & j = 1, \dots, r; j \neq k \\ \frac{(-1)^{d(i)}}{\log 2} \sum_{s=0}^{j+d(i)-1} q(i, j, s) & j = 1, \dots, r; j = k \\ [n_t - d(i)]_{d(i)} \mu_{(e(i))}^{n_t - j - d(i)} & j = n_r + 1, \dots, n_t \end{cases}, \quad (2.28)$$

where  $[a]_n \triangleq a(a-1)\dots(a-n+1)$ . Note that  $[a]_0 \triangleq 1$ . The function  $q(i, j, s)$  is given by

$$q(i, j, s) = \exp(\mu_{(e(i))}) E_1(\mu_{(e(i))}) + \sum_{p=1}^{j+d(i)-1-s} (-1)^{j+d(i)-1-s-p} (p-1)! / \mu_{(e(i))}^p, \quad (2.29)$$

where  $E_1(x) = \int_x^\infty \frac{e^{-w}}{w} dw$  is the exponential integral. The function  $e(i)$  is an indicator function which is defined as the unique integer such that

$$m_1 + \dots + m_{e(i)-1} < i \leq m_1 + \dots + m_{e(i)},$$

and

$$d(i) = \sum_{k=1}^{e(i)} m_k - i.$$

## 2.10 Order Statistics

For a set of random variables,  $X_1, \dots, X_n$ , the order statistics consist of the ordered set such that  $X_{(1)} \leq X_{(2)} \leq \dots \leq X_{(n)}$ . The cumulative distribution function (CDF) of an ordered variable  $X_{(r)}$  is defined as follows in [53, p. 9]:

$$F_{(r)}(x) = \sum_{i=r}^n \binom{n}{i} F^i(x) [1 - F(x)]^{n-i}, \quad (2.30)$$

where  $F(x)$  is the CDF of an unordered variable  $X$ .

### 2.10.1 Concomitants

Consider the pairs  $(X_i, Y_i)$ ,  $i = 1, \dots, n$  which are random samples of a bivariate distribution with CDF  $F(x, y)$ . If the samples are ordered by  $X_i$ , the variable  $Y$  associated with  $X_{r:n}$ , the  $r^{\text{th}}$  largest value of  $X$ , is denoted  $Y_{[r:n]}$ . This is called the *concomitant of the  $r^{\text{th}}$  order statistic* [53, p. 144]. This situation occurs in the imperfect CSI case where the values of the true channel,  $\mathbf{H}$ , are estimated at the receiver using some channel estimation procedure. The resulting channel estimate,  $\hat{\mathbf{H}}$ , is correlated with  $\mathbf{H}$  but not identical. The order statistics,  $X_{r:n}$ , and  $Y_{[r:n]}$ , have the following relationship for  $r = 1, \dots, n$  [53, p. 144]:

$$Y_{[r:n]} = \mu_Y + \rho \frac{\sigma_Y}{\sigma_X} (X_{r:n} - \mu_X) + \epsilon_r \quad (2.31)$$

where  $\rho = \text{Corr}(X, Y)$ ,  $\epsilon_r$  is a zero-mean error term which is independent of  $X_{r:n}$ , and  $\mu_X$ ,  $\sigma_X$  and  $\mu_Y$ ,  $\sigma_Y$  are the mean and standard deviations of  $X$  and  $Y$  respectively.

## 2.11 Optimization

In many systems the aim is to optimize a particular performance metric. For example, it may be necessary to either minimize the power consumption while achieving a given BER, or to optimize the channel rate. The problem can be expressed in a very general form as follows <sup>3</sup> [54]:

$$\begin{aligned} & \text{minimize} && f_0(\mathbf{x}) \\ & \text{subject to} && f_i(\mathbf{x}) \leq 0, \quad i = 1, \dots, m \\ & && h_i(\mathbf{x}) = 0, \quad i = 1, \dots, p \end{aligned} \quad (2.32)$$

where  $\mathbf{x} \in \mathbb{R}^n$ . A subset of optimization is convex optimization, which is a special case. In convex optimization, if the solution is locally optimal, it is also globally optimal due to the convexity of the function.

---

<sup>3</sup>To perform a maximization, minimize over  $-f_0(x)$ .

### 2.11.1 The Lagrangian

Using Lagrangian duality, the constraints in (2.32) can be taken into account by adding a weighted sum of these constraint functions to the objective problem [54]. Hence the *Lagrangian*,  $L$ , associated with (2.32) is defined as

$$L(\mathbf{x}, \boldsymbol{\zeta}, \boldsymbol{\nu}) = f_0(\mathbf{x}) + \sum_{i=1}^m \zeta_i f_i(\mathbf{x}) + \sum_{i=1}^p \nu_i h_i(\mathbf{x}), \quad (2.33)$$

where  $\zeta_i$  is the *Lagrange multiplier* associated with the  $i^{\text{th}}$  inequality constraint,  $f_i(x) \leq 0$ , and  $\nu_i$  is the Lagrange multiplier associated with the  $i^{\text{th}}$  equality constraint,  $h_i(x) = 0$ . The variables  $\zeta$  and  $\nu$  are also referred to as the dual variables for (2.32).

### 2.11.2 Karush-Kuhn-Tucker Conditions

Building on the MSc. thesis of W. Karush [55], H. W. Kuhn and A.W. Tucker wrote a conference paper [56] outlining the conditions necessary for optimization. They can be broken down into parts, each representing a condition for optimality. Given the optimal point of (2.32),  $\mathbf{x}^*$ , and the optimal Lagrange multipliers,  $\boldsymbol{\zeta}^*$  and  $\boldsymbol{\nu}^*$ , [54], the Karush-Kuhn-Tucker (KKT) conditions are defined as follows [54]:

- Stationarity (i.e. the gradient of the Lagrangian,  $\nabla L(\mathbf{x}^*, \boldsymbol{\zeta}^*, \boldsymbol{\nu}^*) = 0$ )

$$\nabla f_0(\mathbf{x}^*) + \sum_{i=1}^m \zeta_i^* \nabla f_i(\mathbf{x}^*) + \sum_{i=1}^p \nu_i^* \nabla h_i(\mathbf{x}^*) = 0 \quad (2.34)$$

- Primal Feasibility

$$f_i(\mathbf{x}^*) \leq 0, \text{ for all } i = 1, \dots, m$$

$$h_j(\mathbf{x}^*) = 0, \text{ for all } j = 1, \dots, p \quad (2.35)$$

- Dual Feasibility [54]

$$\zeta_i^* \geq 0 \quad (2.36)$$

- Complementary Slackness [54, p. 242]

$$\zeta_i^* f_i(\mathbf{x}^*) = 0, \text{ for all } i = 1, \dots, m \quad (2.37)$$

### 2.11.3 Convexity

In order to ensure that the properties of convex optimization hold, it is necessary to determine whether a function is convex. A function  $f : \mathbb{R}^n \rightarrow \mathbb{R}$  is convex if the following conditions hold [54].

1. The domain of the function,  $\mathbf{dom} f$ , is a convex set.
2. For all  $x, y \in \mathbf{dom} f$ ,  $0 \leq \theta \leq 1$

$$f[\theta x + (1 - \theta)y] \leq \theta f(x) + (1 - \theta)f(y). \quad (2.38)$$

Following from the above, a function  $f$  is concave if  $-f$  is convex and vice versa. An alternative approach to test convexity is to look at the second derivative or Hessian, if it exists, for all  $x \in \mathbf{dom} f$ . The function  $f$  is convex if and only if the Hessian satisfies

$$\nabla^2 f(\mathbf{x}) \succeq 0, \quad (2.39)$$

where  $\mathbf{A} \succeq 0$  indicates the matrix  $\mathbf{A}$  is positive semi-definite.

The final condition for optimality is that a feasible point exists within  $\mathbf{dom} f$ , i.e. there is at least one valid  $\mathbf{x}$  such that  $f_i(\mathbf{x}) < 0$ , for all  $i = 1, \dots, m$ , holds. This is referred to as Slater's Condition [54, p. 226]. If this holds and the optimization problem in (2.32) is convex, then the KKT conditions ((2.34), (2.35), (2.36), (2.37)) are necessary for a unique optimal point.

### 2.11.4 Waterfilling

For a single-user MIMO system, with an  $m \times n$  channel matrix,  $\mathbf{H}$ , waterfilling is an algorithm that produces the highest possible rate. The algorithm consists of two parts, a particular covariance structure and a power allocation algorithm.

#### Covariance Structure

It is well-known that in order to maximize the single user MIMO capacity (2.3), the covariance matrix  $\mathbf{Q}_{\text{WF}}$  has the form [1]:

$$\mathbf{Q}_{\text{WF}} = \mathbf{V} \mathbf{X} \mathbf{V}^\dagger, \quad (2.40)$$

where  $\mathbf{X} = \text{diag}(x_1, x_2, \dots, x_m, 0, \dots, 0)$  is a matrix of power allocations to each subchannel,  $\ell = \min(m, n)$  and  $\mathbf{V}$  is a unitary matrix from the SVD of  $\mathbf{H}$  (see Sec. 2.2).

#### Power Allocation Algorithm

The power allocation algorithm itself stems from the convex optimization problem of maximizing the capacity with a set of power constraints. Boyd and Vandenberghe [54, p. 245] describe the problem by dividing the channel into its eigenchannels. This gives the following optimization problem:

$$\max_{x_i : x_i \geq 0} \sum_{i=1}^{\ell} \log_2(\alpha_i + x_i), \quad \sum_{i=1}^{\ell} x_i = 1 \quad (2.41)$$

where  $\lambda_i$  are the eigenvalues of  $\mathbf{H}^\dagger \mathbf{H}$ ,  $\alpha_i = \frac{1}{\lambda_i \text{SNR}}$  and  $x_i$  is the power allocated to each antenna. The total power constraint in this example is that the total allocated power is 1 ( $\sum_{i=1}^{\ell} x_i = 1$ , also expressed as  $\mathbf{1}^T \mathbf{x} = 1$ ), as  $\alpha_i$  is proportional to SNR. To make this problem convex, we can turn it into a

minimization as follows:

$$x_i : x_i \geq 0 \quad \sum_{i=1}^{\ell} x_i = 1 \quad - \sum_{i=1}^{\ell} \log_2 (\alpha_i + x_i). \quad (2.42)$$

To optimize the above equation, we introduce Lagrange multipliers:  $\zeta_i \in \mathbb{R}^n$  for the inequality constraint  $x_i \geq 0$  and the multiplier  $\nu$  for the equality constraint  $\mathbf{1}^T \mathbf{x} = 1$ . These multipliers give the KKT conditions for optimization as:

$$\begin{aligned} x_i^* &\geq 0 & \mathbf{1}^T \mathbf{x}^* &= 1 & \zeta_i^* &\geq 0 \\ \zeta_i^* x_i^* &= 0 & \frac{-1}{\alpha_i + x_i^*} - \zeta_i^* + \nu^* &= 0, \end{aligned} \quad (2.43)$$

for all  $i = 1, \dots, \ell$ .

To complete the minimization, we must solve (2.43) for  $\mathbf{x}^*$ ,  $\zeta^*$  and  $\nu^*$ . We can easily show that  $\zeta_i^*$  is a slack variable in the above equations so it can be eliminated to leave

$$\begin{aligned} x_i^* &\geq 0 & x_i^* (\nu^* - 1/(\alpha_i + x_i^*)) &= 0 \\ \mathbf{1}^T \mathbf{x}^* &= 1 & \nu^* &\geq 1/(\alpha_i + x_i^*). \end{aligned} \quad (2.44)$$

Now looking at these equations closely, we can form a solution by considering two distinct cases. The first case is where  $\nu^* < 1/\alpha_i$ . Under this condition the last equation of (2.44) can only hold if  $x_i^* > 0$ , and with this being the case, the third equation of (2.44) implies that  $\nu^* = 1/(\alpha_i + x_i^*)$ . Solving for  $x_i^*$  gives  $x_i^* = 1/\nu^* - \alpha_i^*$  when  $\nu^* < 1/\alpha_i$ . Logically the other case is where  $\nu^* \geq 1/\alpha_i$ , leading to  $\nu^* \geq 1/\alpha_i > 1/(\alpha_i + x_i^*)$ , which means that  $x_i^* > 0$  is impossible as it would violate the slackness conditions of  $\zeta_i^*$  used to convert (2.43) to (2.44). Thus, by the first equation in (2.44),  $x_i^* = 0$  when  $\nu^* \geq 1/\alpha_i$ . This is expressed neatly as

$$x_i = \begin{cases} 1/\nu^* - \alpha_i^*, & \nu^* < 1/\alpha_i \\ 0, & \nu^* \geq 1/\alpha_i \end{cases}. \quad (2.45)$$

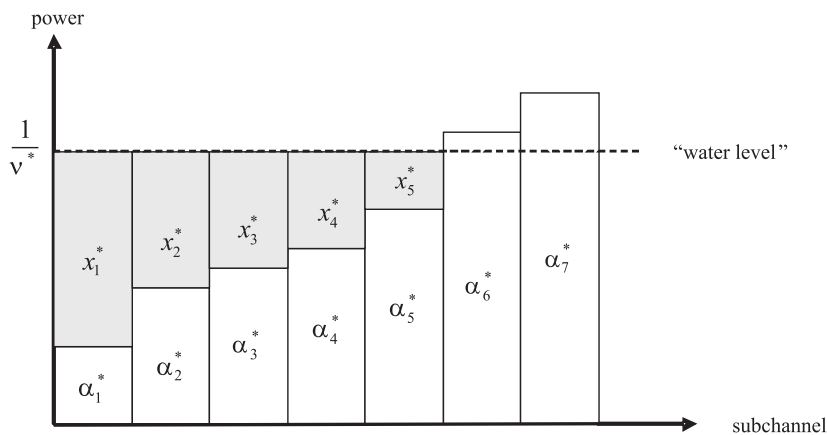


Figure 2.3: Visual interpretation of the waterfilling algorithm.

Equation (2.45) can be simplified to  $x_i^* = \max\{0, 1/\nu^* - \alpha_i\}$ . Combining this with the equality constraint,  $\mathbf{1}^T \mathbf{x}^* = 1$ , we find

$$\sum_{i=1}^n \max\{0, 1/\nu^* - \alpha_i\} = 1. \quad (2.46)$$

This gives

$$\nu^* = \frac{k}{1 + \sum_{i \in \kappa} \alpha_i}, \quad (2.47)$$

where  $\kappa$  is the set of subchannels where  $\nu^* < \frac{1}{\alpha_i}$  and  $k$  is the number of channels in this set.

The reason the above process is called waterfilling is as follows. If one imagines each eigenchannel as a region in a tank, and  $\alpha_i^*$  as the level of the ground in region  $i$ , the solution,  $x_i^*$ , is the height of water above it when a certain amount of water is poured in (the amount of power allocated). The final water level ends up being  $1/\nu^*$ . In the end the shallower regions, i.e. those with higher SNR, get more water as they are the ones with the lower  $\alpha_i^*$  values and thus higher eigenvalues, representing the better eigenchannels for transmission. This is shown schematically in Fig. 2.3

### 2.11.5 Iterative Waterfilling

Unfortunately, the extension of water-filling from a single-user to a multiuser MIMO system is not as straight forward as water-filling each user independently. Instead, one must take into account the mutual interference between users. Jindal *et al.* [17] built upon work by Yu and Cioffi [16] to create a robust and proven iterative algorithm for water-filling a multiuser system in the MIMO-MAC domain with sum-power constraints. Note that the same authors show that the results can also be used in the MIMO-BC domain via *duality* [19]. This iterative approach, named Iterative Waterfilling, first creates generalized channels for each user which include interference from the other users. This generalized channel is calculated during every iteration by the following equation for user  $i$ :

$$\mathbf{G}_i^{(n)} = \mathbf{H}_i \left( \mathbf{I} + \sum_{j=1, j \neq i}^K \mathbf{H}_j^\dagger \mathbf{Q}_j^{(n-1)} \mathbf{H}_j \right)^{-1/2}. \quad (2.48)$$

In (2.48)  $\mathbf{G}_i^{(n)}$  represents the generalized channel for the  $i^{\text{th}}$  user at the  $n^{\text{th}}$  iteration and  $\mathbf{Q}_j^{(n-1)}$  represents the covariance matrix for user  $j$  at the  $(n-1)^{\text{th}}$  iteration. Note that  $\mathbf{Q}_j^{(0)}$  needs to be initialized for all  $j = 1 \dots K$  (see [17]). With (2.48), parallel non-interfering channels have been created which can be water-filled separately (with individual power constraints) or in parallel with a single sum-power constraint. The latter is the next step of Jindal's algorithm with the covariance matrices computed using standard water-filling:

$$\begin{aligned} \left\{ \mathbf{Q}_i^{(n)} \right\}_{i=1}^K = \\ \arg \max_{\left\{ \mathbf{Q}_i \right\}_{i=1}^K : \mathbf{Q}_i \geq 0, \sum_{i=1}^K \text{Tr} \{ \mathbf{Q}_i \} \leq P} \sum_{i=1}^K \log_2 \left| \mathbf{I} + \left( \mathbf{G}_i^{(n)} \right)^\dagger \mathbf{Q}_i \mathbf{G}_i^{(n)} \right| \end{aligned} \quad (2.49)$$

The maximization in (2.49) may look complicated but can be performed simply as a single water-filling problem based on the block diagonal channel with diagonals equal to  $\mathbf{G}_i^{(n)}, \dots, \mathbf{G}_K^{(n)}$ . This can be further simplified [17] as a matrix water-filling problem by taking the eigenvalue decomposition of  $\mathbf{G}_i^{(n)} \left( \mathbf{G}_i^{(n)} \right)^\dagger$ ,

$$\mathbf{G}_i^{(n)} \left( \mathbf{G}_i^{(n)} \right)^\dagger = \mathbf{U}_i \mathbf{D}_i \mathbf{U}_i^\dagger \quad (2.50)$$

with matrices  $\mathbf{U}_i$  unitary and  $\mathbf{D}_i$  square and diagonal. This simply leaves the updated covariance matrices to be:

$$\mathbf{Q}_i^{(n)} = \mathbf{U}_i \mathbf{\Lambda}_i \mathbf{U}_i^\dagger \quad (2.51)$$

where  $\mathbf{\Lambda}_i = [\mu \mathbf{I} - (\mathbf{D}_i)^{-1}]^+$ ,  $[\cdot]^+$  is a element-wise maximum with zero and the water-filling level<sup>4</sup>,  $\mu$ , is chosen for the sum-power constraint such that  $\sum_{i=1}^N \text{Tr}\{\mathbf{\Lambda}_i\} = P$ .

## 2.12 Cellular Layouts and Modelling

### 2.12.1 Single Cell ‘Bagel’ Model

To model a cell and the spatial distribution of users in the cell we use a simple circular model, nicknamed the ‘bagel’. This consists of a uniform distribution of users between two circles, one defining the cell radius,  $R$ , and the other corresponding to an inner exclusion zone,  $R_0$ . This inner exclusion zone is to prevent users from being too close to the transmitter. This prevents the traditional inverse power law models for signal strength from giving arbitrarily high power to users who happen to be very close to the BS. The exclusion zone is not just a mathematical construction since most cellsites are high up on buildings or on cell towers and it is very hard for a mobile user to get within a certain distance of the actual antennas. In this thesis  $R = 100\text{m}$  and

---

<sup>4</sup>Note that  $\mu \equiv \frac{1}{\nu^*}$  in the previous sections.

$R_0 = 10\text{m}$ . This gives a mean distance from the antennas of 67.6m.

The PDF of the distance,  $r$ , from the base station to mobile using the above model is as follows:

$$f(r) = \frac{2r}{R^2 - R_0^2}, \quad R_0 \leq r \leq R, \quad (2.52)$$

where  $R$  is the cell radius and  $R_0$  is the inner exclusion zone radius.

Consider the  $i^{\text{th}}$  user in the cell. The link gain of this user, denoted  $\Gamma_i$ , is defined by the classical model [57]

$$\Gamma_i = AL_i r_i^{-\gamma}, \quad (2.53)$$

where  $L_i$  is the lognormal variable representing shadowing (see Sec. 2.8.1),  $r_i$  is the distance from user  $i$  to the base station,  $\gamma$  is the path loss exponent and  $A$  is a constant such that  $\text{E}\{\Gamma_i\} = 1$  across the cell. This is important as it ensures that the mean SNR received by a user is equal to the ratio of the transmit signal power over noise. In this thesis we refer to the mean SNR as  $\text{SNR}_{\text{av}}$ .

A key metric in investigating the relative effects of various algorithms within this system is the ratio  $\Gamma_i/\Gamma_j$  for  $i \neq j$ . The CDF of the distribution of  $\Gamma_i/\Gamma_j$ ,  $F(z) = \text{Pr}(\Gamma_i/\Gamma_j < z)$  is given as follows (see Appendix A for

the derivation):

$$\begin{aligned}
F(Z) = & \frac{a^2 R^2 R_0^2}{4} \left[ \Phi \left( \frac{w_1 - \mu}{\sigma} \right) - \Phi \left( \frac{w_0 - \mu}{\sigma} \right) \right] \\
& - \left( \frac{1}{2} + \frac{a^2 (R^4 + R_0^4)}{8} \right) \left[ \Phi \left( \frac{w_2 - \mu}{\sigma} \right) - \Phi \left( \frac{w_1 - \mu}{\sigma} \right) \right] \\
& - \frac{a^2 R^4 c^2}{8} \exp[2/\gamma(\sigma^2/\gamma + \mu)] \left[ \Phi \left( \frac{w_1 - \mu - 2\sigma^2/\gamma}{\sigma} \right) - \Phi \left( \frac{w_0 - \mu - 2\sigma^2/\gamma}{\sigma} \right) \right] \\
& - \frac{a^2 R_0^4}{8c^2} \exp[2/\gamma(\sigma^2/\gamma - \mu)] \left[ \Phi \left( \frac{w_1 - \mu + 2\sigma^2/\gamma}{\sigma} \right) - \Phi \left( \frac{w_0 - \mu + 2\sigma^2/\gamma}{\sigma} \right) \right] \\
& + \frac{a^2 R_0^4 c^2}{8} \exp[2/\gamma(\sigma^2/\gamma + \mu)] \left[ \Phi \left( \frac{w_2 - \mu - 2\sigma^2/\gamma}{\sigma} \right) - \Phi \left( \frac{w_1 - \mu - 2\sigma^2/\gamma}{\sigma} \right) \right] \\
& + \frac{a^2 R^4}{8c^2} \exp[2/\gamma(\sigma^2/\gamma - \mu)] \left[ \Phi \left( \frac{w_2 - \mu + 2\sigma^2/\gamma}{\sigma} \right) - \Phi \left( \frac{w_1 - \mu + 2\sigma^2/\gamma}{\sigma} \right) \right] \\
& + \Phi \left( \frac{w_2 - \mu}{\sigma} \right). \tag{2.54}
\end{aligned}$$

where  $a = 2/(R^2 - R_0^2)$ ,  $R_0 < r < R$ ,  $c = z^{-1/\gamma}$ ,  $w_0 = \gamma \log \left( \frac{R_0}{cR} \right)$ ,  $w_1 = \gamma \log \left( \frac{1}{c} \right)$ ,  $w_2 = \gamma \log \left( \frac{R}{cR_0} \right)$ ,  $\Phi(x) = P(\mathbb{N}(0, 1) < x)$  and  $\mu$  and  $\sigma$  are the mean and standard deviation of the normal distribution involved in the lognormal distribution respectively.

Note that the value of  $R$  used ( $R = 100\text{m}$ ) gives a small cell, but Fig. 2.4 shows that the sizes of the cell radius and inner exclusion zone have very little effect on the distribution of the ratio of two users' SNR values within the cell. This suggests that in capacity studies, although the absolute capacity values may change when the cell size is changed, the relative effects between users may remain approximately the same.

## 2.13 Summary

In this chapter we have laid down the foundations for the thesis. Firstly, we reviewed a number of system models including the common statistical channel models, which are used due to their simplicity. Secondly, we covered various techniques used throughout the literature, such as the SVD, order statistics

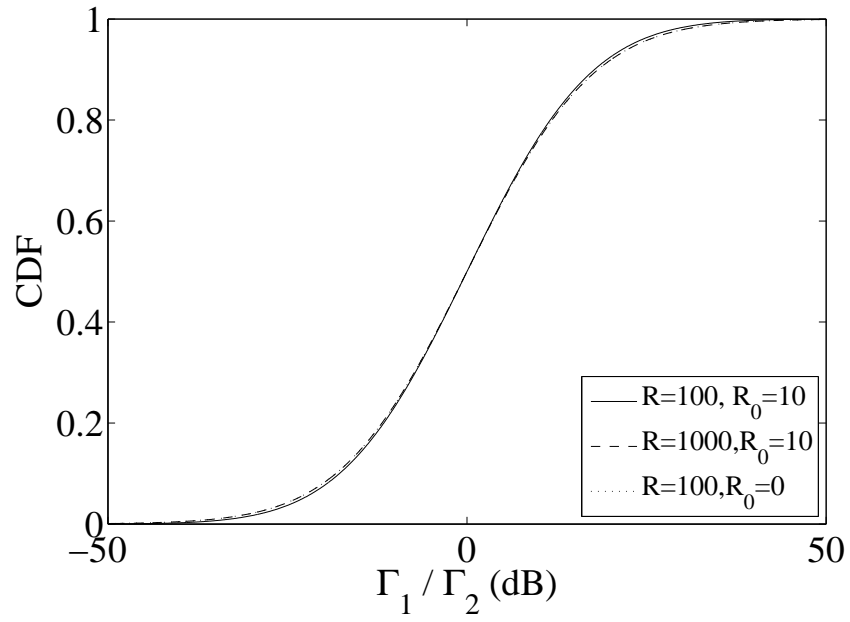


Figure 2.4: CDF of the ratio  $\Gamma_1/\Gamma_2$  for different values of  $R$  and  $R_0$ .

and convex optimization. Finally we introduced models more specific to this thesis, allowing the reader to understand their use in the following chapters.



## Chapter 3

# Single User MIMO: Selection Methods and Analysis

The throughput advantages of MIMO systems are increased by the use of large antenna arrays and a large amount of attention has been given to getting as much out of these systems to realize large potential capacity gains. However, to achieve these gains, the number of antennas in either the transmit or receive array must be increased and in turn the associated baseband complexity to process the MIMO capacity-approaching codes increases significantly. In practice, spatial constraints and the power consumption of the antenna array also are very important issues. An example of this is the continuing miniaturization of cellular mobile terminals and the reduced space for accommodating several antenna elements. Also, each RF chain requires proper amplification prior to transmission. Whilst modern highly linear amplifiers are very power efficient, they are also very expensive. For example, today's typical 3GPP mobile terminal transmitter uses a cheap non-linear amplifier per antenna, which can consume between 20% and 30% of the terminal's limited power budget. Thus, maintaining a large number of these RF chains is very power and/or cost intensive.

In this chapter we consider antenna selection. This is a simple yet very powerful approach for reducing system complexity and the number of RF chains (and thus making the system less power intensive), whilst retaining a large

portion of the increased rates from using MIMO techniques. Using the principle of antenna selection at the transmit and/or receive side, RF chains can be assigned to a subset of the available physical antennas. This is a convenient method to approach the spatial capacity of MIMO without a large increase in the system's hardware needs. On the negative side, a feedback channel from receiver to transmitter is needed in the case of transmit antenna selection; however, very little feedback data (just the antenna indices) is required and most modern communications systems have feedback channels available.

Antenna selection has its historical roots in selection combining which is usually performed at the RX side for single-input-multiple-output (SIMO) channels (see e.g. [32]). This technique has also been generalized to the TX side for multiple-input-single-output (MISO) channels [34]. More recently, many researchers have proposed algorithms for more generalized antenna selection [35–38]. Some of these focus on selection to minimize outage probabilities or error rates [58, 59]. However, in this chapter, we propose selection to increase MIMO capacity as in [36, 60]. Other previous work in this area is based on both simple methods [35, 37, 61, 62], variants of which are discussed in this chapter, as well as more complex methods [63], which can give slightly better performance than the simpler methods at the expense of greater computational complexity.

In this chapter we address antenna selection in a point-to-point single-user MIMO link, building on the ideas in [35–37], analyzing and extending the algorithms discussed. We demonstrate using statistical analysis of the resultant channel capacities that the selection process can be simply modeled as a scaling of the SNR, resulting in a performance gain. Hence, we propose this SNR scaling factor as a *very simple metric* that can be used to compare the performances of various algorithms. Note that this approach is extremely general and can be used for a variety of channels, selection scenarios and also when channel estimation error is considered. Furthermore, our analysis is

valid for all scenarios: transmit selection, receive selection and joint transmit-receive selection. In this chapter we use the scaling factor to assess the impact of different channel types, including i.i.d. Rayleigh, correlated Rayleigh and Ricean fading channels. Also we investigate the presence of imperfect CSI and propose a simplified waterfilling scheme.

## 3.1 Selection Algorithms

We cover a variety of antenna selection algorithms, some pre-existing, some novel. The aim of all of the algorithms is to select an  $r \times t$  ( $r$  receive antennas and  $t$  transmit antennas) submatrix  $\mathbf{S}$  from  $\mathbf{H}$ , the  $m \times n$  ( $m$  receive antennas and  $n$  transmit antennas) single-user complex channel matrix (see Sec. 2.1). We focus on two scenarios: selection only at the transmitter (TX selection) and selection at both the transmitter and receiver (TX-RX selection). Selection at the receiver (RX selection) is not covered in detail as it is analogous to TX selection and all TX selection algorithms can be simply transferred to the RX selection domain. TX selection is our major focus in this chapter as TX-RX selection algorithms are also very similar to their TX selection cousins.

### 3.1.1 Transmit Selection Algorithms

We study three main algorithms for TX selection are considered as well as two additional approaches that are derivatives of these. The first method is the Optimal Selection Algorithm (OSA) which performs selection by choosing the submatrix  $\mathbf{S}_{OSA}$  which results in the highest capacity.  $\mathbf{S}_{OSA}$  is chosen over all possible  $m \times t$  submatrices of  $\mathbf{H}$  and thus provides the maximum capacity for pure antenna selection. OSA can be described mathematically by:

$$\mathbf{S}_{OSA} = \arg \max_{\{\mathbf{S} \in \mathbf{H}\}} \log_2 \left| \mathbf{I}_r + \frac{\text{SNR}}{t} \mathbf{S} \mathbf{S}^\dagger \right|, \quad (3.1)$$

where the set  $\{\mathbf{S} \in \mathbf{H}\}$  contains all  $m \times t$  submatrices of  $\mathbf{H}$ .

The second algorithm, the Arbitrary Selection Algorithm (ASA), is based on the selection of a random (arbitrary)  $m \times t$  subset of  $\mathbf{H}$ ,  $\mathbf{S}_{ASA}$ . If the antennas are uncorrelated and the channel is random in nature, a deterministic subset of  $\mathbf{H}$  can be chosen for  $\mathbf{S}_{ASA}$ . Also, in such random uncorrelated channels, ASA is directly comparable to an independent system with  $m \times t$  antennas in which no selection is performed. This algorithm is not a sensible approach to increasing capacity but provides a useful baseline (based on no channel knowledge) with which to compare the other techniques.

The third algorithm is the Norm-based Selection Algorithm (NSA). This performs antenna selection by using the norms of the columns of  $\mathbf{H}$ ,  $P_j^{(u)} = \sum_{i=1}^m |h_{ij}|^2$  (for column  $j$ ), as a measure of the received power from each antenna. Note that unless specified by the  $(u)$  superscript, all  $P_j$  variables are assumed to be ordered. Hence  $P_j$  is the  $j^{\text{th}}$  largest column norm, whereas  $P_k^{(u)}$  is the norm of column  $k$ . To perform the selection we create  $\mathbf{S}_{NSA}$  from the columns with the  $t$  biggest norms,  $P_j, j = 1 \dots t$ . This algorithm is not novel and has been described previously in the literature (examples are [35,37]) under other guises. The advantages of NSA are its computational simplicity and its close-to-optimal capacity results. Both of these advantages will be discussed in more detail throughout the chapter. We note that NSA works better in i.i.d. channels. In the presence of spatial correlation its performance is degraded, which is further studied in Sec. 3.5. In practise, more complex variations on NSA might be used to handle the correlated nature of the channel rows or columns. However, this is not considered here.

Two more selection algorithms can be derived from the above three to provide interesting benchmarks for comparison. The first one is WSA, the Worst-Case Selection Algorithm, the antithesis of OSA. Thus to perform WSA, we pick  $\mathbf{S}_{WSA}$  to be the subset of  $\mathbf{H}$  that minimizes capacity

$$\mathbf{S}_{WSA} = \arg \min_{\{\mathbf{S} \in \mathbf{H}\}} \log_2 \left| \mathbf{I}_r + \frac{\text{SNR}}{t} \mathbf{S} \mathbf{S}^\dagger \right|, \quad (3.2)$$

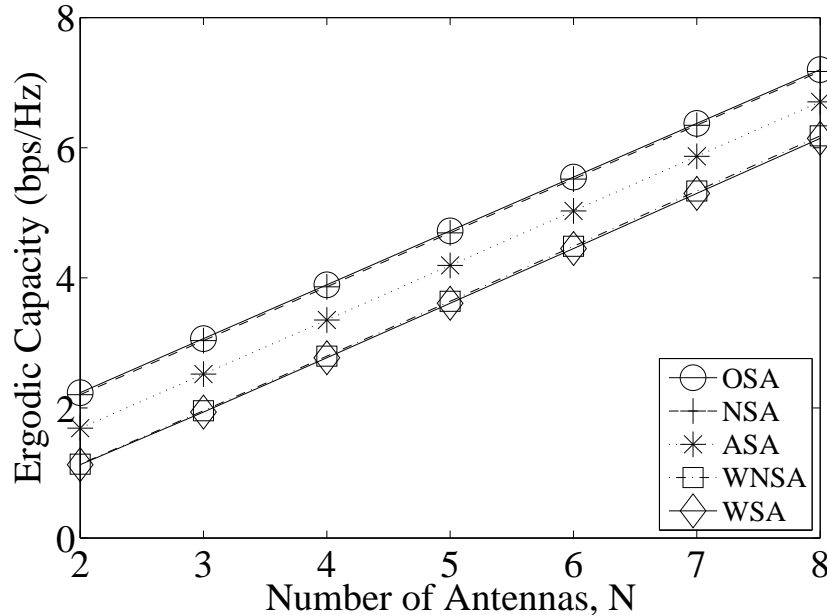


Figure 3.1: Comparison of selection schemes for a  $(N, N + 2)$  choose  $(N, N)$  system (SNR = 0dB).

where  $\{\mathbf{S} \in \mathbf{H}\}$  contains all  $m \times t$  submatrices of  $\mathbf{H}$ .

Although not intended for use, WSA provides us a lower bound for the selection process as well as interesting relationships to OSA and ASA. These will be discussed in more detail later in the chapter. The other method is the converse of NSA, WNSA (Worst-Case Norm-based Selection Algorithm) in which one selects the submatrix  $\mathbf{S}_{WNSA}$  from the  $t$  columns of  $\mathbf{H}$  with the lowest norms,  $P_j, j = n - t + 1 \dots n$ . WNSA is used for comparison to its opposite, NSA and the benchmark ASA. The basic selection algorithms are shown for an  $(N, N + 2)$  select  $(N, N)$  system in Figs. 3.1, 3.2 and 3.3 for a i.i.d. Rayleigh channel with a variety of SNRs. Notice that the worst-case variants are effectively mirrors of their best-case equivalents around ASA. These graphs also illustrate that NSA is a very good approximation to OSA especially at lower SNRs.

Figure 3.4 illustrates the effects of increasing the number of redundant antennas. Note that the absolute selection gain of OSA (and NSA) with respect

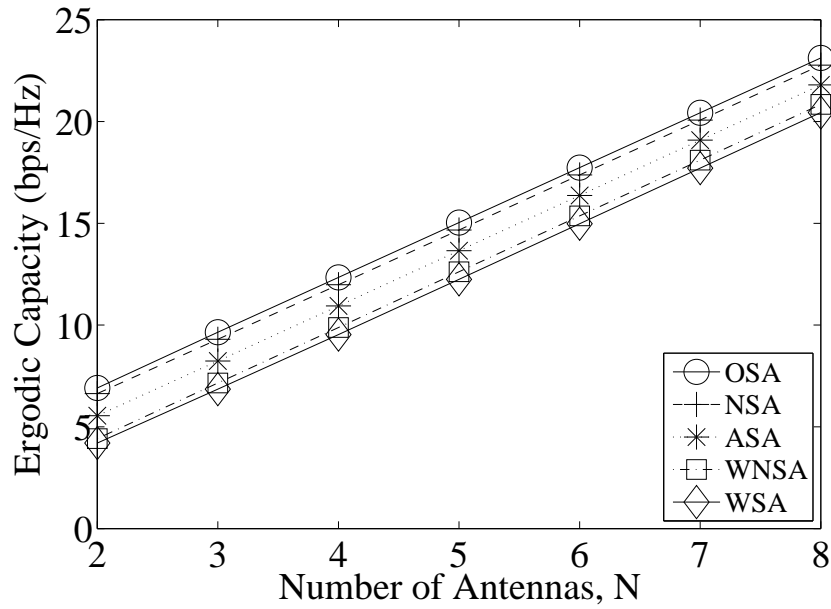


Figure 3.2: Comparison of selection schemes for a  $(N, N + 2)$  choose  $(N, N)$  system (SNR = 10dB).

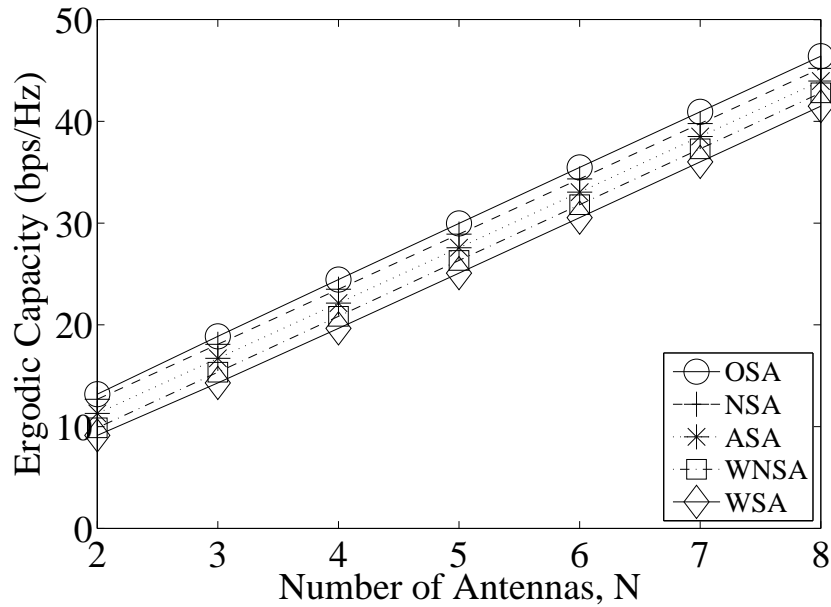


Figure 3.3: Comparison of selection schemes for a  $(N, N + 2)$  choose  $(N, N)$  system (SNR = 20dB).

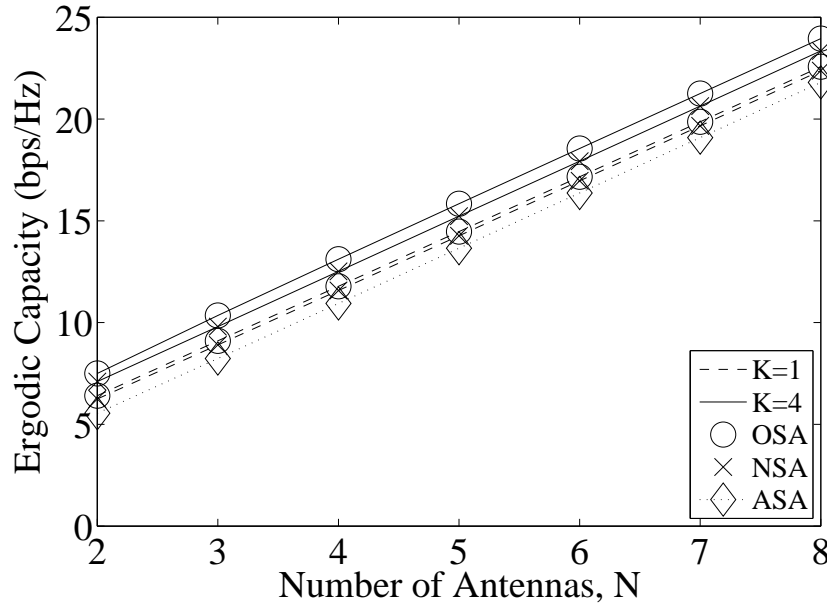


Figure 3.4: Comparison of selection schemes for a  $(N, N + K)$  choose  $(N, N)$  system with variable  $K$  (SNR = 10dB).

to ASA is dependent on the number of redundant antennas,  $n - t$ , not the number of total antennas,  $n$ . This is a key point as it allows a system designer to know how much system gain they can introduce to a system by introducing redundant antennas, or how many redundant antennas they need to introduce for a required increase in capacity.

### 3.1.2 Algorithms for Transmitter-Receiver Selection

All of the TX selection algorithms can be easily extended to RX selection by performing the selections over the rows instead of the columns of  $\mathbf{H}$ . From this, TX and RX selection can be simply combined to create joint selection algorithms. For OSA (and its converse WSA) we select submatrices  $\mathbf{S}$  for comparison which are  $r \times t$ . Note there are many more submatrices to be considered in joint OSA than in standard OSA. Hence, joint OSA can be much more computationally intensive as discussed in Sec. 3.4. It can be mathematically described by (3.1) with a slight change: now the selection  $\{\mathbf{S} \in \mathbf{H}\}$

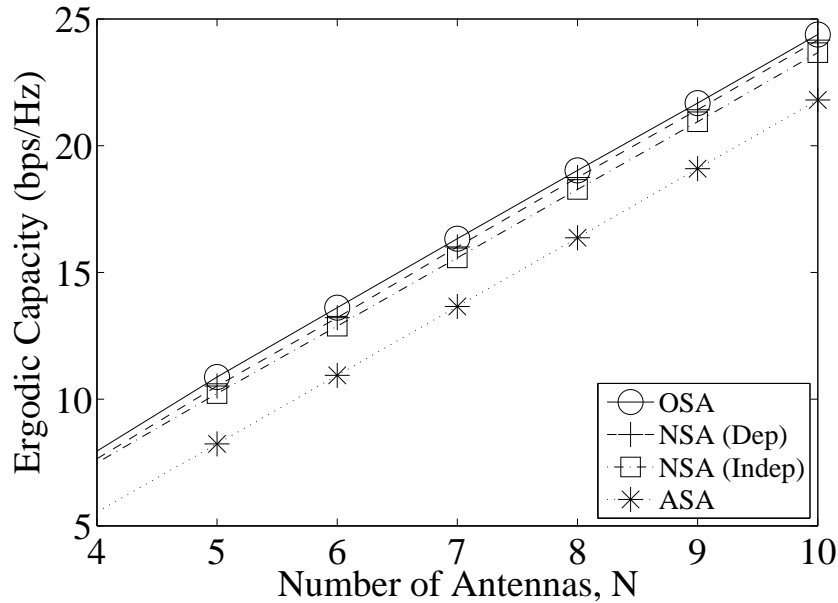


Figure 3.5: Comparison of TX-RX selection schemes for a  $(N + 2, N + 2)$  choose  $(N, N)$  system (SNR = 10dB).

encompasses all  $r \times t$  submatrices of  $\mathbf{H}$ . Similarly, ASA consists of a random  $r \times t$  submatrix drawn from the set  $\{\mathbf{S} \in \mathbf{H}\}$ . For NSA, the selection procedure might involve an independent concatenation: performing TX selection then RX selection or vice versa. Order can be important here, and we should intuitively select the dimension with the greatest choice (i.e. select RX antennas first if  $m > n$  and TX antennas first if  $m \leq n$ ) to increase diversity gains. Further improvements can be made if we perform the above selection iteratively, one row/column at a time from the dimension with the greatest choice after each step. This gives a small gain over the independent concatenation but at the increase of complexity. The relative performance of independent and dependent selection can be seen in Fig. 3.5. Note that the gain of joint over independent selection is only very slight.

A full joint approach to NSA would involve cycling through all possible  $r \times t$  submatrices and computing the norms. In terms of complexity this approach is similar to OSA and is not therefore considered.

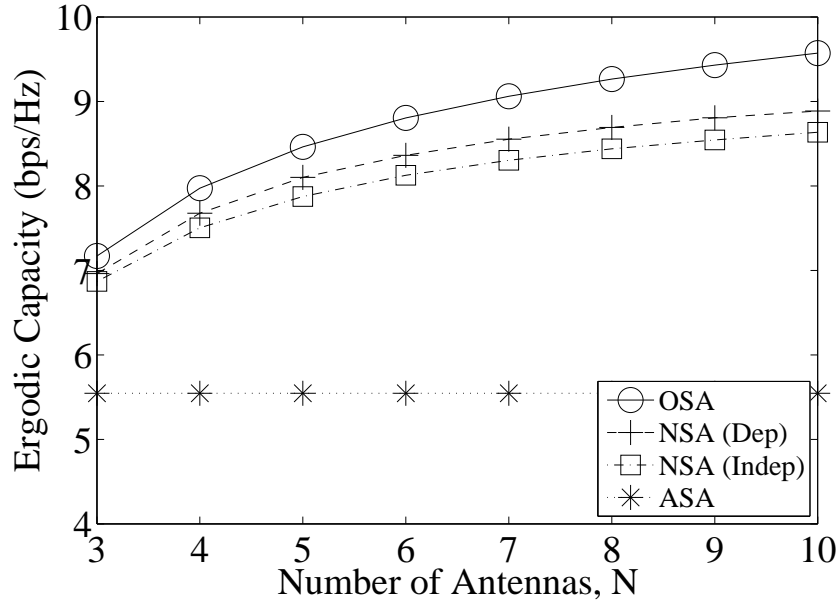


Figure 3.6: Comparison of TX-RX selection schemes for a  $(N, N)$  choose  $(2, 2)$  system (SNR = 10dB).

### 3.1.3 Poor Man's Waterfilling

The methods discussed so far are pure selection methods, where the power levels of each selected antenna are equal. In this section we introduce a novel power allocation algorithm called “*Poor Man's Waterfilling*” (PMWF). The name is derived from its greatly reduced complexity compared to the standard power allocation scheme, waterfilling. Consider a TX selection case where NSA is used and there are  $t$  selected antennas with norms  $P_1, P_2, \dots, P_t$ . The PMWF approach follows by allocating powers based on these norms. The resultant power to a column with norm  $P_j$  is the fraction,  $P_j / \sum_{k=1}^t P_k$  of the total power. After PMWF the norm of the vector including the column norms becomes  $tP_j^2 / \sum_{k=1}^t P_k$ . Figures 3.7 and 3.8 illustrate PMWF for various SNRs. In Sec. 3.2.6 PMWF is analyzed and it is shown that at low SNRs, NSA with PMWF can outperform the more computationally intensive OSA<sup>1</sup>.

<sup>1</sup>Note that PMWF will also benefit a system in which OSA has been used.

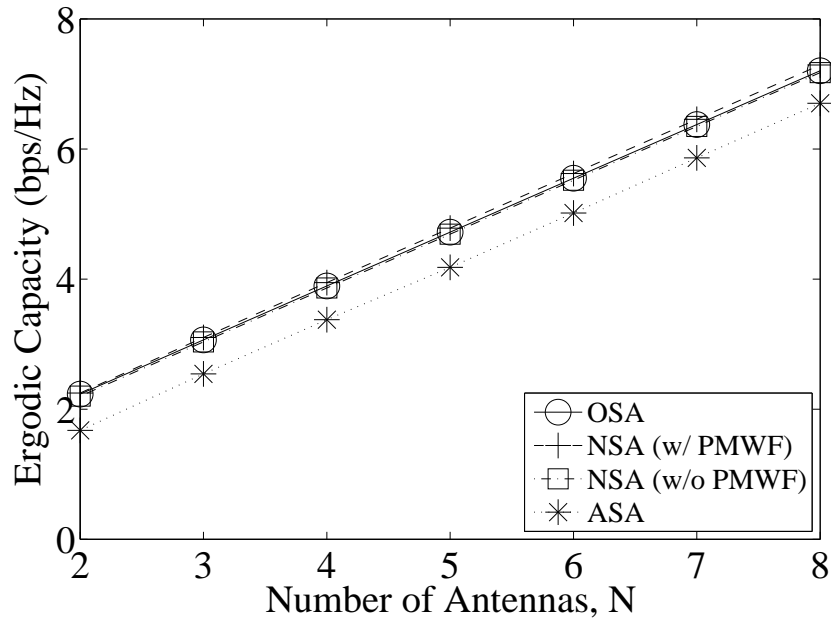


Figure 3.7: Comparison of selection schemes and PMWF for a  $(N, N + 2)$  choose  $(N, N)$  system (SNR = 0dB).

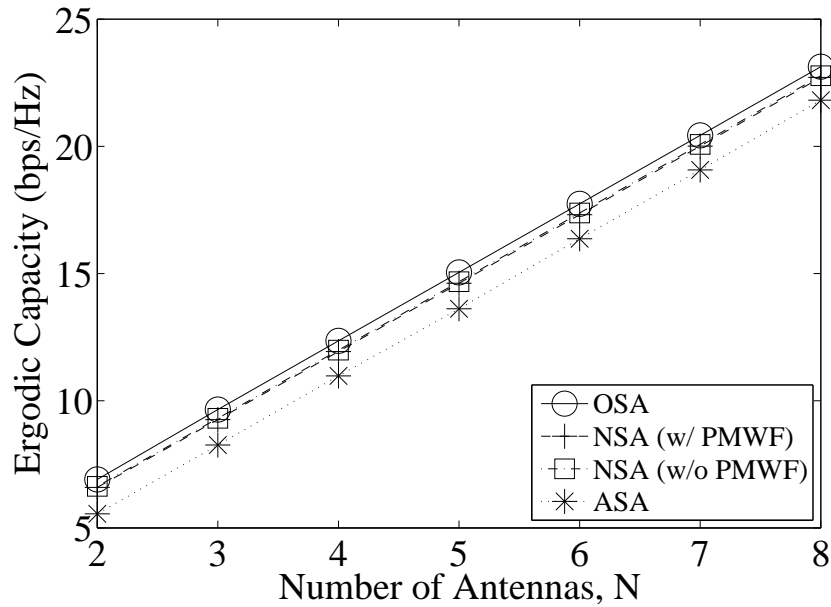


Figure 3.8: Comparison of selection schemes and PMWF for a  $(N, N + 2)$  choose  $(N, N)$  system (SNR = 10dB).

## 3.2 Algorithm Analysis

Of the three main algorithms, ASA is the easiest to evaluate as it leads to the standard capacity results [14]. OSA on the other hand is highly non-linear and difficult to analyze. At present there are no known approaches to computing the capacity of the OSA and simulations are required. Hence, in this section, we focus our analysis on the NSA. Our analysis leads to effective methods to calculate the gains made by norm-based antenna selection. The statistical analysis is based mainly on the fact that capacity, although exactly defined by the joint distributions of the elements of *all* possible submatrices of  $\mathbf{H}$ , is strongly affected by the moments of these elements.

### 3.2.1 NSA Analysis

In this analysis we examine the simplest MIMO Rayleigh fading system, the  $2 \times 2$  case. The channel matrix,  $\mathbf{H}$ , has column norms  $P_1^{(u)}$  and  $P_2^{(u)}$ . We assume for simplicity and without loss of generality that the first column  $[h_{11}, h_{21}]^T$  has the largest norm. We consider the selection of one transmit antenna, so that  $\mathbf{S} = [h_{11}, h_{21}]^T$ . Note that the elements of  $\mathbf{S}$  are no longer Gaussian, but instead are conditionally distributed due to the fact  $P_1^{(u)} > P_2^{(u)}$ . We can find the exact distribution of  $\mathbf{S}$  by computing the joint density function  $f(h_{11}, h_{21} | P_1^{(u)} > P_2^{(u)})$ . Due to the fact that  $P_1^{(u)} > P_2^{(u)}$  we can clearly see that the elements of  $\mathbf{S}$  have a larger variance than those of  $\mathbf{H}$ . The derivation of the PDF of the column of  $\mathbf{H}$  with the  $k^{\text{th}}$  largest norm (for the general  $m \times n$  case) is given in Appendix B. From this derivation we show that the columns retain their isotropic nature. This allows the replacement of the zero-mean complex Gaussian entries of  $\mathbf{H}$ , with zero-mean isotropic entries in  $\mathbf{S}$ .

From Appendix B it is straightforward to show that in the  $2 \times 2$  case the joint density of the largest column is flattened slightly compared to the Gaussian. This flattening is caused by the selection of large column norms pushing the probability away from zero. Overall this means that the elements of  $\mathbf{S}$

maintain the isotropic structure of those of  $\mathbf{H}$  but have increased variances. From this observation, a heuristic model for TX selection is that the scaling is a simple scaling of the original elements of  $\mathbf{H}$ . Given that column  $j$  of  $\mathbf{S}$  (ordered) has norm  $P_j$ , we propose to model  $\mathbf{S}$  as having elements with the same distribution as those of  $\mathbf{H}$  but with scaled variances,  $E\{P_j\}/m = \mu_j/m$ , instead of 1 for column  $j$ . This yields a simple power scaling due to the selection process. This approximation for  $\mathbf{S}$  is given by:

$$\mathbf{S} \approx \mathbf{V} \text{diag}(\sqrt{\mu_1}, \sqrt{\mu_2}, \dots, \sqrt{\mu_t})/\sqrt{m}, \quad (3.3)$$

where the  $m \times t$  matrix  $\mathbf{V}$  is statistically identical to a  $m \times t$  submatrix of  $\mathbf{H}$  picked at random. Note that  $\mathbf{V} \equiv \mathbf{S}_{ASA}$ . Defining  $\mathbf{M} = \text{diag}(\mu_1, \mu_2, \dots, \mu_t)/m$  and using equation (3.3) this leads to the approximate capacity:

$$C_{\text{sel,pa}} \approx \log_2 \left| \mathbf{I}_r + \frac{\text{SNR}}{t} \mathbf{V} \mathbf{M} \mathbf{V}^\dagger \right| \text{ bps/Hz}, \quad (3.4)$$

where the subscript, “pa”, denotes the fact that the diagonal matrix,  $\mathbf{M}$ , can be interpreted as performing power allocation over the antennas. Thus, we refer to this as the Power Allocation (PA) approximation. We can find a further approximation to (3.4) by replacing the power allocation matrix ( $\mathbf{M}$ ) with a single power scaling factor,

$$P_{\text{av}} = \frac{1}{mt} \sum_{j=1}^t \mu_j. \quad (3.5)$$

This leads to the capacity:

$$C_{\text{sel,ps}} \approx \log_2 \left| \mathbf{I}_r + P_{\text{av}} \frac{\text{SNR}}{t} \mathbf{V} \mathbf{V}^\dagger \right| \text{ bps/Hz}, \quad (3.6)$$

where the subscript, “ps”, refers to the power scaling provided by the SNR inflation factor,  $P_{\text{av}}$ . This is a very simple approximation to NSA, suggesting that it can be interpreted as a simple power scaling effect. This scaling is thus

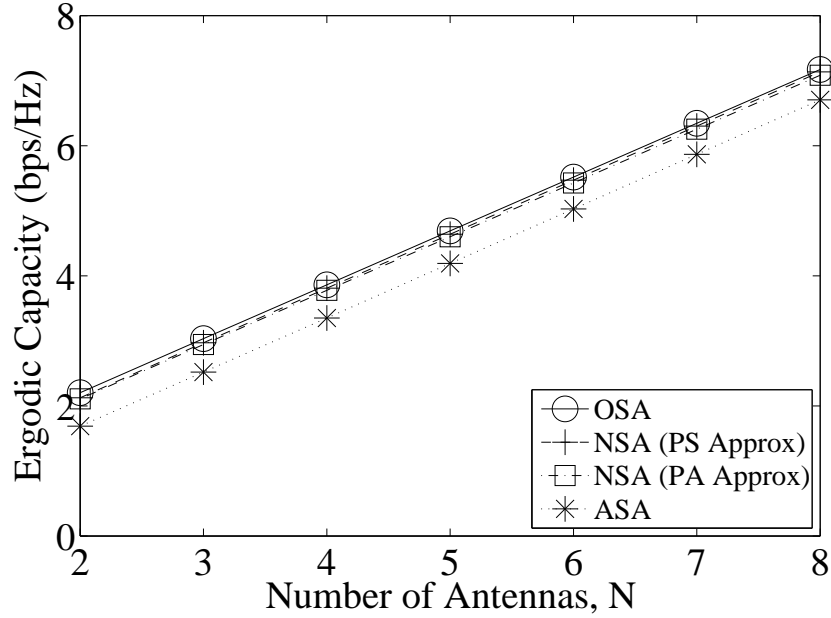


Figure 3.9: Comparison of NSA and approximations for a  $(N, N + 2)$  choose  $(N, N)$  system (SNR = 0dB).

denoted as the Power Scaling (PS) approximation. Implementations of both the PA and PS methods require both a knowledge of  $\mu_1, \mu_2, \dots, \mu_t$  and the statistics of (3.4) and (3.6) for the particular channel. For all the channels studied in this chapter the mean capacity is known [14, 48, 64]. Figures 3.9 and 3.10 show NSA and its approximations at SNR = 0dB and SNR = 10dB. Note that both the PA and PS approximations are very accurate, and PS performs at least as well as PA for all cases. Thus, since PS is a simpler approximation, this approach is the focus of further results.

We now discuss the relevant capacity results for a variety of channels.

### 3.2.2 Rayleigh Flat Fading Channels

The Rayleigh channel defined earlier in Sec. 2.6.1 has complex Gaussian channel matrix elements  $h_{ij}$ . Hence, the unordered column norm powers,  $P_j^{(u)}$ , are i.i.d. complex  $\chi^2$  distributed with  $m$  degrees of freedom, and a mean value of

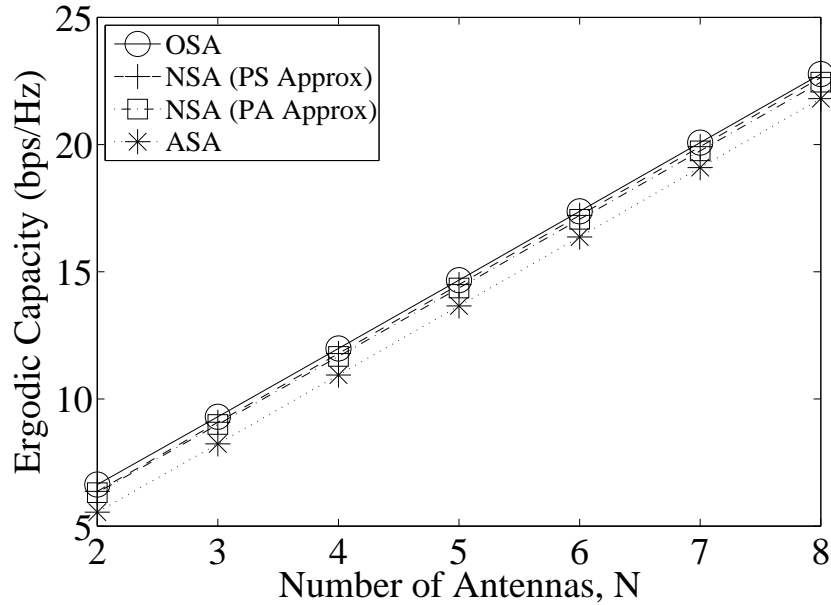


Figure 3.10: Comparison of NSA and approximations for a  $(N, N + 2)$  choose  $(N, N)$  system (SNR = 10dB).

$E\{P_j^{(w)}\} = m$ . The PDF and CDF of the complex  $\chi^2$  distribution are respectively [65]:

$$f_\chi(x; m) = \frac{x^{m-1}}{(m-1)!} \exp(-x) \quad (3.7)$$

$$F_\chi(x; m) = 1 - \exp(-x) \sum_{k=0}^{m-1} \frac{x^k}{k!}. \quad (3.8)$$

Some simple order statistics results are required to calculate the moments of the ordered column norms. In general the  $\ell^{\text{th}}$  moment of the  $j^{\text{th}}$  order statistic is [53]

$$E\{P_j^\ell\} = \frac{n!}{(n-j)!(j-1)!} \int_{-\infty}^{\infty} x^\ell F(x)^{n-j} [1 - F(x)]^{j-1} f(x) dx, \quad (3.9)$$

where  $f(\cdot)$  and  $F(\cdot)$  are the PDF and CDF respectively of the unordered variables. Substituting (3.7) and (3.8) into (3.9) leads to [66, p. 38]:

$$E\{P_j^\ell\} = \frac{n!}{(n-j)!(j-1)!(m-1)!} \sum_{r=0}^{n-j} (-1)^r \binom{n-j}{r} \quad (3.10)$$

$$\times \sum_{s=0}^{(m-1)(j+r-1)} \frac{c_s(j+r-1)(\ell+m+s-1)!}{(j+r)^{\ell+m+s}}, \quad (3.11)$$

where  $c_s(N)$  is the coefficient of  $x^s$  in  $(\sum_{v=0}^{m-1} \frac{x^v}{v!})^N$ .

Another simpler method for computing approximations to  $\mu_j$  and generally to  $E\{P_j^\ell\}$  is based on the well-known quantile approximations [53, 66]. These are of the form,  $\mu_j \approx F^{-1}\left(\frac{n+1-j-\alpha}{n-\beta}\right)$ , where  $F(\cdot)$  is the CDF of each column norm. However, for these approximations to be accurate, especially when  $j = 1$ , the correction factors  $\alpha$  and  $\beta$  need to be chosen differently for each value of  $j$  and  $n$ . Since simulations show that this approximation is not particularly accurate and requires fine tuning of  $\alpha$  and  $\beta$  for every pair of  $j$  and  $n$ , we prefer to use the exact results.

Using (3.5) and (3.11) the PS factor,  $P_{av}$ , can be computed for any system size. Sample results are given in Tables 3.1–3.3. The value of  $P_{av}$  gives a good indication of the gains offered by transmit selection in terms of an equivalent scaled SNR.

		$n$				
		2	3	4	5	6
$t$	1	1.375	1.607	1.774	1.904	2.011
	2		1.259	1.439	1.578	1.690
	3			1.199	1.347	1.465
	4				1.162	1.288
	5					1.137

Table 3.1:  $P_{av}$  Values for Various  $n$  and  $t$  ( $m = 2$ )

		$n$				
		2	3	4	5	6
$t$	1	1.313	1.499	1.631	1.733	1.815
	2		1.221	1.367	1.478	1.567
	3			1.170	1.293	1.389
	4				1.140	1.245
	5					1.119

Table 3.2:  $P_{av}$  Values for Various  $n$  and  $t$  ( $m = 3$ )

		$n$				
		2	3	4	5	6
$t$	1	1.274	1.433	1.544	1.630	1.700
	2		1.194	1.321	1.416	1.491
	3			1.151	1.258	1.340
	4				1.125	1.217
	5					1.107

Table 3.3:  $P_{av}$  Values for Various  $n$  and  $t$  ( $m = 4$ )

Tables 3.1-3.3 show a few key points:

- The effective SNR gain is increased when the number of redundant antennas ( $n - t$ ) is increased.
- The effective SNR gain decreases with increasing  $m, n$ . This is due to the fact that for a particular  $n - t$ , the absolute gain in capacity is very similar no matter what the original capacity. With increasing  $m, n$ , the ASA capacity increases, and this reduces the relative gain of the redundant antennas, thus reducing the effective SNR gain.
- The effective SNR gains range from 10% to 100% for the given values. For example, to give an effective SNR increase of 50%, systems such as 4 pick 2 or 6 pick 3 could be used if  $m = 2$ . For  $m = 3$ , 3 pick 1 and 5 pick 2 would also give a similar gain. For  $m = 4$ , 4 pick 1 and 6 pick 2 would also give approximately 50% increases in effective SNR.

### 3.2.3 Semi-Correlated Rayleigh Channels

Consider a semi-correlated (SC) Rayleigh channel matrix,  $\mathbf{H}_{SC}$ , given by,

$$\mathbf{H}_{sc} = \mathbf{R}^{1/2} \mathbf{H}, \quad (3.12)$$

where  $\mathbf{R}^{1/2}$  is the square root of the channel spatial correlation matrix at the receiver. The unordered column norms of  $\mathbf{H}_{sc}$  are now  $P_j^{(u)} = h_j^\dagger \mathbf{R} h_j$ ,  $j = 1, \dots, n$  where  $h_j$  is the  $j^{\text{th}}$  column of  $\mathbf{H}$  in (3.12). This is a well known quadratic form as described in [67] and can be rewritten as  $P_j^{(u)} = \sum_{i=1}^m \lambda_i |h_{ij}|^2$  where  $\lambda_i, i = 1, \dots, m$  is the  $i^{\text{th}}$  eigenvalue of  $\mathbf{R}$ . The PDF and CDF of  $P_j^{(u)}$

are, respectively,

$$f(x) = \sum_{j=1}^m \frac{b_j}{\lambda_j} \exp\left(-\frac{x}{\lambda_j}\right), \quad (3.13)$$

$$F(x) = \sum_{j=1}^m b_j \left[1 - \exp\left(-\frac{x}{\lambda_j}\right)\right], \quad (3.14)$$

where

$$b_j = \lambda_j^{m-1} \prod_{k=1, k \neq j}^m (\lambda_j - \lambda_k)^{-1}.$$

We can easily extend the capacity approximations of (3.4) and (3.6) to this case. Note that  $\mathbf{V}$  is now semi-correlated and can be defined by  $\mathbf{V} = \mathbf{R}^{1/2}\mathbf{U}$  where  $\mathbf{U}$  is an i.i.d. Rayleigh channel matrix. We can rewrite the capacity approximations as:

$$C_{\text{sel,pa}} \approx \log_2 \left| \mathbf{I}_r + \frac{\text{SNR}}{t} \mathbf{R}^{1/2} \mathbf{U} \mathbf{M} \mathbf{U}^\dagger \mathbf{R}^{1/2} \right| \text{ bps/Hz} \quad (3.15)$$

$$C_{\text{sel,ps}} \approx \log_2 \left| \mathbf{I}_r + P_{\text{av}} \frac{\text{SNR}}{t} \mathbf{R}^{1/2} \mathbf{U} \mathbf{U}^\dagger \mathbf{R}^{1/2} \right| \text{ bps/Hz.} \quad (3.16)$$

Again we can derive the values of  $\mu_1, \dots, \mu_t$  and hence, using order statistics, can find  $P_{\text{av}}$ . Note that (3.9) and (3.5) are applicable to this situation by substituting the  $\chi^2$  distribution with the quadratic form distribution defined in (3.13) and (3.14). From this we can derive a closed-form expression for  $\mu_j = \text{E}\{P_j\}$ . Firstly, note that the density of  $P_j$  is given by [66]

$$f_{P_j}(x) = \frac{n!}{(j-1)!(n-j)!} F(x)^{n-j} [1 - F(x)]^{j-1} f(x). \quad (3.17)$$

Substituting  $f(x)$  and  $F(x)$  from (3.13) and (3.14) into (3.17) we write:

$$\begin{aligned} \mu_j = \frac{n!}{(j-1)!(n-j)!} \int_0^\infty x \left(1 - \sum_{t=1}^m b_t e^{-x/\lambda_t}\right)^{n-j} \left(\sum_{r=1}^m b_r e^{-x/\lambda_r}\right)^{j-1} \\ \times \sum_{s=1}^m \frac{b_s}{\lambda_s} e^{-x/\lambda_s} dx. \end{aligned} \quad (3.18)$$

Expanding the binomial term in (3.18), we finally have

$$\begin{aligned}
\mu_j &= \frac{n!}{(j-1)!(n-j)!} \int_0^\infty x \sum_{t=0}^{n-j} (-1)^t \binom{n-j}{t} \left( \sum_{r=1}^m b_r e^{-x/\lambda_r} \right)^{t+j-1} \sum_{s=1}^m \frac{b_s}{\lambda_s} e^{-x/\lambda_s} dx \\
&= \frac{n!}{(j-1)!(n-j)!} \sum_{t=0}^{n-j} (-1)^t \binom{n-j}{t} \sum_{K(t+j-1)} c_{K(t+j-1)} \\
&\quad \times \sum_{s=1}^m \frac{b_s}{\lambda_s} \int_0^\infty x e^{-(d_{K(t+j-1)}+1/\lambda_s)x} dx \\
&= \frac{n!}{(j-1)!(n-j)!} \sum_{t=0}^{n-j} (-1)^t \binom{n-j}{t} \sum_{K(t+j-1)} c_{K(t+j-1)} \sum_{s=1}^m \frac{b_s}{\lambda_s} \left( d_{K(t+j-1)} + \frac{1}{\lambda_s} \right)^{-2},
\end{aligned} \tag{3.19}$$

where

$$\left( \sum_{r=1}^m b_r e^{-x/\lambda_r} \right)^L = \sum_{K(L)} c_{K(L)} \exp \{ -d_{K(L)} x \},$$

with

$$c_{K(L)} = L! \prod_{i=1}^m \frac{b_i^{k_i}}{k_i!}, \quad d_{K(L)} = \sum_{i=1}^m \frac{k_i}{\lambda_i}$$

and the sum is over all partitions of  $L$  (i.e.,  $K(L) = (k_1, \dots, k_m)$  where  $\sum_{i=1}^m k_i = m$ ).

Figures 3.11 and 3.12 show that the NSA algorithm is a good approximation to the optimal capacity, even under correlated channel conditions. For simulation purposes, we use an exponential correlation structure to model SC Rayleigh channels. This gives a receiver correlation matrix,  $\mathbf{R}$ , with elements given by [68]

$$r_{ij} = \begin{cases} \varrho^{j-i} & i \leq j \\ r_{ji}^\dagger & i > j \end{cases}, \quad |\varrho| \leq 1, \tag{3.20}$$

where  $\varrho$  is the (complex) correlation coefficient between adjacent receive antennas. In our simulations, we used the value of  $\varrho = 0.8$ .

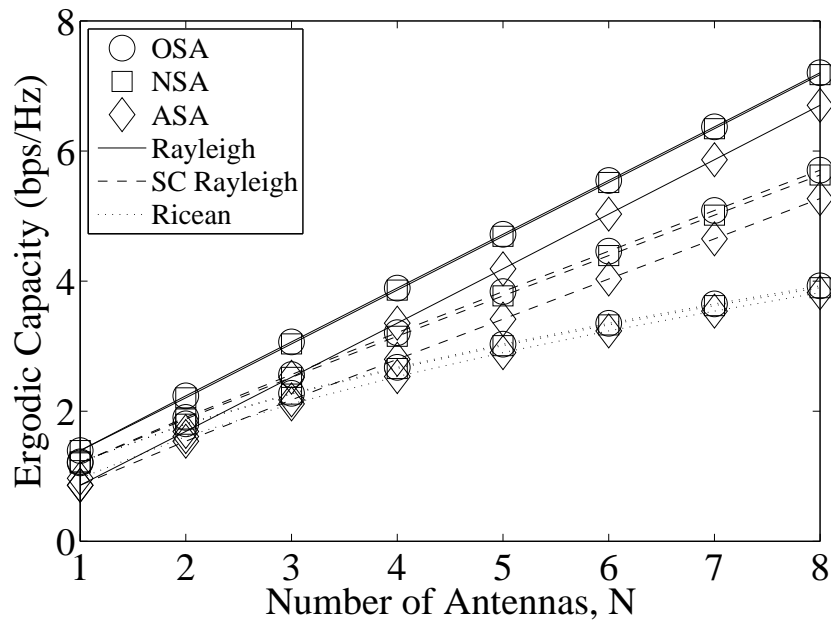


Figure 3.11: Comparison of selection algorithms over different channels for a  $(N, N + 2)$  choose  $(N, N)$  system (SNR = 0dB).

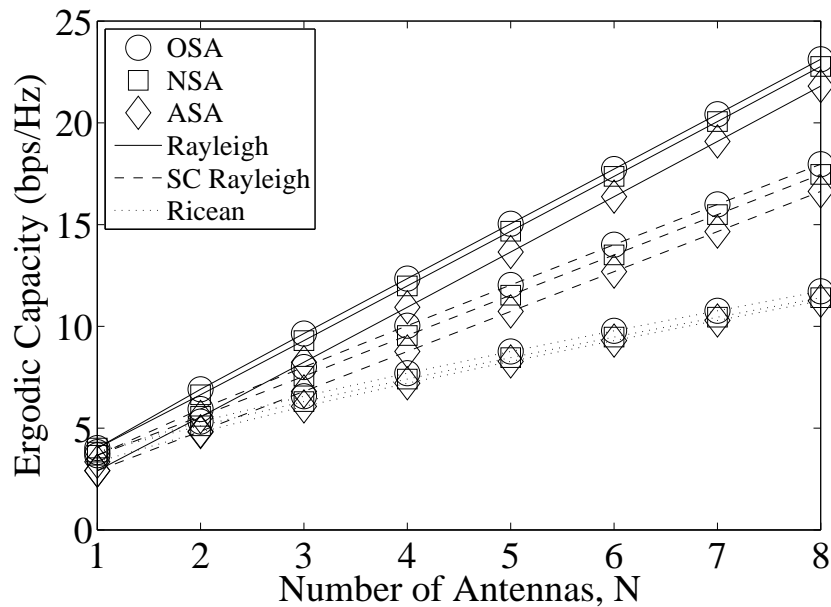


Figure 3.12: Comparison of selection algorithms over different channels for a  $(N, N + 2)$  choose  $(N, N)$  system (SNR = 10dB).

### 3.2.4 Ricean Channels

An i.i.d. Ricean channel can be simply expressed as the weighted sum of a LOS channel and a Rayleigh flat-fading channel as follows:

$$\mathbf{H}_{\text{rice}} = a \mathbf{H}_{\text{LOS}} + b \mathbf{H}, \quad (3.21)$$

where  $a^2 + b^2 = 1$  and the entries of  $\mathbf{H}_{\text{LOS}}$  and  $\mathbf{H}$  have unit variance. If we assume the common model of a unit rank  $\mathbf{H}_{\text{LOS}}$  matrix, then we can assume without loss of generality that the elements of  $\mathbf{H}_{\text{LOS}}$  are all unity. This leads to the  $j^{\text{th}}$  unordered column norm of  $\mathbf{H}_{\text{rice}}$  being given by  $P_j^{(u)} = [a \mathbf{1} + b \mathbf{h}_j]^\dagger [a \mathbf{1} + b \mathbf{h}_j]$ , where  $\mathbf{1} = [1, \dots, 1]^T$  and  $\mathbf{h}_j$  is again the  $j$ -th column of the i.i.d. Rayleigh matrix  $\mathbf{H}$ . This is a non-central quadratic form with PDF and CDF respectively given by [67]

$$f(x) = \frac{1}{b^2} \left( \frac{2x}{b^2 \delta} \right)^{(m-1)/2} I_{m-1} \left( \frac{2x \sqrt{\delta}}{b^2} \right) \times \exp \left[ - \left( \frac{2x}{b^2} + \delta \right) / 2 \right] \quad (3.22)$$

$$F(x) = \exp \left( -\frac{\delta}{2} \right) \sum_{j=0}^{\infty} \frac{(\delta/2)^j}{j! (m+j-1)! 2^{m+j}} \times \int_0^{2x/b^2} u^{m+j-1} \exp \left( -\frac{u}{2} \right) du, \quad (3.23)$$

where  $\delta = 2m a^2/b^2$  and  $I_k(\cdot)$  is a modified Bessel function. Although the integral in the CDF can be expressed as a finite sum there is no closed-form solution that avoids either numerical integration or an infinite series. To find the means,  $\mu_1, \dots, \mu_t$ , we can use (3.9) with (3.3) and (3.6) to compute the corresponding capacity approximations. Figures 3.11 and 3.12 show that the NSA algorithm is a good approximation to the optimal capacity, even under Ricean channel conditions. Note that the simulated Ricean channel has K-factor  $K = 10\text{dB}$  and is defined in Sec. 2.6.2.

### 3.2.5 Transmitter-Receiver Antenna Selection

In Sec. 3.1.2 we showed that TX selection algorithms can be easily extended to RX selection and TX-RX selection. Using the analysis in Sec. 3.2.1 for the TX-RX selection case leads to two power scaling factors, one for TX selection  $P_{av,t}$  and the other for RX selection  $P_{av,r}$ . If joint selection is performed, the results from Sec. 3.2.1 and Sec. 3.2.4 can be leveraged to approximate the capacity. Assuming TX selection occurs first, the selected matrix  $\mathbf{S}_t \approx \mathbf{V}\mathbf{M}^{1/2}$  is calculated using (3.3). For an i.i.d. Rayleigh channel, the resultant row (RX) selection problem is exactly the same as the column (TX) selection problem for the semi-correlated case. This is due to the fact that the forms of the rows of  $\mathbf{S}_t$  are equivalent to that of the columns of  $\mathbf{H}_{sc}$  in (3.12). Hence, both (3.4) and (3.6) can be evaluated for the i.i.d. Rayleigh case.

The capacity of TX-RX selected SC Rayleigh and i.i.d. Ricean channels can also be approximated in the form of (3.4) by using similar methods. Thus, we can use the SNR scaling approximation of (3.6) effectively in TX-RX selection. Using TX selection leads to the submatrix  $\mathbf{S}_t \approx P_{av,t}^{1/2}\mathbf{V}$ . Following with RX selection now yields the submatrix  $\mathbf{S} \approx P_{av,r}^{1/2}\mathbf{S}_t \approx P_{av,r}^{1/2}P_{av,t}^{1/2}\mathbf{V}$ . This result now allows us to use (3.6) with the new power scaling factor,  $P_{av} = P_{av,r}P_{av,t}$ .

### 3.2.6 Poor Man's Waterfilling

After the initial selection techniques, an algorithm like conventional waterfilling, where the transmit power is allocated over the eigenmodes of the selected channel, can be used. However, this can be computationally intensive, and thus we propose a simpler algorithm to achieve suboptimal gains but at a highly reduced complexity level. PMWF uses the values of the column norms,  $P_j$ , to allocate power to the system as described in Sec. 3.1.3. As with standard antenna selection, the effects of this procedure can be simply approximated by a power scaling factor. After TX selection has been performed, column  $j$  in  $\mathbf{S}$  has norm  $P_j$ . Under PMWF this norm is scaled by  $tP_j / \sum_{k=1}^t P_k$  and

the resulting selection matrix is denoted  $\mathbf{S}_{\text{pmwf}}$ . The total norm of  $\mathbf{S}_{\text{pmwf}}$  is  $\|\mathbf{S}_{\text{pmwf}}\|^2 = \sum_{j=1}^t tP_j^2 / \sum_{k=1}^t P_k$ . The average modulus squared value of an element of  $\mathbf{S}_{\text{pmwf}}$  is  $\|\mathbf{S}_{\text{pmwf}}\|^2 / (mt)$ . The mean of this gives the power scaling factor:

$$P_{\text{av,pmwf}} = \frac{1}{m} \mathbb{E} \left\{ \frac{\sum_{j=1}^t P_j^2}{\sum_{k=1}^t P_k} \right\}. \quad (3.24)$$

For TX-RX selection using PMWF (for TX-selection) the power scaling factor is now  $P_{\text{av}} = P_{\text{av},r} P_{\text{av,pmwf}}$ . Exact evaluation of (3.24) is very difficult as the PDF of a sum of  $\chi^2$  order statistics is extremely complex (see for example, [69]). However, the so-called ‘‘delta method’’ can be employed with good effect [70]. Note that (3.24) involves the mean of a ratio of 2 random variables. The delta method approach for this scenario is based on the Taylor series expansion

$$\mathbb{E} \left( \frac{X}{Y} \right) \triangleq \mathbb{E}[g(X, Y)] = \mathbb{E} \left[ \sum_{d,f} \frac{g^{(d,f)}(\mu_X, \mu_Y)}{d! f!} (X - \mu_X)^d (Y - \mu_Y)^f \right] \quad (3.25)$$

where

$$g^{(d,f)}(\mu_X, \mu_Y) = \left. \frac{\partial^{d+f}}{\partial x^d \partial y^f} g(x, y) \right|_{x=\mu_X, y=\mu_Y},$$

$\mu_X = \mathbb{E}(X)$ ,  $\mu_Y = \mathbb{E}(Y)$  and  $\mathbb{E}[g(X, Y)]$  is usually approximated by only the first few terms. Taking terms up to order two ( $d + f \leq 2$ ), we find:

$$\mathbb{E} \left( \frac{X}{Y} \right) \approx \frac{\mu_X}{\mu_Y} + \frac{\mu_X}{\mu_Y^3} \text{var}(Y) - \frac{\mathbb{E}[(X - \mu_X)(Y - \mu_Y)]}{\mu_Y^2} = \frac{\mu_X \mathbb{E}(Y^2)}{\mu_Y^3} - \frac{\text{cov}(X, Y)}{\mu_Y^2}. \quad (3.26)$$

Comparing (3.24) with (3.26) we need to compute the following variables:  $\mu_X = \sum_{j=1}^t \mathbb{E}(P_j^2)$ ,  $\mu_Y = \sum_{j=1}^t \mathbb{E}(P_j)$ ,  $\mathbb{E}(Y^2) = \sum_{j=1}^t \sum_{k=1}^t \mathbb{E}(P_j P_k)$ , and  $\text{cov}(X, Y) = \sum_{j=1}^t \sum_{k=1}^t \mathbb{E}(P_j^2 P_k) - \mu_X \mu_Y$ . However, from (3.11), the components  $\mathbb{E}(P_j)$ ,  $\mathbb{E}(P_j^2)$ , and  $\mathbb{E}(P_j^3)$  are already known for the i.i.d. Rayleigh fading case. To compute (3.26), we need to know the variables  $\mathbb{E}(P_j P_k)$  and  $\mathbb{E}(P_j^2 P_k)$  as well. For the Rayleigh fading case we can find these from  $\mathbb{E}(P_i^s P_j^q)$ . Without loss of generality, we set  $i > j$  so that  $0 < W \triangleq P_i < Z \triangleq P_j < \infty$ . Thus

the joint density of  $(W, Z)$ , or  $(P_i, P_j)$ , is [66]:

$$f_{W,Z}(w, z) = \frac{n!}{(n-i)!(i-j-1)!(j-1)!} F(w)^{n-i} [F(z) - F(w)]^{i-j-1} \times [1 - F(z)]^{j-1} f(w) f(z). \quad (3.27)$$

For the Rayleigh case, substituting  $f(w)$  and  $F(w)$ , using (3.7) and (3.8), into (3.27), we find

$$f_{W,Z}(w, z) = \Delta \left( 1 - e^{-w} \sum_{k=0}^{m-1} \frac{w^k}{k!} \right)^{n-i} \left( e^{-w} \sum_{h=0}^{m-1} \frac{w^h}{h!} - e^{-z} \sum_{\ell=0}^{m-1} \frac{z^\ell}{\ell!} \right)^{i-j-1} \times \left( e^{-z} \sum_{u=0}^{m-1} \frac{z^u}{u!} \right)^{j-1} \frac{w^{m-1} e^{-w}}{(m-1)!} \frac{z^{m-1} e^{-z}}{(m-1)!}, \quad (3.28)$$

where  $\Delta = n! / [(n-i)!(i-j-1)!(j-1)!]$ . Expanding the binomial terms, the first two bracketed terms in (3.28) yield

$$f_{W,Z}(w, z) = \frac{\Delta}{[(m-1)!]^2} \sum_{k=0}^{n-i} \sum_{\ell=0}^{i-j-1} (-1)^{k+\ell} \binom{n-i}{k} \binom{i-j-1}{\ell} w^{m-1} z^{m-1} \times \left( \sum_{h=0}^{m-1} \frac{w^h}{h!} \right)^{k+i-j-\ell-1} \left( \sum_{u=0}^{m-1} \frac{z^u}{u!} \right)^{\ell+j-1} e^{-(k+i-j-\ell)w} e^{-(\ell+j)z}. \quad (3.29)$$

Expanding the two power series in (3.29), we finally have

$$f_{W,Z}(w, z) = \frac{\Delta}{[(m-1)!]^2} \sum_{k=0}^{n-i} \sum_{\ell=0}^{i-j-1} (-1)^{k+\ell} \binom{n-i}{k} \binom{i-j-1}{\ell} \times \sum_{h=0}^{N(i,j,k,\ell,m)} c_h(N(i,j,k,\ell,m)) \times \sum_{u=0}^{N(j,\ell,m)} c_u(N(j,\ell,m)) w^{m+h-1} z^{m+u-1} e^{-(k+i-j-\ell)w} e^{-(\ell+j)z}, \quad (3.30)$$

where  $N(i, j, k, \ell, m) = (m - 1)(k + i - j - \ell - 1)$ ,  $N(j, \ell, m) = (m - 1)(\ell + j - 1)$  and  $c_s(N)$  is defined after (3.11). The calculation of  $E\{W^s Z^q\}$  is now straightforward using the result

$$\int_0^\infty \int_0^\infty w^a z^b e^{-cw} e^{-gz} dw dz = g^{-(b+1)} \sum_{v=0}^b \frac{b!}{(b-v)!} \frac{(a+b-v)!}{(c+1)^{a+b-v+1}},$$

where  $a, b \in \mathbb{Z}^+$ . Finally, we write the joint moment as

$$\begin{aligned} E\{P_i^s P_j^u\} &= \frac{\Delta}{[(m-1)!]^2} \sum_{k=0}^{n-i} \sum_{\ell=0}^{i-j-1} (-1)^{k+\ell} \binom{n-i}{k} \binom{i-j-1}{\ell} \\ &\times \sum_{h=0}^{N(i,j,k,\ell,m)} c_h(N(i, j, k, \ell, m)) \sum_{u=0}^{N(j,\ell,m)} c_u(N(j, \ell, m)) \\ &\times \sum_{v=0}^{m+r+q-1} \frac{(m+u+q-1)!}{(m+u+q-1-v)!} \\ &\times \frac{(2m+u+h+s+q-2-v)!}{(k+i-j-\ell+1)^{2m+u+h+s+q} (\ell+j)^{m+u+q}}. \end{aligned} \quad (3.31)$$

This derivation is already complicated for the i.i.d. Rayleigh case. The equivalent calculation for the other channel models is possible in principle but the mathematics becomes extremely cumbersome and is therefore of limited use. Hence, these results are omitted from the thesis.

Figures 3.13 and 3.14 highlight the performance of PMWF relative to NSA at SNR values of 0dB and 10dB respectively. In the 0dB SNR case (Fig. 3.13) NSA with PMWF outperforms OSA. In addition the PS approximation is excellent for the mixture of NSA and PMWF and also provides an accurate approximation to OSA. Note that NSA with PMWF outperforms OSA only for low SNR, but for higher SNRs, OSA becomes superior again, although the difference is small. This comparison is shown in more detail in Fig. 3.15 for an i.i.d. Rayleigh channel. We observe that as the SNR varies from -10dB to 10dB the percentage improvement of OSA over NSA is at most 4%. Also, NSA with PMWF offers improvements over OSA of up to about 6.5% at -10dB. These

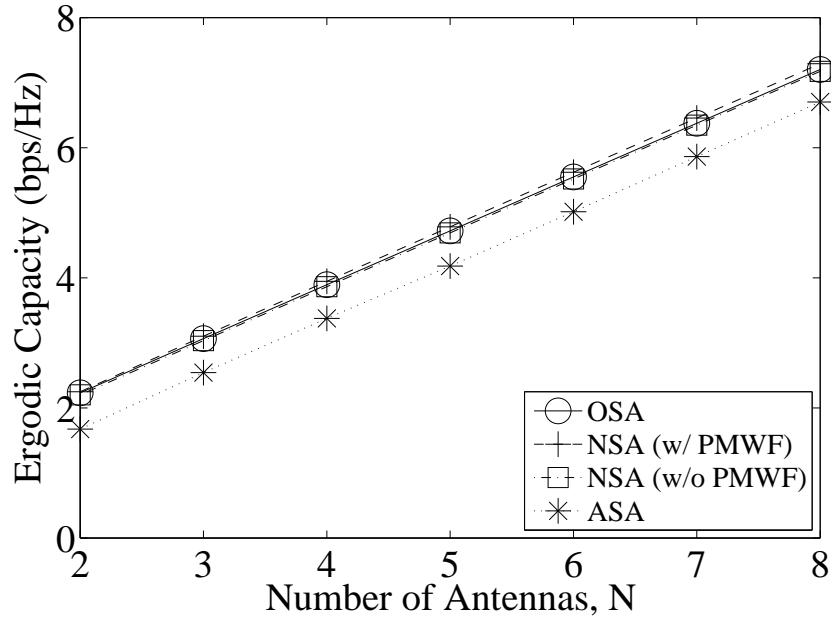


Figure 3.13: Comparison of NSA and approximations using PMWF for a  $(N, N + 2)$  system (SNR = 0dB).

gains reduce with increasing SNR and at 10dB OSA has a slight superiority (see Sec. 4.5.3 for more discussion on proportional power algorithms). Overall, the performance of the simple norm-based approaches compare very favorably with OSA.

### 3.3 Effects of Imperfect Channel State Information

In this section we cover the impact of imperfect CSI on TX selection and the power scaling approach. Taking column  $j$  of (2.22), we can write

$$h_j = \rho \hat{h}_j + \sqrt{1 - \rho^2} e_j, \quad (3.32)$$

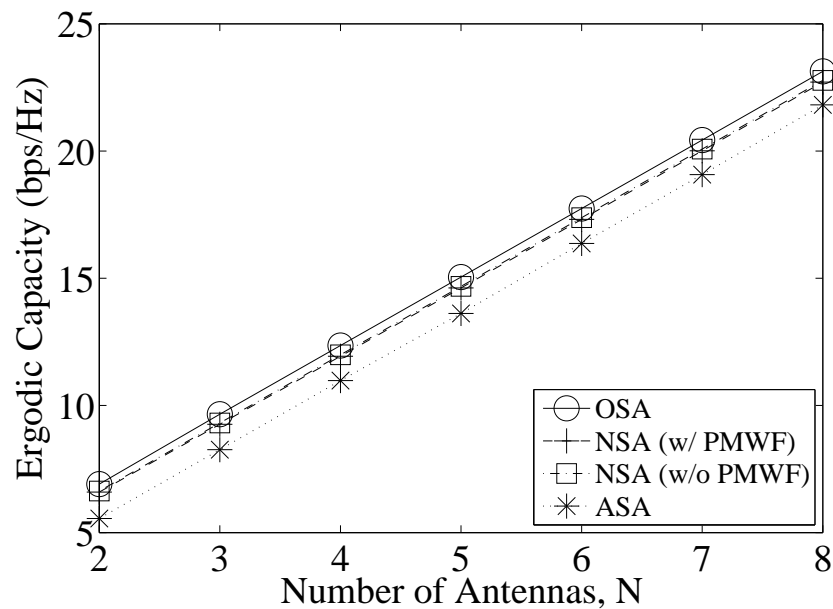


Figure 3.14: Comparison of NSA and approximations using PMWF for a  $(N, N+2)$  choose  $(N, N)$  system ( $\text{SNR} = 10\text{dB}$ ).

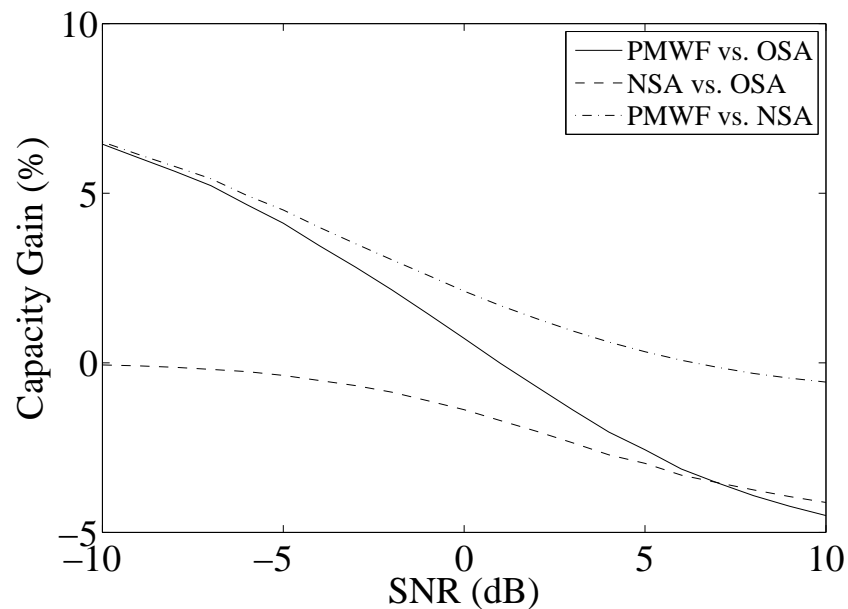


Figure 3.15: Percentage capacity improvement of PMWF, NSA and OSA relative to each other in a  $(2, 4)$  choose  $(2, 2)$  system for an i.i.d. Rayleigh channel.

with  $\mathbf{h}_j$ ,  $\hat{\mathbf{h}}_j$  and  $\mathbf{e}_j$  being the  $j^{\text{th}}$  columns of  $\mathbf{H}$ ,  $\hat{\mathbf{H}}$ ,  $\mathbf{E}$  respectively. Taking the column norms of (3.32), we have

$$P_j^{(u)} = \rho^2 \hat{P}_j^{(u)} + (1 - \rho^2) \|\mathbf{e}_j\|^2 + \Delta \quad (3.33)$$

where  $\Delta$  is the cross product term given by

$$\Delta = \rho \sqrt{1 - \rho^2} \left( \hat{\mathbf{h}}_j^\dagger \mathbf{e}_j + \mathbf{e}_j^\dagger \hat{\mathbf{h}}_j \right). \quad (3.34)$$

Since  $E\{\hat{P}_j^{(u)}\} = E\{\|\mathbf{e}_j\|^2\} = m$ , we can rewrite (3.33) as

$$P_j^{(u)} = \rho^2 (\hat{P}_j^{(u)} - m) + m + \epsilon_j \quad (3.35)$$

where  $\epsilon_j = \Delta + (1 - \rho^2)(\|\mathbf{e}_j\|^2 - m)$ . In the process of TX selection columns of  $\mathbf{H}$  are selected on the basis of the measurements of  $\hat{\mathbf{H}}$ . This leads to the area of order statistics called concomitants [53]. Note that (3.35) is simple and linear and thus when  $\epsilon_j$  is independent of  $\hat{P}_j^{(u)}$  the following relationship holds:

$$\mu_{[j]} = \rho^2 (\mu_j - m) + m, \quad (3.36)$$

where  $\mu_j$  is as before but  $\mu_{[j]}$  represents the mean norm of column  $j$  of  $\mathbf{H}$  selected on the basis of  $\hat{\mathbf{H}}$ . Note that in the TX selection scenarios covered,  $\epsilon_j$  is uncorrelated with  $\hat{P}_j^{(u)}$  but not independent. This can be seen from (3.34). The cross product  $\Delta$  contains  $\hat{\mathbf{h}}_j$  and  $\hat{P}_j^{(u)}$ . Hence, it is a function of  $\hat{\mathbf{h}}_j$ . Parameters  $\Delta$  and  $\hat{P}_j^{(u)}$  are dependent. However, due to the multiplication by  $\mathbf{e}_j$  in (3.34)  $E(\hat{P}_j^{(u)}) = 0$  and  $E(\Delta) = 0$ . Hence  $\hat{P}_j^{(u)}$  and  $\Delta$  are uncorrelated. Thus we use (3.36) as an approximate result. Since the column norms now have means  $\mu_{[j]}$ , we can adjust  $P_{\text{av},t}$  to give  $P_{\text{av,CSI}} \triangleq \sum_{j=1}^t \mu_{[j]} / (mt)$  which, after substituting (3.36), can be rewritten as

$$P_{\text{av,CSI}} = 1 - \rho^2 + \rho^2 P_{\text{av},t}. \quad (3.37)$$

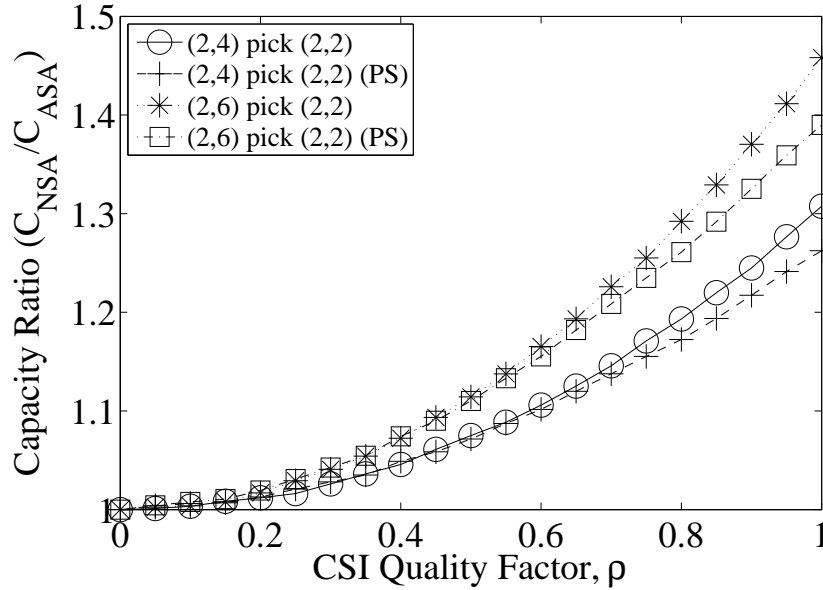


Figure 3.16: Comparison of selection algorithms and PS approximations under imperfect CSI (SNR = 0dB).

This shows that the effect of imperfect CSI can be simply accommodated in the power scaling factor.

Figure 3.16 shows the gains of NSA over ASA under the effects of imperfect CSI. It covers various system sizes and both the actual NSA value and PS approximation. We see that the PS approximation holds even when the CSI is not perfectly known.

### 3.4 Algorithm Complexity

Both NSA and PMWF are low complexity compared to OSA. Breaking down the computation of NSA, the basic steps are the calculation of the column norms and their ordering. The calculation of a column norm of  $\mathbf{H}$  requires  $m$  multiplications and  $m$  additions, giving a complexity of  $O(m)$ . Since there are  $n$  columns to compare, the total computation is  $O(mn)$ . These norms need to be sorted which is an  $O(n \log n)$  operation if the fastest search methods are used. In most cases,  $mn > n \log n$ , so it is safe to approximate the total

computational complexity of NSA as  $O(mn)$ . OSA, on the other hand, involves a matrix multiplication, addition and determinant calculation for each submatrix. The determinant calculation is by far the most complex part and is approximately  $O(t^3)$ . For TX selection this calculation occurs  $\binom{n}{t}$  times. Overall, this makes the total complexity approximately  $O(n^t)$  as shown in [71]. The enormous difference in complexity, especially for high  $t$  and  $n$ , is a strong motivation for using NSA despite the slight capacity penalty. In addition, this penalty can be reduced at low SNR levels by using PMWF which does not increase the complexity of NSA as it uses information already calculated.

### 3.5 System Size

In some systems, especially in hand-held devices, there is a space constraint. Although we have shown increasing gains with the number of redundant antennas (see Sec. 3.1.1), packing multiple antennas into a small space soon causes correlation between the antennas. In such a system one can model the effect of this as a semi-correlated Rayleigh channel (see Sec. 3.2.3). Naturally, increasing antenna correlation will reduce capacity, but at the same time increasing antennas increases the selection gains. The method of selection now becomes very important. Since OSA selects columns based both on the size and the relationship between the columns, we might expect that OSA would increase in superiority over NSA in this correlated case. This is due to the intrinsic dependence between the columns that OSA could possibly exploit. However, in the limiting case of perfect correlation each column becomes identical, and thus it does not matter which columns are chosen and all selection methods become equivalent.

This correlated scenario is also important in another sense. Consider the selection gains available from selecting a few antennas from a densely packed array of a large number of antennas confined to a fixed space. In this situation, the columns become correlated due to the small antenna spacing. As more

antennas are packed into the space there are now two opposing factors: the selection gain due to greater choice versus the increased correlation between the columns.

To explore this situation in detail, we consider an equi-spaced linear array of both fixed and variable length. The decorrelation distance is assumed to be half a wavelength so that the correlation between channel coefficients separated by half a wavelength is  $\rho(0.5) = 0.5$ . We use the well-known simple exponential model for correlation [68], where  $\rho(d) = \exp(-ad)$  and choose  $a$  to match the decorrelation distance. With this correlation model we compare the relative performance of OSA and NSA and also investigate the competition between reduced spacing and antenna numbers.

Figure 3.17 shows the mean capacities achieved by NSA, OSA and ASA in a (4,8) choose (4,4) and (2,4) choose (2,2) system where the transmitter picks half of the total available antennas. The  $x$ -axis is the total antenna array span in wavelengths ( $\lambda$ ), and as predicted, when the intra-antenna spacing is small the three methods converge. For systems of this size NSA works acceptably, giving more than 70% of the gains of OSA over ASA.

Figure 3.18 shows a more complex scenario. In Fig. 3.18, we consider (4, $N$ ) choose (4,4) and (2, $N$ ) choose (2,2) scenarios, where the  $N$  antennas are constrained to a total array length of one wavelength. Figure 3.18 shows the increasing superiority of OSA over NSA and the potential decrease in performance of NSA as  $N$  increases. This is caused by two key effects. The first effect is the ability of OSA to use the correlation structure of the channel, whilst NSA cannot. The second effect is the fact that in the presence of heavy correlation NSA tends to select consecutive antennas since the antenna with the highest norm is often surrounded by others with similar high norms. However, due to the high correlation between selected antennas, the channel gains are similar, leading to reduced capacity. Hence, in densely packed arrays or other highly correlated scenarios, NSA needs to be adjusted to account for correlation patterns in addition to the simple norms.

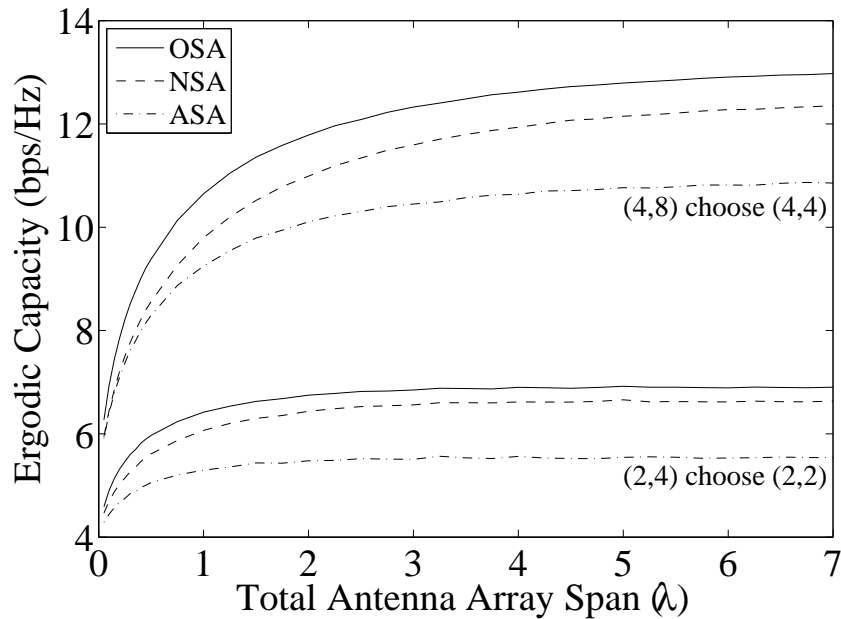


Figure 3.17: Comparison of selection algorithms under correlation with a variable width and a  $(N, N + 2)$  choose  $(N, N)$  system (SNR = 10dB).

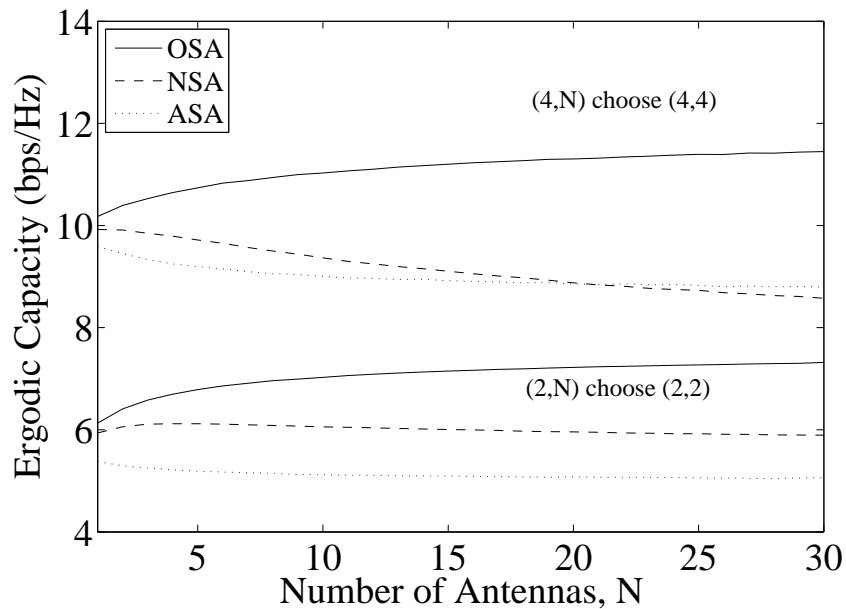


Figure 3.18: Comparison of selection algorithms under correlation with a fixed width (1 wavelength) and a  $(N, N + 2)$  choose  $(N, N)$  system (SNR = 10dB).

## 3.6 Summary

In this chapter we have shown that antenna selection can provide significant gains in a system, with NSA being a benchmark algorithm. Although not as effective as OSA, it is similar in performance and is considerably simpler to implement. Also, at low SNRs the combination of NSA and PMWF provides gains which are superior to OSA. We also show that a closed form analysis for NSA is possible which results in a robust power scaling approximation to the capacity. The beauty of this power scaling approach is its generality and its ability to gauge the effect of selection in a single finite number.



## Chapter 4

# Multiuser MIMO: Broadcast Channel Capacity

Up to now, the vast majority of work on the MIMO-BC has made the basic assumption that the users have equal SNR. In practise this is very unlikely if the multiple users are not co-located. In this chapter, we focus on the MIMO-BC where the users are located separately and thus experience different SNRs due to distance and shadowing effects. We compare this scenario to the equal SNR case. The unequal SNR effects have a considerable impact on the capacity and also the relative merits of different broadcast algorithms. Furthermore, with the sometimes considerable variations in SNR comes an increasing likelihood that the capacity allocations are highly unequal. Thus, fairness becomes an increasingly important concern. Hence, in this chapter, our focus includes the effects of shadowing and also subsequent fairness issues.

The key algorithm we use in this chapter is ITWF developed by [16] and implemented for the MIMO-MAC with sum-power constraints by [17]. This is proven to provide the optimal capacity for any MIMO-BC system [17]. In [17] the iterative algorithms are used to find the sum-rate of a MIMO-BC channel. These ITWF methods are complex and do not result in a fair sharing of the resources at lower SNRs. Recently researchers have derived the capacity for the MIMO-BC with the perfectly fair approach of each user achieving the same capacity [40]. Again the approach is complex, and in scenarios with variable

SNRs it may offer considerably less capacity than the higher SNR users would expect. Thus, we look at simpler techniques which could approach ITWF capacity but with lower complexity and reasonable fairness to all users at a variety of SNRs.

Eigenbeamforming is one alternative method to ITWF in which multiple antennas and the transmitter and receiver can be used to provide array and diversity gains in place of capacity gains [72]. In BF, transmission takes place across one or more eigenchannels. Another alternative is antenna selection which provides a cost effective solution to the increasing hardware needs of MIMO systems [33] (see Chapter 3). Antenna selection can be applied to either or both ends of the MIMO link. In previous chapters we considered transmit and receive antenna selection methods for a single user system. The single user analysis gave a simple power scaling factor as a good approximation to the effect of the selection methods. These methods can also be applied to multiple user systems. In addition to BF and selection, we also consider a baseline case where the transmitter sends independent signals to each user with an equal share of the power. The above methods provide a useful hierarchy of complexity beginning with ITWF, being the most complex, requiring extensive processing at the transmitter and full channel feedback. BF requires less processing and feedback whilst the selection algorithms are simple in comparison. The baseline case requires no feedback nor extra processing.

For a direct comparison of these methods we employ the same analysis philosophy of Chapter 3. This gives us a set of approximately “equivalent” single-user capacities with varying SNR and system size.

We begin this chapter by defining a number of algorithms that we use in our analysis and simulations. We then develop an equivalent single user analysis for these algorithms. We continue with a section on MIMO-MAC design and algorithm complexity analysis. We finish the chapter with a set of comprehensive simulated results and discussion of these results.

## 4.1 Performance Metrics and Algorithms

For the multiuser MIMO case two key metrics of link performance are link throughput and fairness. To evaluate link throughput, we consider the sum capacity of ITWF along with the sum-rates of the suboptimal approaches. From the viewpoint of the dual MIMO-MAC, we can write the sum capacity as [17], [16], (see Sec. 2.3.1)

$$C = \max_{\mathbf{Q}_1, \dots, \mathbf{Q}_K} \log_2 \left| \mathbf{I}_t + \sum_{i=1}^K \mathbf{H}_i^\dagger \mathbf{Q}_i \mathbf{H}_i \right| \text{ bps/Hz}, \quad (4.1)$$

where the maximization in (4.1) is performed over all positive, semi-definite matrices,  $\mathbf{Q}_i$ , that satisfy  $\sum_{i=1}^K \text{Tr}(\mathbf{Q}_i) \leq P$  where  $P$  is the total power available to the system. When we use the suboptimal algorithms to select the  $\mathbf{Q}_i$  matrices in (4.1), then an achievable rate is obtained.

The other key metric we consider in this chapter is that of the ‘fairness’ of each proposed allocation strategy. The fairness metrics considered are outlined in Sec. 2.3.4.

### 4.1.1 Iterative Waterfilling

Iterative waterfilling has been shown in [17] to achieve the sum-capacity of both the MIMO-BC and MIMO-MAC channels. Using the duality properties discussed in [19], we can perform ITWF in the MAC domain and can convert the resulting  $\mathbf{Q}_i$  matrices to optimal  $\mathbf{\Sigma}_i$  matrices for use at the BC transmitter. This approach avoids the direct optimization problem in the BC domain, which is non-convex and highly difficult to solve.

### 4.1.2 Equal Power Independent Uncorrelated Transmission

Equal Power Independent Uncorrelated Transmission, or EPIUT, is the simplest suboptimal power allocation method. In the MIMO-MAC this consists of setting  $\mathbf{Q}_i = \frac{P}{Kr_i} \mathbf{I}_{r_i}$  and if performed in the MIMO-BC,  $\mathbf{\Sigma}_i = \frac{P}{Kt} \mathbf{I}_t$ . This method acts as a convenient benchmark to the performance of all algorithms as it is a convenient baseline approach requiring no transmit processing and no CSI at the transmitter. As we have noted, EPIUT can be performed in both the MIMO-MAC and MIMO-BC domains. However, we have found that EPIUT in the MIMO-MAC produces a slightly better mean rate as compared to MIMO-BC EPIUT (see Sec 4.3) and thus we use it in this thesis. We then use duality principles to find the equivalent MIMO-BC covariance matrices.

### 4.1.3 Beamforming Techniques

Like the simple EPIUT, we can implement BF in either MIMO-MU domain. However, like EPIUT, we found that the BF implementation in the MIMO-MAC domain achieved higher rates in the systems applicable to this thesis. Thus, we consider only BF in the MIMO-MAC and we need to use duality to determine the MIMO-BC.

Beamforming in the MIMO-MAC consists of user  $i$  transmitting  $\ell_i$  symbols along the  $\ell_i$  principal eigenvectors. More specifically, user  $i$  selects the top  $\ell_i \leq \min(r_i, t)$  eigenchannels which have eigenvalues  $\lambda_1^{(i)} > \lambda_2^{(i)} > \dots > \lambda_{\ell_i}^{(i)}$ . Note that these are the ordered eigenvalues of the  $r_i \times r_i$  matrix  $\mathbf{H}_i \mathbf{H}_i^\dagger$ . Then, beamforming results if a  $\mathbf{Q}_i$  matrix is used, defined by

$$\mathbf{Q}_i = \left[ \mathbf{v}_1^{(i)} \mathbf{v}_2^{(i)} \dots \mathbf{v}_{\ell_i}^{(i)} \right] \mathbf{P}_i \left[ \mathbf{v}_1^{(i)} \mathbf{v}_2^{(i)} \dots \mathbf{v}_{\ell_i}^{(i)} \right]^\dagger \quad (4.2)$$

where  $\mathbf{P}_i = \text{diag}(P_{i1}, P_{i2}, \dots, P_{i\ell_i})$  is a diagonal matrix which allocates powers to the eigenchannels and  $\mathbf{v}_j^{(i)}$  denotes the eigenvector of  $\mathbf{H}_i \mathbf{H}_i^\dagger$  corresponding

to  $\lambda_j^{(i)}$ . We consider both  $P_{ij}$  constant and  $P_{ij} \propto \lambda_j^{(i)}$  as power allocations in this thesis.

One of the key decisions we make in the BF approach is choosing the number of eigenchannels to be employed by each user. We use two approaches here. The first, denoted BF2, is a fair (in terms of user fairness) approach where each user selects their  $L$  largest eigenchannels ( $L \leq \min(r_1, r_2, \dots, r_K)$ ). The other approach, denoted BF1, selects the best  $L'$  eigenchannels from the system irrespective of the user and performs beamforming across these.

#### 4.1.4 Selection Techniques

Selection can be split into two distinct categories: user selection and antenna selection.

##### User Selection

A sensible approach to user selection is to select the user(s) with the highest single-user capacity(s). This would mean that the selection process involves waterfilling, which is complex, time consuming and requires a high degree of feedback. Thus, we also use a suboptimal selection approach, where users are selected based on the size of the single-link gain,  $\|\mathbf{H}_i\|_F^2$ . This is denoted SLG. Note that this requires much less system feedback than waterfilling as only the link gains need to be fed back. Once the user(s) are selected, it is assumed that EPIUT is used. It is important to note that user selection is inherently unfair as only a subset of the users are active at any one time.

##### Antenna Selection

In a multiuser broadcast system, antenna selection can take two distinct forms. The first, which we denote S2, is where each user performs selection independently, picking their best  $L$  antennas ( $L \leq \min(r_1, r_2, \dots, r_K)$ ) and allocating a fair share of the total power across the selected antennas evenly. Note that

this approach is fair in terms of users. The other approach is performance based and selects the best  $L'$  antennas of the entire system irrespective of the user. We denote this S1. For simplicity the antennas are selected using NSA rather than OSA. Hence, user  $i$  ranks antenna  $j$  first if row  $j$  of  $\mathbf{H}_i$  has the largest row norm, denoted  $\Gamma_i \alpha_{ij} = \|(\mathbf{H}_i)_j\|^2$ , where  $(\mathbf{H}_i)_j$  is row  $j$  of  $\mathbf{H}_i$ . The ordered row norms are thus denoted by  $\Gamma_i \alpha_{i(1)} > \dots > \Gamma_i \alpha_{i(r_i)}$ . As with the beamforming approaches, power allocation is also an issue and to address it, we take the same two approaches as beamforming. Thus a selected antenna for user  $i$ , for example antenna  $j$ , can be allocated power  $P_{ij}$  where  $P_{ij}$  is either a constant or  $P_{ij} \propto \Gamma_i \alpha_{ij}$ .

## 4.2 Equivalent Single-user System Analysis

We now attempt to analyze the algorithm defined in Sec. 4.1.

Due to the high complexity and iterative nature of the optimal iterative waterfilling solution, little analytical progress can be made and thus we have to use simulations instead. For most other approaches we can achieve further insight by converting the systems in to their “equivalent” single-user forms. From these, we can employ well-known and established capacity results. The dimensions of an “equivalent” single-user MIMO system with  $n_r$  receiver antennas and  $n_t$  transmitter antennas are denoted by  $(n_r, n_t)$ .

### 4.2.1 Equal Power Independent Uncorrelated Transmission

With the EPIUT approach the MIMO-MAC gives us  $\mathbf{Q}_i = \frac{P}{Kr_i} \mathbf{I}_{r_i}$ . In the special case where  $r_i = r$  and  $\Gamma_i = \Gamma$  for all users then (4.1) yields the rate  $R$  where

$$R = \log_2 \left| \mathbf{I}_t + \frac{P\Gamma}{Kr} \mathbf{U}^\dagger \mathbf{U} \right| \text{ bps/Hz}, \quad (4.3)$$

with  $\mathbf{U} = [\mathbf{U}_1^\dagger \dots \mathbf{U}_K^\dagger]$ , where  $\mathbf{U}_i$  are  $r \times t$  i.i.d.  $\mathbb{C}\mathcal{N}(0,1)$  matrices. The resulting rate is that of a single-user MIMO system with  $t$  transmit antennas and  $Kr$  receive antennas (i.e. a  $(Kr, t)$  system) with equivalent  $SNR = P\Gamma$  for an i.i.d. Rayleigh channel. In more general cases with differing link gains ( $\Gamma_i$ ) or antenna numbers, we can still express these in a single-user system although the channel is no longer i.i.d. Instead the rate equation is

$$R = \log_2 |\mathbf{I}_M + \mathbf{U}^\dagger \mathbf{D}_1 \mathbf{U}| \quad \text{bps/Hz}, \quad (4.4)$$

with  $\mathbf{U}$  defined as above and block diagonal matrix  $\mathbf{D}_1$  made up of  $K$  diagonal matrices of the form  $\frac{P\Gamma_i}{Kr_i} \mathbf{I}_{r_i}$ . We can compute the mean rate for such a system using the techniques explained in Sec. 2.9.

## 4.2.2 Beamforming Techniques

We can construct a basic approximation to beamforming in the following way. For simplicity, we only show the approach for the BF2 case with  $L = 1$  will be shown (this is where the user communicates over their maximum eigenchannel). In this case (4.2) collapses neatly to  $\mathbf{Q}_i = v_1^{(i)} P_{i1} v_1^{(i)\dagger}$ . Consider the SVD,  $\mathbf{H}_i = \mathbf{V}_i \mathbf{S}_i \mathbf{W}_i^\dagger$ , with the principal  $r_i \times r_i$  submatrix of  $\mathbf{S}_i$  given by  $\text{diag}(\sqrt{\lambda_1^{(i)}}, \dots, \sqrt{\lambda_{r_i}^{(i)}})$  and  $v_1^{(i)}$  is the first column of  $\mathbf{V}_i$ . Now substituting  $\mathbf{Q}_i$  as well as the SVD for  $\mathbf{H}_i$  into (4.1), we can write

$$\begin{aligned} R &= \log_2 \left| \mathbf{I}_M + \sum_{i=1}^K \mathbf{W}_i^\dagger \text{diag}(P_{i1} \lambda_1^{(i)}, 0, \dots, 0) \mathbf{W}_i \right| \\ &= \log_2 |\mathbf{I}_M + \mathbf{W}^\dagger \mathbf{D}_2 \mathbf{W}| \quad \text{bps/Hz}, \end{aligned} \quad (4.5)$$

where  $\mathbf{W}^\dagger = [(\mathbf{W}_1^\dagger)_{\cdot 1} \ (\mathbf{W}_2^\dagger)_{\cdot 1} \ \dots \ (\mathbf{W}_K^\dagger)_{\cdot 1}]$  is a  $t \times K$  matrix containing the first columns of the  $\mathbf{W}_i^\dagger$  matrices and  $\mathbf{D}_2 = \text{diag}(P_{11} \lambda_1^{(1)}, \dots, P_{K1} \lambda_1^{(K)})$ . Due to the nature of the SVD,  $\mathbf{W}^\dagger$  contains independent columns with column norms

equal to 1. Hence we can find a rough approximation by replacing (4.5) with

$$R = \log_2 \left| \mathbf{I}_M + \mathbf{U}^\dagger \mathbf{D}_3 \mathbf{U} \right| \quad \text{bps/Hz}, \quad (4.6)$$

where  $\mathbf{U} : K \times t$  is i.i.d.  $\mathbb{CN}(0, 1)$  and  $\mathbf{D}_3 = \mathbf{D}_2/t$ . Note that in (4.6) the singular matrix  $\mathbf{S}$ , containing the singular vectors, is replaced by an i.i.d. Gaussian matrix with the same mean and column power. This analysis is accurate to within 10% for reasonable channel models due to the approach in [73], where it is shown that the mutual information of a system is more dependent on the moments of the channel distribution rather than the distribution itself.

### 4.2.3 Selection Techniques

We can handle user selection that is based on link gain (SLG) using the approach developed in previous chapters. For simplicity, we consider the easiest case where  $r_i = r$  for all users. The link gain for the  $i^{\text{th}}$  user is then  $\Gamma_i \alpha_i = \Gamma_i \sum_{j=1}^r \alpha_{ij} = \Gamma_i Y_i$ , where  $Y_i$  has a complex  $\chi^2$  distribution with  $rt$  degrees of freedom. Thus, the selected user's link gain is  $g_{\max} = \max(\Gamma_1 Y_1, \dots, \Gamma_K Y_K)$ . Our approach is to create an equivalent  $r \times t$  channel matrix for the chosen user,  $\mathbf{H}_{\text{equiv}} = \sqrt{E(g_{\max})/(rM)} \mathbf{U}$ , which has the same mean link gain as the original user and  $\mathbf{U}$  is i.i.d.  $\mathbb{CN}(0, 1)$ . This gives the rate

$$R = \log_2 \left| \mathbf{I}_t + \frac{E(g_{\max})}{rt} \mathbf{U}^\dagger \mathbf{U} \right| \quad \text{bps/Hz}. \quad (4.7)$$

Also note that we can obtain  $E(g_{\max})$  using standard order statistic results for non-identical independent random variables.

Our approach for antenna selection methods is very similar. We now describe our approach for the S2 method with  $L = 1$  but the methodology can also be applied to all other cases. In S2 (with  $L = 1$ ), user  $i$  selects antenna  $j$  if  $\alpha_{ij} = \max(\alpha_{i1}, \dots, \alpha_{ir_i})$  and allocates power  $P_{ij}$ . This results in a corresponding matrix  $\mathbf{Q}_i = \text{diag}(0, \dots, P_{ij}, \dots, 0)$  with the non-zero entry in position  $j$ .

However, for the special case of  $L = 1$  we can further simplify the notation by denoting the  $j^{\text{th}}$  row of  $\mathbf{H}_i$  by  $\mathbf{h}_i$ , dropping the  $j$  subscript in  $P_{ij}$  and using the order statistic notation  $\alpha_{i(1)}$  for the maximum row norm. Substituting for  $\mathbf{Q}_i$  in (4.1), we can write

$$R = \log_2 \left| \mathbf{I}_t + \sum_{i=1}^K P_i \mathbf{h}_i^\dagger \mathbf{h}_i \right| \text{ bps/Hz.} \quad (4.8)$$

Using techniques from Chapter 3, we can replace the rows  $\mathbf{h}_i$  by  $\sqrt{\Gamma_i E(\alpha_{i(1)})} \mathbf{u}_i$ , where  $\mathbf{u}_i$  is an i.i.d.  $\mathbb{CN}(0, 1)$  vector and (4.8) becomes

$$R = \log_2 \left| \mathbf{I}_t + \mathbf{U}^\dagger \mathbf{D}_4 \mathbf{U} \right| \text{ bps/Hz.} \quad (4.9)$$

where  $\mathbf{U}$  is a  $K \times M$  i.i.d.  $\mathbb{CN}(0, 1)$  matrix and

$$\mathbf{D}_4 = \text{diag}[P_1 \Gamma_1 E(\alpha_{1(1)}), \dots, P_K \Gamma_K E(\alpha_{K(1)})].$$

Note that we can obtain the values of  $E(\alpha_{i(1)})$  by using the same methods as those employed to find  $P_{\text{av}}$  in Chapter 3.

#### 4.2.4 System Comparison

Of the equivalent systems constructed, only (4.3) and (4.7) are in the form of rates for i.i.d. MIMO channels. The remaining equivalent systems, e.g., (4.4), (4.5), (4.6) and (4.9), have diagonal  $\mathbf{D}_i$  matrices in the quadratic forms. This form of log determinant can be analyzed [74], but we achieve greater insight by converting all of the cases to approximate single-user MIMO systems in i.i.d. channels. Hence we construct approximations to these systems by replacing  $\mathbf{D}_i$  by  $E\{\text{Tr}(\mathbf{D}_i)/\nu_i\} \mathbf{I}_{\nu_i}$ , where  $\nu_i$  is the dimension of  $\mathbf{D}_i$ . Using this approach, we can compare the different algorithms in terms of a single equivalent SNR and dimension, as shown in Table 4.1. Note that the terms, *constant* and *proportional* used in Table 4.1 refer to the power allocation method used, which

Method	Dimension ( $n_t, n_r$ )	Equivalent SNR
EPIUT ( $r_i = r, \Gamma_i = \Gamma$ )	$(Kr, t)$	$P\Gamma$
EPIUT (general case)	$(\sum_{i=1}^K r_i, t)$	$\frac{P}{K} \sum_{i=1}^K \Gamma_i$
BF2 (constant)	$(KL, t)$	$\frac{P}{K} \sum_{i=1}^K \Gamma_i \mathbb{E} \left[ \frac{\sum_{j=1}^L \lambda_j^{(i)}}{ML} \right]$
BF2 (proportional)	$(KL, t)$	$\frac{P}{K} \sum_{i=1}^K \Gamma_i \mathbb{E} \left[ \frac{\sum_{j=1}^L \lambda_j^{(i)2}}{t \sum_{j=1}^L \lambda_j^{(i)}} \right]$
SLG	$(r_i, t)$	$\mathbb{E}(g_{\max})/t$
S2 (constant)	$(KL, t)$	$\frac{P}{K} \sum_{i=1}^K \Gamma_i \mathbb{E} \left[ \frac{\sum_{j=1}^L \alpha_{i(j)}}{Lt} \right]$
S2 (proportional)	$(KL, t)$	$\frac{P}{K} \sum_{i=1}^K \Gamma_i \mathbb{E} \left[ \frac{\sum_{j=1}^L \alpha_{i(j)}^2}{t \sum_{j=1}^L \alpha_{i(j)}} \right]$

Table 4.1: Equivalent MIMO Systems

can be constant or proportional to the eigenvalues (in BF1 and BF2) or the row norms (in S1 and S2). Table 4.1 gives the approximations:

$$R \approx \log_2 \left| \mathbf{I}_M + \frac{\text{SNR}}{n_t} \mathbf{U}^\dagger \mathbf{U} \right| \text{ bps/Hz}, \quad (4.10)$$

where SNR and  $n_t$  are from Table 4.1 and  $\mathbf{U}$  is  $n_t \times t$ .

Using the equivalent system SNR values from Table 4.1 and the mean capacity calculations from Sec. 2.9, Figs. 4.1 and 4.2 show that the equivalent SNR formulations are a very good approximation to the actual sum-rate even in the case of highly variant individual SNRs. One key point to note from Table 4.1 is that the equivalent SNR of selection is less than that of beamforming. This is due to the fact that S2 and BF2 tend to become efficient when the leading norms or eigenvalues dominate. Since leading eigenvalues tend to dominate more than dominant row norms, BF2 gives better performance and a higher equivalent SNR than the S2 case. This point is reinforced in the majority of the figures in this chapter. Note that both the equivalent SNR and

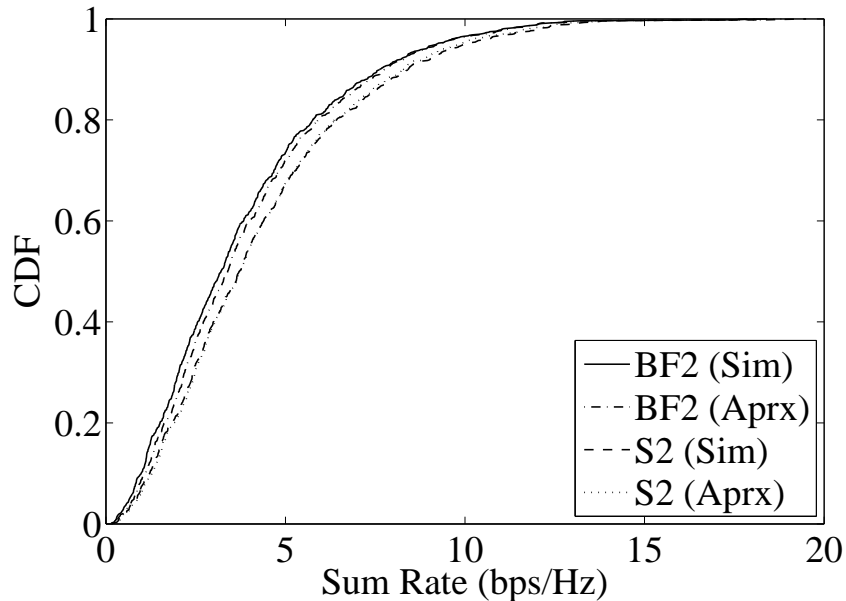


Figure 4.1: Comparison between simulation (Sim) and equivalent SNR approximation (Aprx) for BF2 and S2 algorithms ( $\text{SNR}_{\text{av}} = 10\text{dB}$ , (2,4) three user system with shadow fading effects).

the system dimension need to be taken into account when comparing systems.

### 4.3 MAC Design

Throughout the chapter we have used various suboptimal covariance matrices, based on EPIUT, selection and beamforming. In all cases these matrices were constructed for the MAC and transformed to the BC using the duality results in [19]. Intuitively, designing the  $\mathbf{Q}_i$  matrices is easier, since the users are decoupled in the MAC system. The BC design is hampered by intrinsic problems of interference, and the  $\mathbf{\Sigma}_i$  matrices affect all users. Although MAC design is not universally better than BC design, it is usually preferable for typical system dimensions. We demonstrate this below for some simple examples.

We consider the S2 approach where the best single antenna is selected. In the MAC this makes perfect sense. Each user selects a single antenna leading

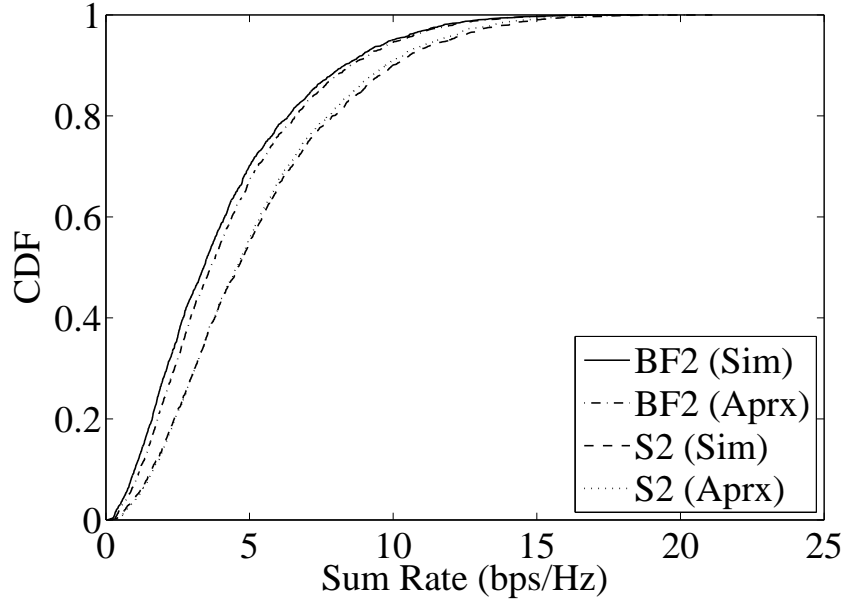


Figure 4.2: Comparison between simulation (Sim) and equivalent SNR approximation (Aprx) for BF2 and S2 algorithms ( $\text{SNR}_{\text{av}} = 10\text{dB}$ , (4,4) three user system with shadow fading effects).

to a BC channel with  $n_t$  transmit antennas and  $K$  single antenna users with optimized links to the BS. For the BC, we choose one antenna at the BS for each user to maximize the link. It is possible that one antenna maximizes the link for all users. This is not a practical solution as the dimensionality of the resulting system (i.e. 1 transmit antenna) cannot support  $K$  users. Hence, simple selection works at the MAC end but more complex versions would be required in the BC.

Next, we consider the EPIUT approach. For ease of exposition, we assume two users with  $n_r$  antennas. Furthermore, we let both users have the same link strength and undergo i.i.d. Rayleigh fading. This scenario gives:

$$C_{\text{MAC}} = \log_2 \left| \mathbf{I} + \frac{1}{n_r} \mathbf{H}_1^\dagger \mathbf{H}_1 + \frac{1}{n_r} \mathbf{H}_2^\dagger \mathbf{H}_2 \right| \text{ bps/Hz} \quad (4.11)$$

and

$$\begin{aligned}
C_{\text{BC}} = & \log_2 \left| \mathbf{I} + \frac{1}{n_t} \mathbf{H}_1 \mathbf{H}_1^\dagger \right| \\
& - \log_2 \left| \mathbf{I} + \frac{1}{n_t} \mathbf{H}_2 \mathbf{H}_2^\dagger \right| \\
& + \log_2 \left| \mathbf{I} + \frac{2}{n_t} \mathbf{H}_2 \mathbf{H}_2^\dagger \right| \quad \text{bps/Hz}, \tag{4.12}
\end{aligned}$$

since  $\mathbf{Q}_1 = \mathbf{Q}_2 = \frac{1}{n_r} \mathbf{I}$  and  $\mathbf{\Sigma}_1 = \mathbf{\Sigma}_2 = \frac{1}{n_t} \mathbf{I}$ . The mean capacities are

$$\text{E}\{C_{\text{MAC}}\} = \text{E} \left[ \log_2 \left| \mathbf{I} + \frac{1}{n_r} \begin{pmatrix} \mathbf{H}_1^\dagger & \mathbf{H}_2^\dagger \end{pmatrix} \begin{pmatrix} \mathbf{H}_1 \\ \mathbf{H}_2 \end{pmatrix} \right| \right] \quad \text{bps/Hz} \tag{4.13}$$

and

$$\text{E}\{C_{\text{BC}}\} = \text{E} \left[ \log_2 \left| \mathbf{I} + \frac{2}{n_t} \mathbf{H}_2 \mathbf{H}_2^\dagger \right| \right] \quad \text{bps/Hz}, \tag{4.14}$$

since the first two terms in (4.12) cancel out. From (4.13) and (4.14) we observe that the MAC has the capacity of a single user system of dimension  $(n_t \times 2n_r)$  and an SNR of 2. The BC system has an equivalent dimension of  $(n_r \times n_t)$  and an SNR of 2. The number of channels available in the MAC is  $\min(n_t, 2n_r)$  and the number in the BC is  $\min(n_r, n_t)$ . Hence the two systems have the same SNR and the MAC has a greater or equal number of channels. In general, therefore, the MAC has a higher capacity. This is not always true, since for small  $n_t$  and large  $n_r$  the number of channels is the same and the BC system has  $n_r$  receive antennas and benefits from diversity. This is not a particularly useful scenario since small  $n_t$ , large  $n_r$ ,  $K > 1$  leads to an overloaded BC system. Our simulation results show that the BC superiority can be achieved but only in asymmetric cases, where the total number of receive antennas is around three times higher than the number of transmit antennas. In such scenarios EPIUT is impractical, and so the MAC design is the best approach in realistic cases.

## 4.4 Complexity Analysis

Although ITWF provides optimal performance, it is a highly complex algorithm. The most complex step in ITWF (see Sec. 2.11.5) is the SVD. This can be made linear with respect to the number of users [17] by taking the SVD of each effective channel separately. This leads to a complexity per iteration of approximately  $O(Kr^3)$ . The other complex processes such as calculating the effective channels can be streamlined as discussed in [17].

The other algorithms we use are more straightforward. BF is the next complex as it needs  $K$  eigendecompositions each of  $O(t^3)$  and a sort of  $O(Kt \log(Kt))$ . Although the order of BF is slightly more than that of ITWF, we only need one iteration, making it considerably more straightforward. Selection follows with row norm calculations and a sort, leading to a complexity of  $O(Krt)$  (see Sec. 3.4). EPIUT is very simple by comparison and requires no computations at all.

## 4.5 Simulation Results

The baseline system we used for simulations is a  $2 \times 4$  MIMO-BC system with varying numbers of users. Shadowing and path loss effects are included in some results. Definitions of these effects can be found in Sec. 2.12.1. The constant,  $A$ , in (2.53) is adjusted so that the mean user SNR,  $\text{SNR}_{\text{av}}$ , is either 0dB or 10dB as specified in each plot. Also, we considered  $2 \times 8$  and  $4 \times 4$  MIMO-BCs, each with 3 users.

The methods we simulated include ITWF, EPIUT (also referred to as EP), S1 (best  $K$  antennas), S2 (best antenna per user), BF1 (best  $K$  eigenchannels) and BF2 (best eigenchannel per user). We also show proportional power allocation versions of S1 and BF1. We denote these S1P and BF1P respectively. It is important to note the different flavours of SNR used:  $\text{SNR}_{\text{av}}$  represents the mean user SNR defined above,  $\Gamma_i$  is the SNR of user  $i$ , and SNR with no

subscript represents the SNR for the case where there is equal SNR for each user.

We display the results on two types of graph. The first is a standard CDF, from which the statistical performance of the algorithms can be simply compared. Examples of this type of graph include Figs. 4.4, 4.18 and 4.21. The second set of graphs, which are shown in Figs. 4.7, 4.8, 4.9 and 4.10, show the effects of changing the relative link gains ( $\Gamma_i$ ) of two links in the cellular environment. They compare the performance of certain algorithms with the optimal ITWF capacity. The  $x$  axis of these graphs corresponds to the  $y$  axis of the c.d.f. in Fig. 4.3 (with  $R = 100$  and  $R_0 = 10$ ). This c.d.f. is then inverted to give a value of  $\Gamma_1/\Gamma_2$  and this ratio is used in the capacity simulations. For example, at  $x = 0.5$  in Fig. 4.7 we invert the c.d.f. in Fig. 4.3 to obtain  $\Gamma_1/\Gamma_2 = 0\text{dB}$ . Hence all channel pairs where  $\Gamma_1/\Gamma_2 \approx 0\text{dB}$  are used to simulate capacity. The final percentage capacity is the average percentage capacity for all simulations where  $\Gamma_1/\Gamma_2 \approx 0\text{dB}$ . Note that the distribution of this ratio is given in both Sec. 2.12.1 and Appendix A. The first notable point about these graphs is their symmetry around  $P(\Gamma_1/\Gamma_2 < x) = 0.5$ . This relates to symmetry about  $\Gamma_1 = \Gamma_2$  due to the fact that  $\Gamma_1$  and  $\Gamma_2$  are i.i.d. variables. Thus, to read these graphs only one half needs to be considered. As an example, consider Fig. 4.8. Look at the BF2 algorithm relative to the EP algorithm. These lines cross at approximately  $P(\Gamma_1/\Gamma_2 < x) = 0.17$ . Therefore, taking into account the symmetry of the graphs, EP is greater than BF2 approximately 34% of the time and conversely BF2 is greater than EP for approximately 66% of the time in this scenario. Also note that this is an average result. At each point,  $\Gamma_1/\Gamma_2 = x$ , there are many values of  $\Gamma_1$  and  $\Gamma_2$  which give the same value of  $x$ . Hence the curves are averages over all such simulated points. In practice, this is achieved by binning all pairs of  $(\Gamma_1, \Gamma_2)$  values in a small region around  $\Gamma_1/\Gamma_2 = x$ . However, in reading these graphs there are a couple of points of note:

1. At the edges, the relative mean SNR of the samples is inflated compared

to  $\text{SNR}_{\text{av}}$ , the desired average SNR. This is due to the fact that, in general, samples with a large ratio of  $\Gamma_1/\Gamma_2$ , have either  $\Gamma_1$  or  $\Gamma_2$  significantly greater than  $\text{SNR}_{\text{av}}$ .

2. The center, where  $\Gamma_1 = \Gamma_2$ , should not be confused with an i.i.d. Rayleigh system. It is equivalent to the mean of a number of Rayleigh systems each with a different  $\text{SNR} = \Gamma_1$  such that their mean is  $\text{SNR}_{\text{av}}$ .

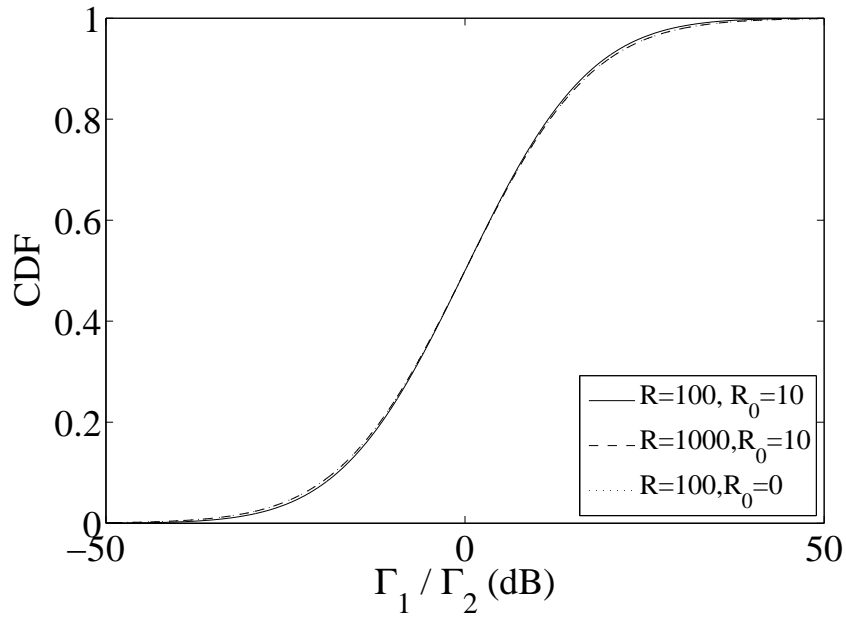


Figure 4.3: CDF of the ratio  $\Gamma_1/\Gamma_2$  for different values of  $R$  and  $R_0$ .

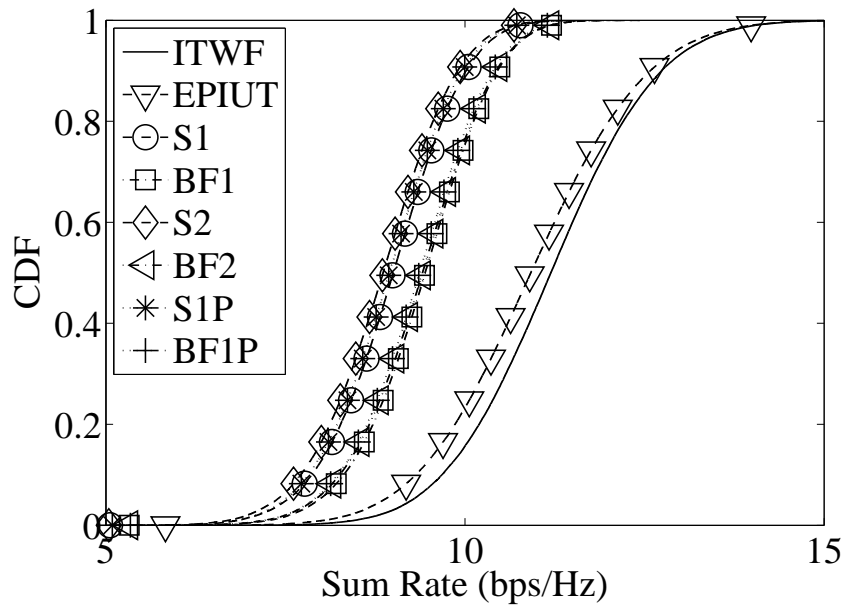


Figure 4.4: Algorithm comparison for a (2,4) two user system ( $\text{SNR}_{\text{av}} = 10\text{dB}$ , no shadow fading effects).

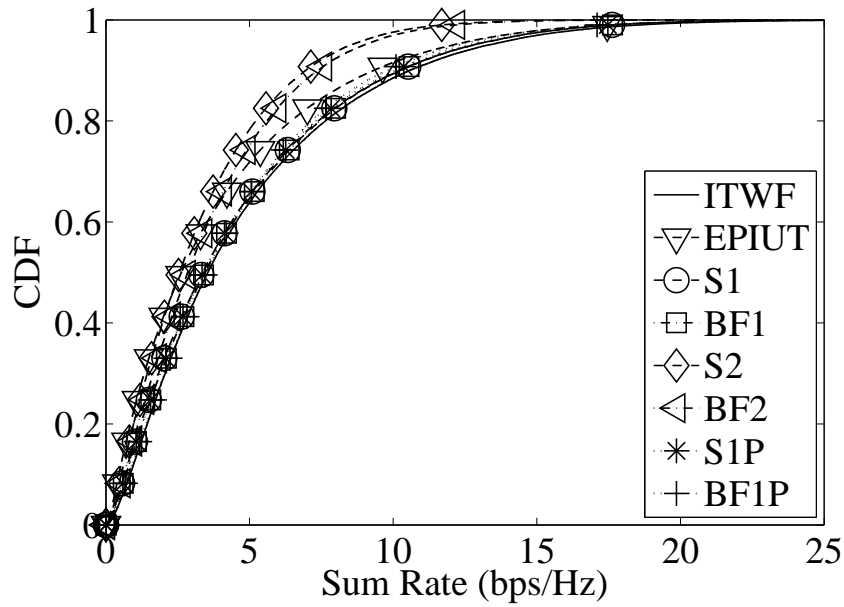


Figure 4.5: Algorithm comparison for a (2,4) two user system ( $\text{SNR}_{\text{av}} = 10\text{dB}$ , shadow fading effects).

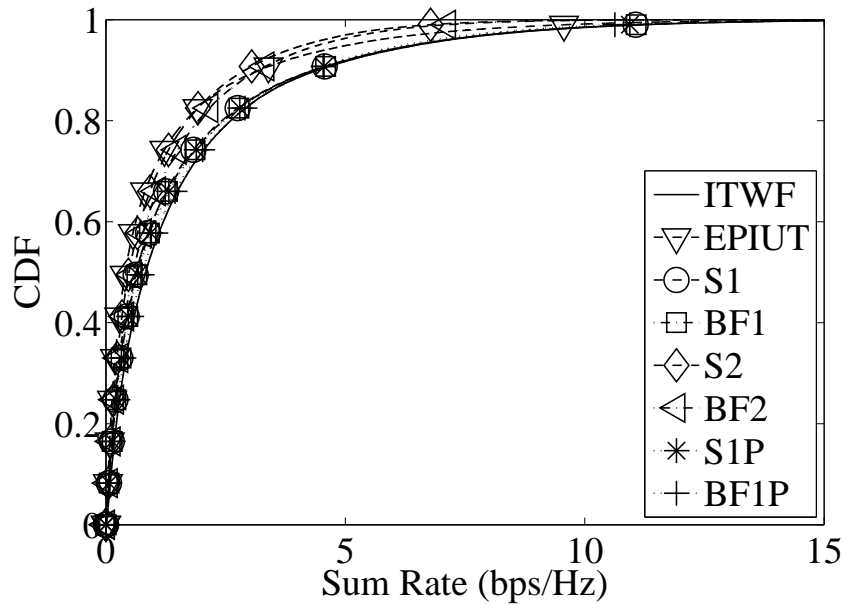


Figure 4.6: Algorithm comparison for a (2,4) two user system ( $\text{SNR}_{\text{av}} = 0\text{dB}$ , shadow fading effects).

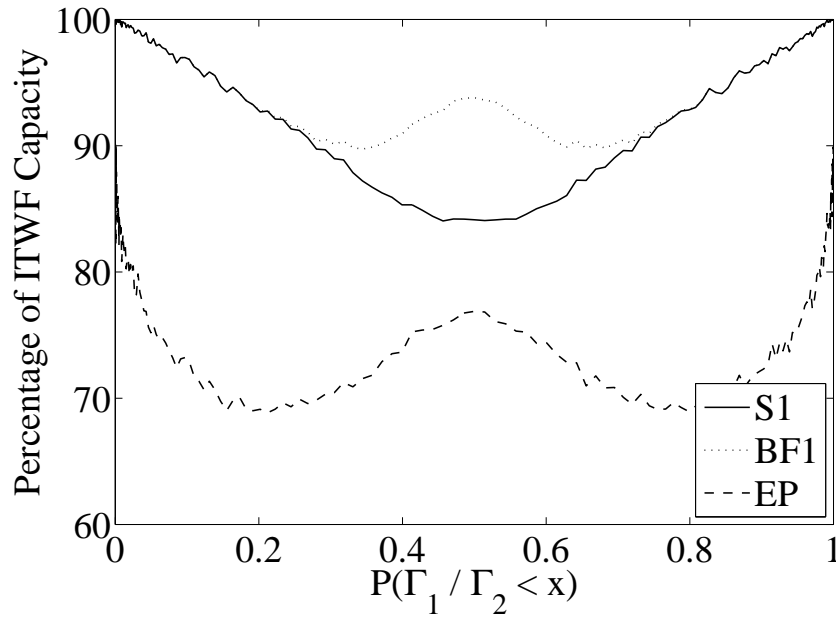


Figure 4.7: Algorithm comparison for a (2,4) two user system for varying ratios of link gain ( $\text{SNR}_{\text{av}} = 10\text{dB}$ ).

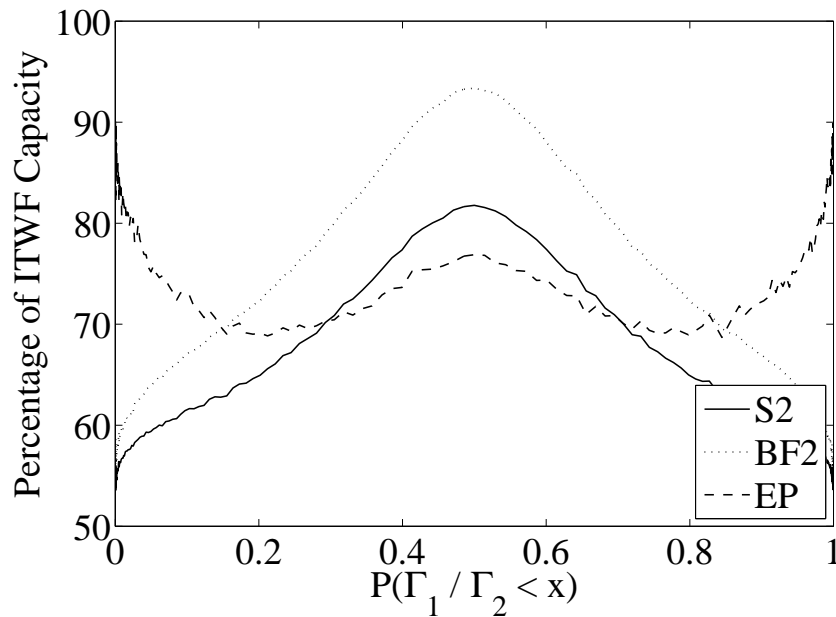


Figure 4.8: Algorithm comparison for a (2,4) two user system for varying ratios of link gain ( $\text{SNR}_{\text{av}} = 10\text{dB}$ ).

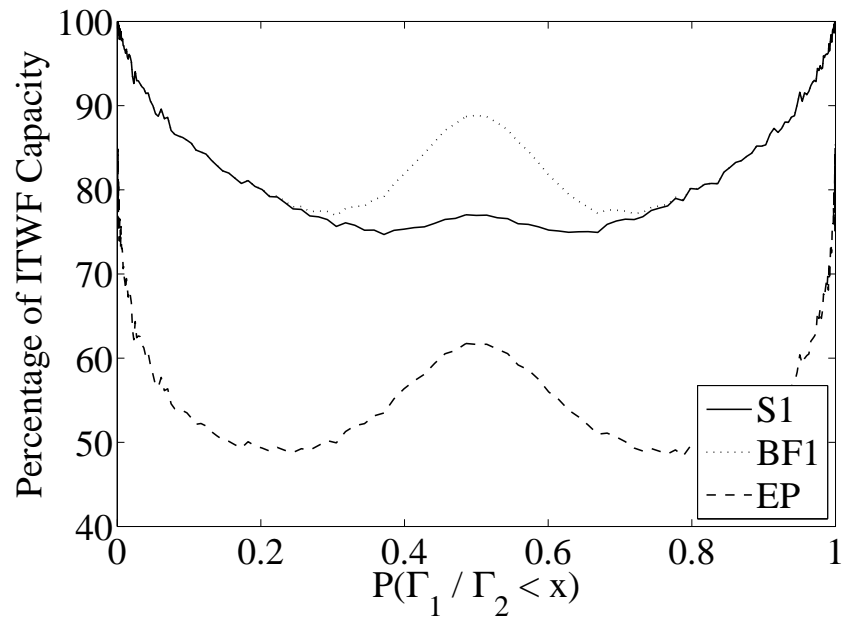


Figure 4.9: Algorithm comparison for a (2,4) two user system for varying ratios of link gain ( $\text{SNR}_{\text{av}} = 0\text{dB}$ ).

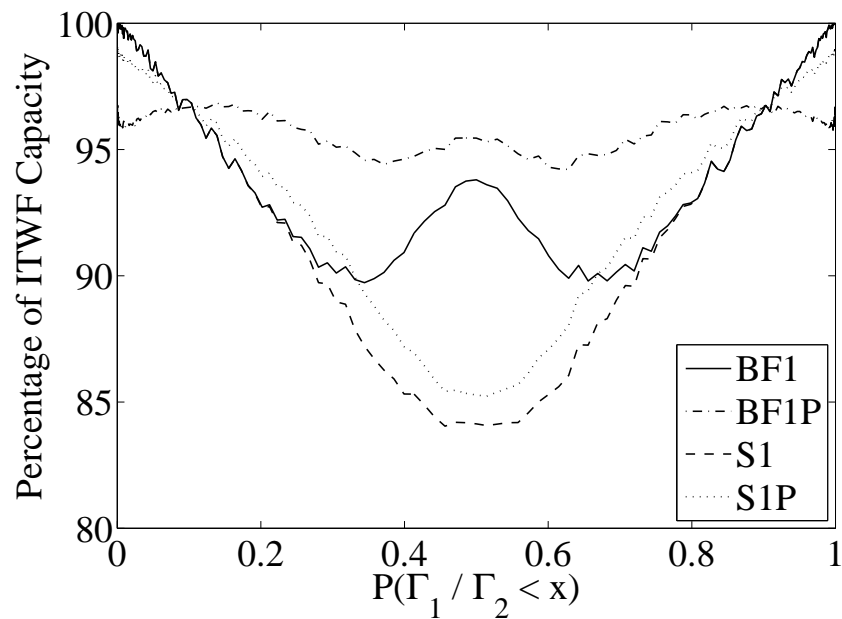


Figure 4.10: Proportion power allocation algorithm comparison for a (2,4) two user system for varying ratios of link gain ( $\text{SNR}_{\text{av}} = 10\text{dB}$ ).

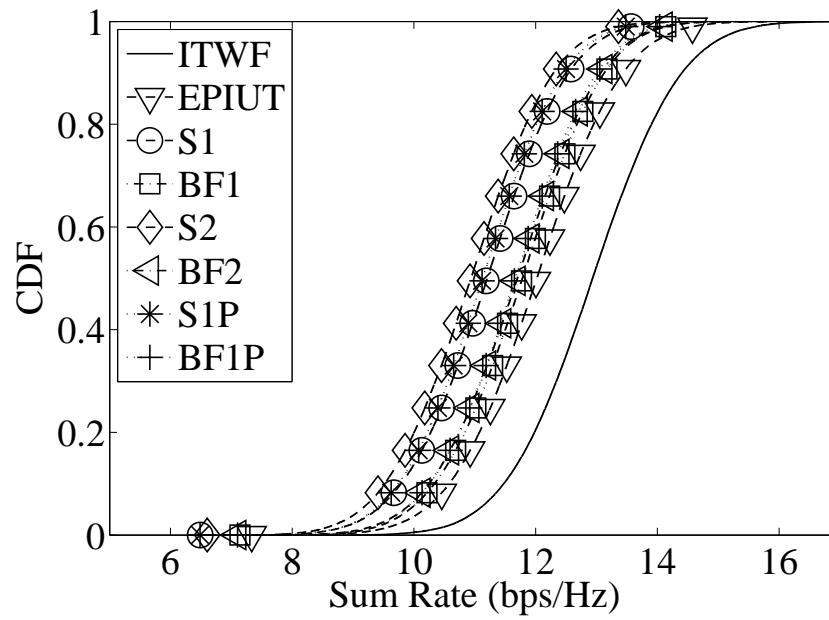


Figure 4.11: Algorithm comparison for a (2,4) three user system ( $\text{SNR}_{\text{av}} = 10\text{dB}$ , no shadow fading effects).

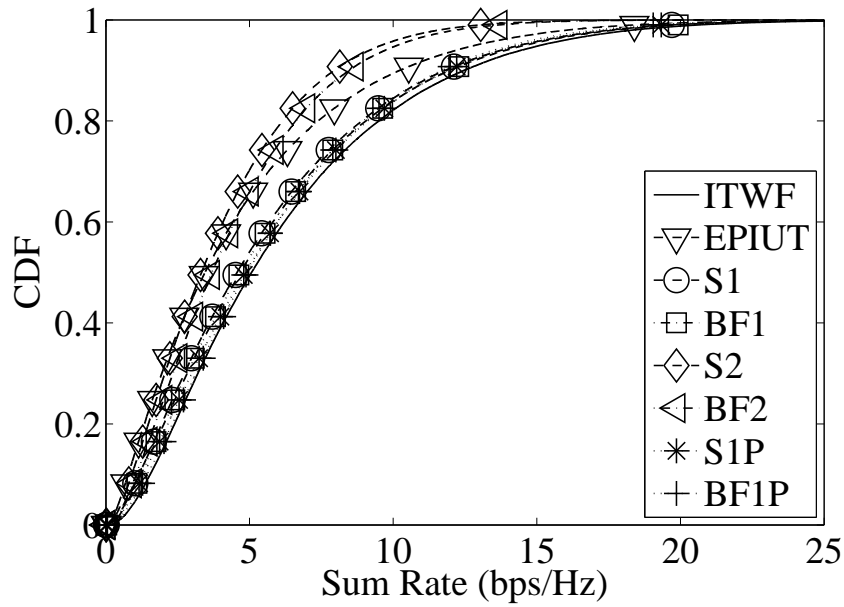


Figure 4.12: Algorithm comparison for a (2,4) three user system ( $\text{SNR}_{\text{av}} = 10\text{dB}$ , shadow fading effects).

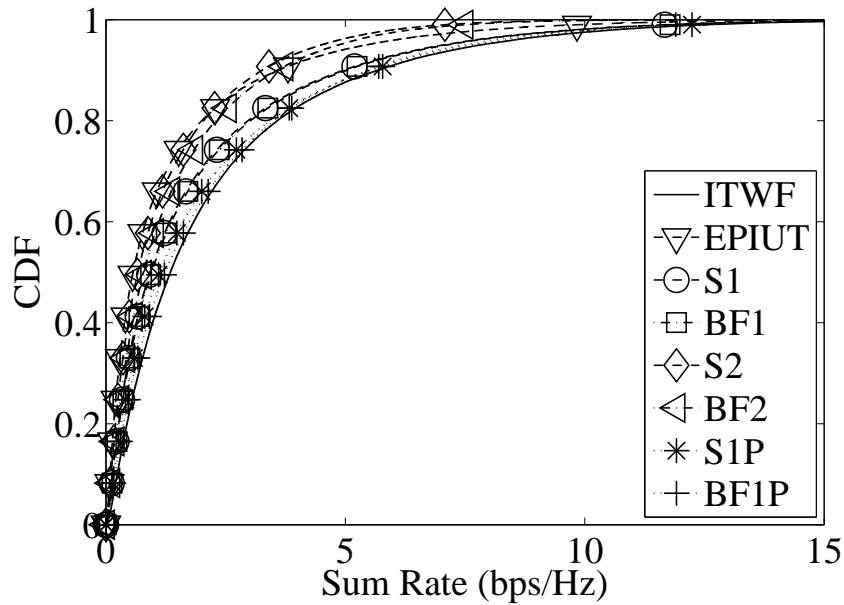


Figure 4.13: Algorithm comparison for a (2,4) three user system ( $\text{SNR}_{\text{av}} = 0\text{dB}$ , shadow fading effects).

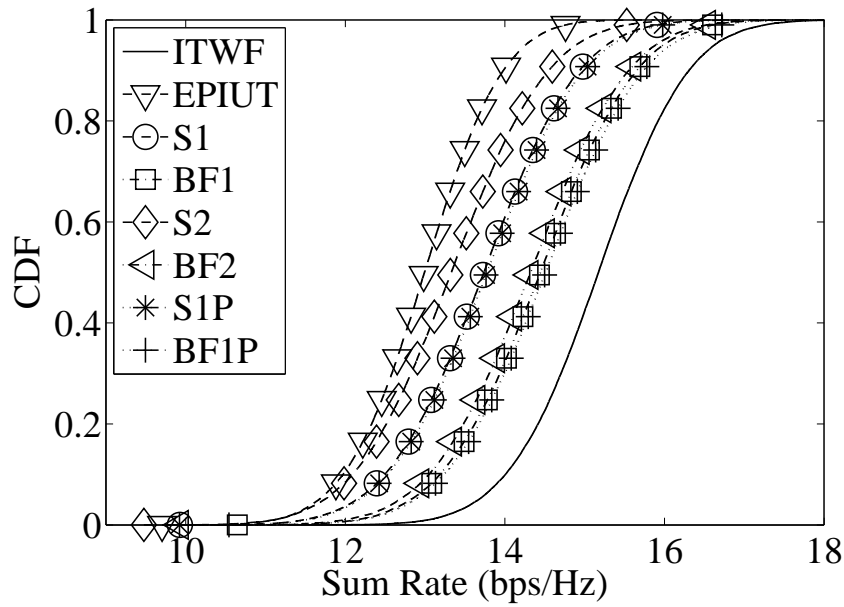


Figure 4.14: Algorithm comparison for a (2,4) six user system ( $\text{SNR}_{\text{av}} = 10\text{dB}$ , no shadow fading effects).

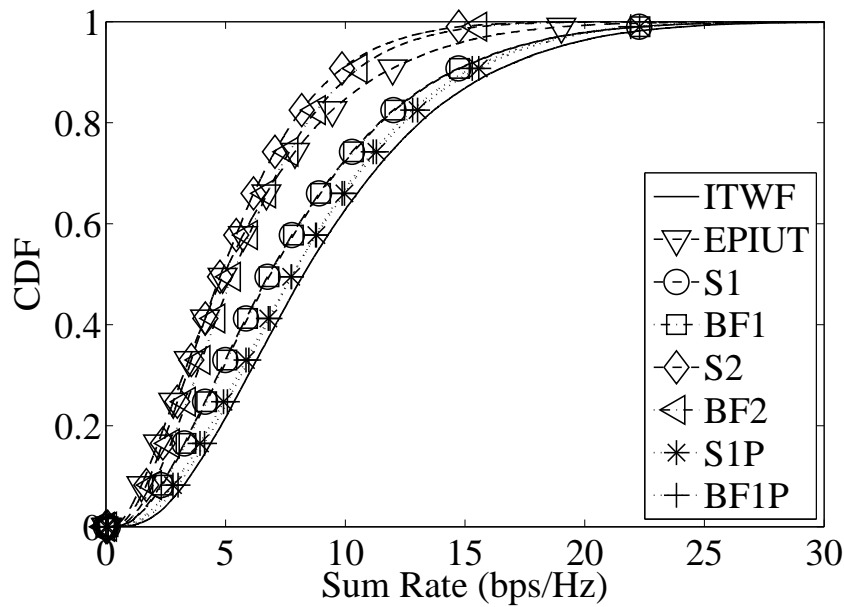


Figure 4.15: Algorithm comparison for a (2,4) six user system ( $\text{SNR}_{\text{av}} = 10\text{dB}$ , shadow fading effects).

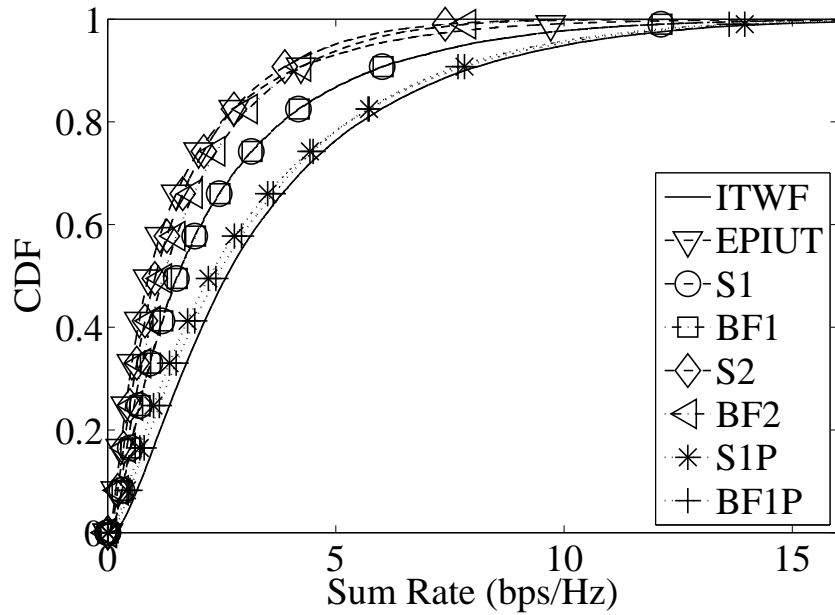


Figure 4.16: Algorithm comparison for a (2,4) six user system ( $\text{SNR}_{\text{av}} = 0\text{dB}$ , shadow fading effects).

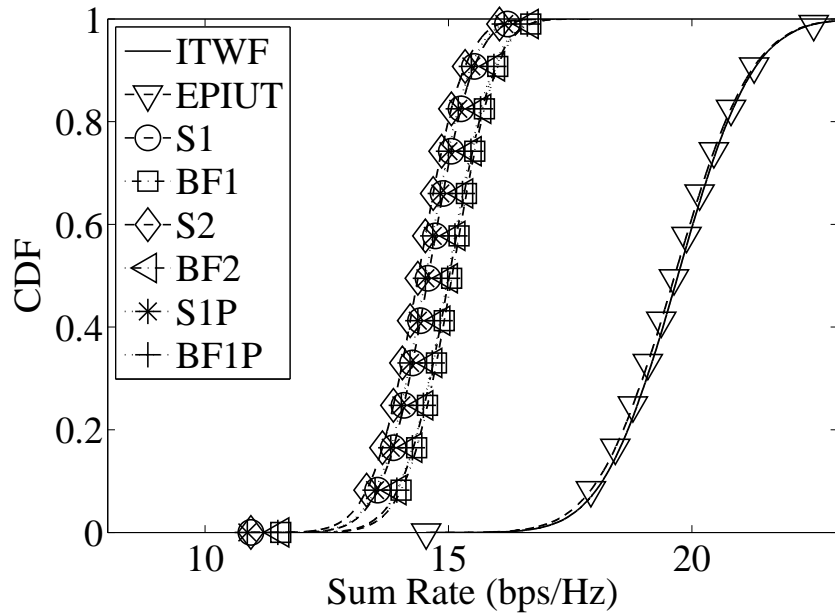


Figure 4.17: Algorithm comparison for a (2,8) three user system ( $\text{SNR}_{\text{av}} = 10\text{dB}$ , no shadow fading effects).

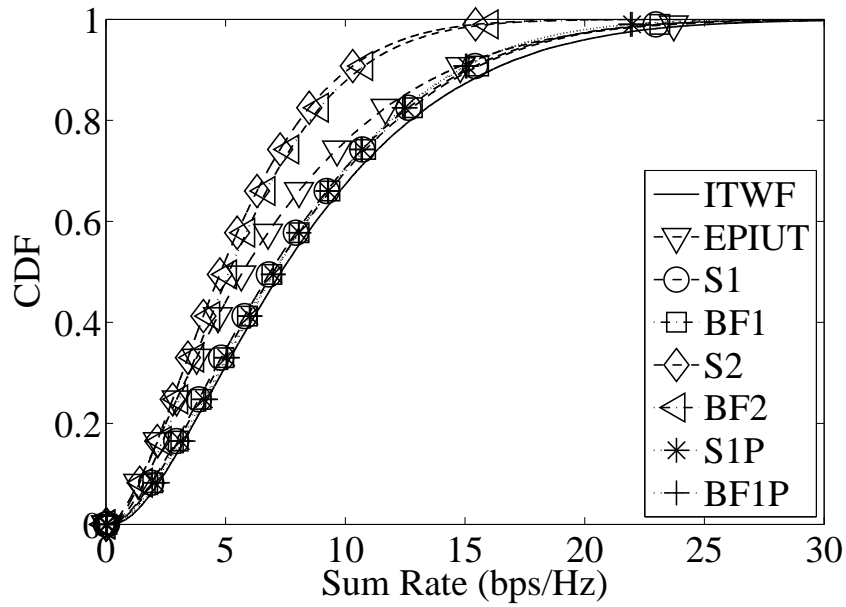


Figure 4.18: Algorithm comparison for a (2,8) three user system ( $\text{SNR}_{\text{av}} = 10\text{dB}$ , shadow fading effects).

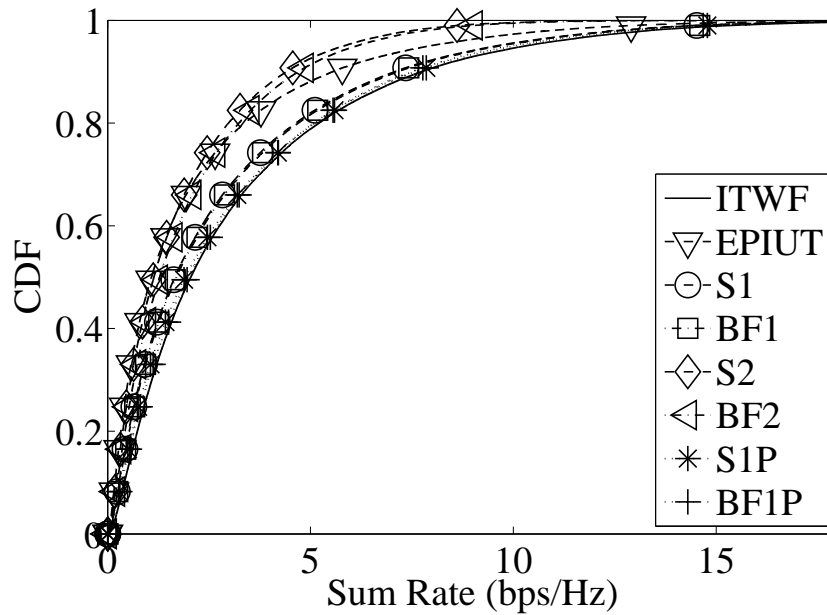


Figure 4.19: Algorithm comparison for a (2,8) three user system ( $\text{SNR}_{\text{av}} = 0\text{dB}$ , shadow fading effects).

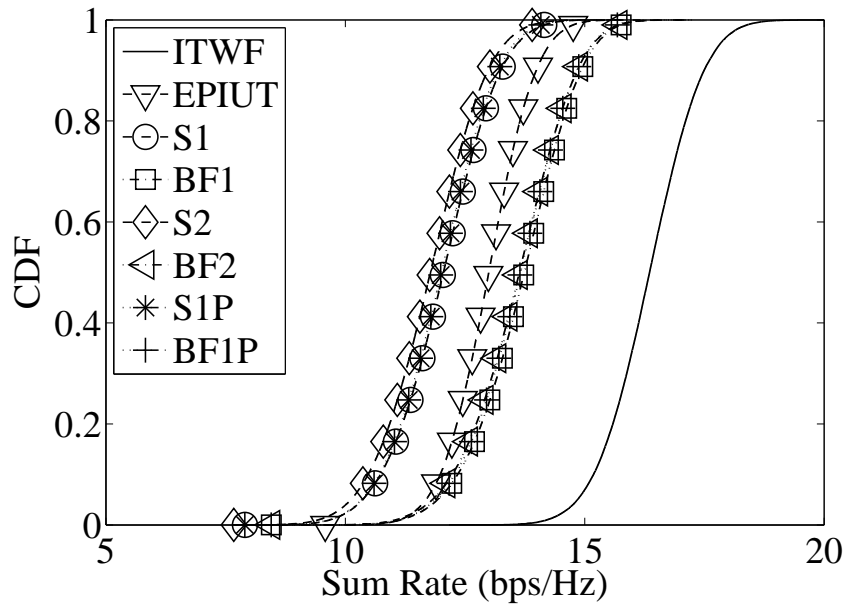


Figure 4.20: Algorithm comparison for a (4,4) three user system ( $\text{SNR}_{\text{av}} = 10\text{dB}$ , no shadow fading effects).

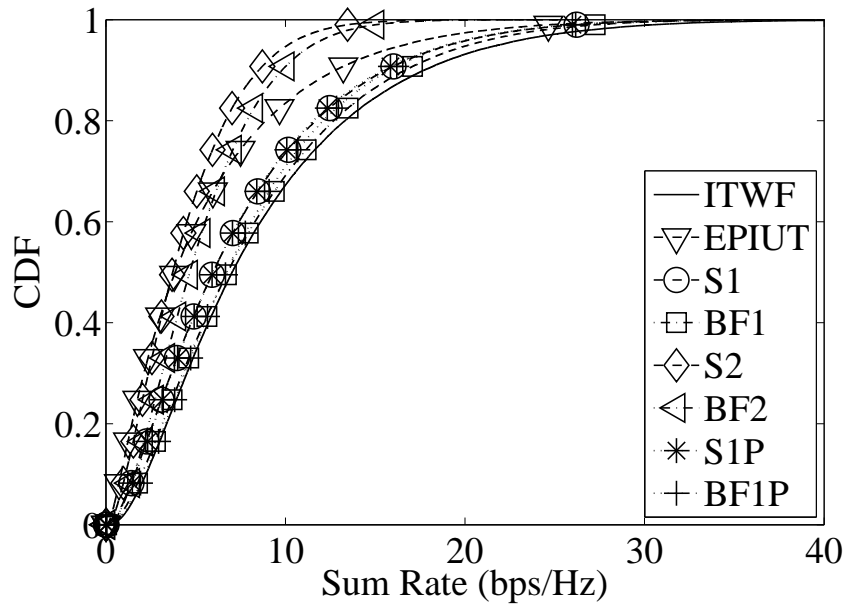


Figure 4.21: Algorithm comparison for a (4,4) three user system ( $\text{SNR}_{\text{av}} = 10\text{dB}$ , shadow fading effects).

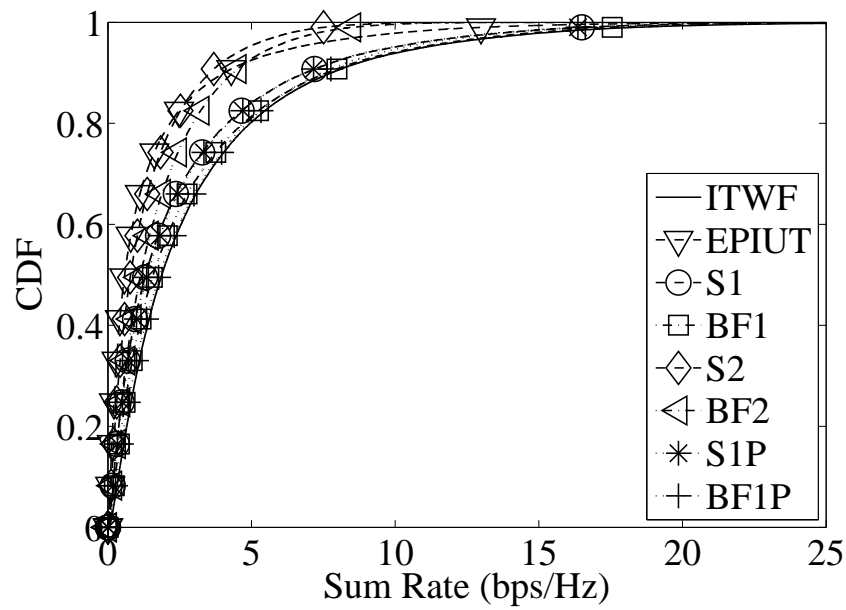


Figure 4.22: Algorithm comparison for a (4,4) three user system ( $\text{SNR}_{\text{av}} = 0\text{dB}$ , shadow fading effects).

### 4.5.1 Results Overview

The previous figures showed a considerable subset of MIMO-BC systems of different sizes and in different conditions. A number of key points arise from these figures.

Firstly, the shape of the CDF graphs are split into two distinct types. In the absence of shadowing Figs. 4.4, 4.11, 4.14, 4.17 and 4.20 show the well-known approximately Gaussian CDF shape. The equivalent systems with shadowing (Figs. 4.5, 4.12, 4.15, 4.18 and 4.21) show a very different shape to averaging over the  $\Gamma_i$  variables. These are similar to those found in [57].

Next, our comparison of the algorithms in the various scenarios leads to a discussion on the issue of performance versus fairness. We consider fairness issues in detail in Sec. 4.5.2. Also, the use of proportional power appeared in the results. We discuss this in detail in Sec 4.5.3, covering both selection and beamforming algorithms.

### 4.5.2 Performance vs. Fairness

In this thesis we measure fairness in a number of ways as discussed in Sec. 2.3.4. One measure is the number of active subchannels. This is a key metric as it shows how many subchannels are closed and how many are open for communication. Note that a high number of subchannels in some circumstances does not necessarily mean a high number of users are available for active communication as the channels may come from the same user. However, Fig. 4.23 shows that these two measures of fairness are closely linked for the ITWF algorithm.

With ITWF being the only algorithm with a variable (var) amount of open subchannels, it provides more flexibility for the algorithm to be fairer/less fair depending on the system state as shown in Fig. 4.23. The decreasing flexibility of S1 and BF1 means that they are less able to adjust their fairness to maximize performance which is highlighted especially in the high SNR Rayleigh cases (Figs. 4.4, 4.11, 4.14, 4.17 and 4.20). The complete lack of flexibility and full

Algorithm	No. OS	No. AU
ITWF	var	var
S1	3	var
BF1	3	var
S2	3	3
BF2	3	3

Table 4.2: Number of Active Users (AU) and Open Subchannels (OS) Available to Various Algorithms for Simulated (2,4) Three User Systems

user fairness of the S2 and BF2 algorithms hampers their ability to maximize performance in nearly all scenarios. On the positive side, S2 and BF2 are completely fair algorithms in terms of active users. The flexibility/lack of flexibility of certain algorithms is summarized in Table 4.5.2.

An important trend to note with the performance/fairness tradeoff is that the algorithms with a similar fairness/power allocation structure to ITWF in a particular scenario tend to have near-optimal performance in that scenario. This can be seen in the Rayleigh conditions, especially at moderate to high-SNR, where EPIUT comes close to optimal capacity as both algorithms have many subchannels and full active users in these cases (for examples, see Figs. 4.11, 4.17 and 4.14). In the other case, where there is a variable power allocation and/or low-SNR, ITWF tends to allocate power to fewer users and subchannels. In these cases S1 and BF1 become very close to optimal, as is shown in Figs. 4.12, 4.13 and 4.22. This is also reflected in Figs. 4.7 and 4.8 where the S1 and BF1 algorithms tend to do well in a channel with greater difference in SNR between the two users. Note that S1 and BF1 match ITWF in the extremes. S2 and BF2, however, do well in a channel where each user has approximately equal link gains. A key point to note in comparing the EPIUT approach with the S2 and BF2 approaches is that it has a higher dimensionality (sending 6 rather than 3 symbols in a (2,4) 3 user case for example). This increase in dimensionality yields better performance in most situations.

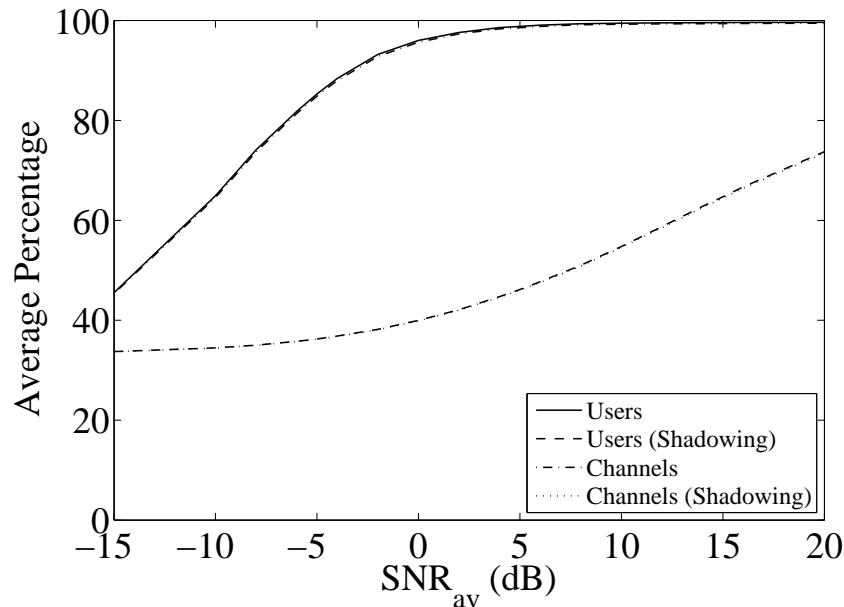


Figure 4.23: Percentage of spatial channels open and active users for ITWF in a (2,4) three user system for variable  $\text{SNR}_{\text{av}}$ .

### 4.5.3 Proportional Power

The use of proportional power is also of considerable interest. In Sec. 3.2.6, we showed that gains made by allocating power based on column norms have a positive effect in low-SNR regions. However, this benefit is SNR dependent and decreases with SNR to such an extent that it becomes a deficit at high SNR. For the multiuser system, a similar effect happens. Figure 4.24 shows that the S1 and BF1 algorithms both have good gains from proportional power allocations at low SNR while this approach results in a deficit at high SNR.

The number of antennas per user<sup>1</sup> does not have much bearing on the gains/losses of proportional power allocations as can be seen by comparing Figs. 4.12, 4.18 and 4.21. However, increasing the numbers of users tends to increase the relative gains of proportional power, which can be seen by comparing Figs. 4.5, 4.12 and 4.15. These effects are due to the fact that proportionality decreases the fairness of an algorithm by encouraging allocation

<sup>1</sup>Note that all users in these results have the same number of antennas.

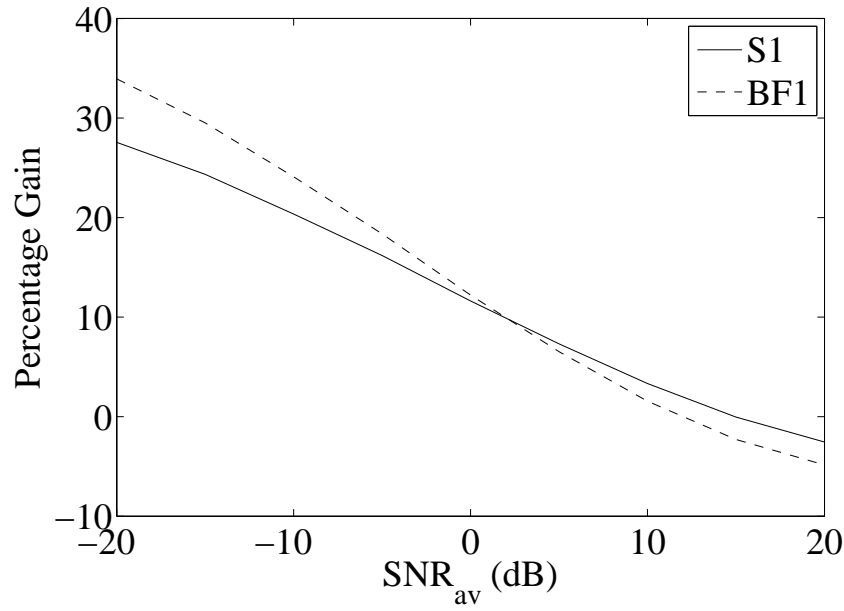


Figure 4.24: Gains of proportional power allocation over fixed power allocation for a (2,4) three user system (shadow fading effects).

to the best subchannels at the expense of the weaker ones. Thus, it is typical to see the benefits of proportional allocation in situations which discourage fairness, such as the low power per user case.

Figure 4.10 shows the effects of proportional power allocation where the link gains are varied. The proportional algorithms perform well, outperforming their non-proportional counterparts except at the edges. This is due to the fact that, as noted before, the mean SNR at the edges is higher than  $\text{SNR}_{\text{av}}$ , and this causes the proportional power algorithms to provide deficits rather than gains as highlighted above.

## 4.6 Summary

In this chapter we have studied the effects of shadowing and the performance and fairness properties of a variety of MIMO-BC algorithms, both optimal and suboptimal. As we have shown, shadowing can have a large impact on both the relative and absolute performances of the algorithms as well as their

fairness in distributing the channel resources. ITWF always achieves optimal capacity, but sometimes at the cost of fairness, especially in shadowing and/or low-SNR conditions. This is due to the fact that it tends to allocate all of the resources to the dominant user. In contrast, the relatively simple selection and beamforming algorithms can approach optimal sum-capacity whilst retaining a higher level of fairness than ITWF for varying SNR conditions. Finally, we have developed a new analytical approximation for the MIMO-BC capacity, by breaking down the systems into power-scaled equivalent single-user channels. This should prove to be a useful tool for better understanding the channels.

## Chapter 5

# Multiuser MIMO: Broadcast Channel Capacity and Modifications to the Waterfilling Algorithm

A well-known problem in modern communications is that of maximizing the mutual information of a channel composed of several subchannels subject to a global power constraint [14, 75, 76]. These subchannels can range from frequency bins in a frequency selective system to variations over time to spatially parallel channels as found in MIMO systems. The solution to this problem is also well-known and is given by the capacity-achieving waterfilling algorithm.

Waterfilling, or waterpouring as it is sometimes known, gets its name from the visual interpretation of pouring a set amount of water over the inverse of the subchannel gains (see Fig. 2.3). Many applications and variations of waterfilling now exist. A common example is to modify the waterfilling algorithm to reduce the mean-squared error of a system [75, 77–80]. Other variations can be used to maximize the minimum signal to interference and noise ratio or minimize the bit error rate [81]. However, relatively few researchers [82] have modified the waterfilling algorithm to increase multiuser system fairness (fairness relative to system users rather than relative to individual channels).

This is the focus of this chapter.

Two approaches to multiuser MIMO (MIMO-MU) capacity problems have recently been investigated. The first is the maximization of the sum capacity with no fairness constraints. These techniques typically employ waterfilling on a multiuser scale, both under individual user power constraints [16] and sum power constraints [17]. The key finding of Vishwanath *et al.*'s on duality [19] allows the convex optimization of the MIMO-MAC to be applied to the MIMO-BC. These techniques were shown in Chapter 4 to lack fairness in some circumstances. The second category is research focussed on fairness and quality of service [83], at the expense of overall throughput. A good example is the work by Lee *et al.*'s on symmetric capacity [40].

In this chapter, we propose modifications to the waterfilling algorithm which increase fairness by encouraging the allocation of power into each sub-channel. We approach this in two ways: firstly via a 'hard' minimum power allocation which modifies the constraints of the waterfilling algorithm. This approach is similar to previous work [82]. In addition we provide a brief analysis as well as an upper bound on the algorithm's performance relative to classical optimal waterfilling. The second, novel approach provides a 'soft' constraint by adjusting the waterfilling problem by using utility functions.

We can clearly see fairness issues on a channel-by-channel basis in the conventional WF algorithm described in Chapter 2. The form of (2.45) in Sec. 2.11.4 implies that the solution,  $x_i^*$ , may be zero at certain times. This implies that a channel is zero or inactive, which may be undesirable in some systems. In order to discourage this possibility, in this chapter we look at various modifications to the waterfilling algorithm. However, note that the main thrust of this work is multiuser fairness. We develop this from the single user work described in Sections 5.1 and 5.2.

## 5.1 Constraint Modification

In classic waterfilling,<sup>1</sup> (2.42) is minimized subject to the constraints,  $\mathbf{1}^T \mathbf{x} = 1$  and  $x_i \geq 0$ . Changing or adding-to these constraint functions is one possible modification to the waterfilling algorithm. In this chapter we look at the effects of adding the constraints,  $x_i \geq u$  and  $x_i \leq w$  where  $0 < u, w \leq 1$ . Note that  $u$  and  $w$  need to be such that a feasible point exists. Thus, a more practical definition of  $u$  is that  $0 < u \leq 1/m$  and that  $w \geq 1/m$ , where  $m$  is the number of non-zero singular values of  $\mathbf{H}$  as given in Sec. 2.11.4. Using the notation in [54], the first KKT condition is that  $f_i(x_i) \leq 0$ , where  $f_i(x)$ ,  $i = 1, \dots, m$  represent the inequality constraints [54].

It is easy to see that imposing minimum power constraints increases the fairness of a system by giving power to channels which may have previously been allocated none. However, it is not as easy to see that imposing maximum power constraints also increases system fairness. It does this in two ways. Firstly, imposing these constraints reduces the power in the dominant user. Secondly, the power that was in the dominant user(s) is now redistributed amongst the weaker users, increasing overall system fairness.

### 5.1.1 Minimum Power Constraints

For a minimum power constraint, we introduce the constraint  $x_i \geq u$ , which is equivalent to  $f_i(x_i) = u - x_i$ . Note that the constraint  $x_i \geq 0$  is now unnecessary. Using the new inequality in the KKT conditions gives:

$$\begin{aligned} u - x_i^* &\leq 0, & \mathbf{1}^T \mathbf{x}^* &= 1, & \zeta_i^* &\geq 0, \\ \zeta_i^*(x_i^* - u) &= 0, & \frac{-1}{\alpha_i + x_i^*} - \zeta_i^* + \nu^* &= 0. \end{aligned} \quad (5.1)$$

---

<sup>1</sup>See Sec. 2.11.4

Equating the 4<sup>th</sup> KKT condition in (5.1) with the 5<sup>th</sup> and using  $\zeta_i$  as a slack variable gives:

$$(x_i^* - u) \left( \nu^* - \frac{1}{\alpha_i + x_i^*} \right) = 0, \quad (5.2)$$

Equation (5.2) has solutions at  $x_i^* = u$  and  $\nu^* = \frac{1}{\alpha_i + x_i^*}$ . The latter gives the standard waterfilling solution  $x_i^* = \left( \frac{1}{\nu^*} - \alpha_i \right)$  as long as  $x_i^* > u$ . We can see that this holds as long as  $\nu^* < \frac{1}{\alpha_i + u}$ , and thus the final value of  $x_i^*$  can be expressed as:

$$x_i^* = \begin{cases} \frac{1}{\nu^*} - \alpha_i, & \nu^* < \frac{1}{\alpha_i + u} \\ u, & \nu^* \geq \frac{1}{\alpha_i + u} \end{cases}. \quad (5.3)$$

In (5.3),  $\nu^*$  can be found by using the 2<sup>nd</sup> KKT condition, so that

$\sum_{i=1}^m \max \left\{ u, \frac{1}{\nu^*} - \alpha_i \right\} = 1$ . This gives:

$$\nu^* = \frac{k}{1 - (m - k)u + \sum_{i \in \kappa} \alpha_i}, \quad (5.4)$$

where  $\kappa$  is the set of subchannels where  $\nu^* < \frac{1}{\alpha_i + u}$  and  $k$  is the number of subchannels in this set. In practise we can solve this by adjusting the classical waterfilling implementations to check if  $x_i \geq u$  rather than  $x_i \geq 0$  to find a valid solution.

## 5.1.2 Maximum Power Constraints

For a maximum power constraint<sup>2</sup>, we introduce the constraint  $x_i \leq w$ . This is equivalent to  $f_i(x_i) = x_i - w$ . Using this inequality in the KKT conditions gives:

$$\begin{aligned} -x_i^* &\leq 0, & x_i - w &\leq 0, & \mathbf{1}^T \mathbf{x}^* &= 1, \\ \zeta_{j,i}^* &\geq 0, & \zeta_{1,i}^* x_i^* &= 0, & \zeta_{2,i}^* (x_i^* - w) &= 0, \\ & & & & \frac{-1}{\alpha_i + x_i^*} - \zeta_{1,i}^* + \zeta_{2,i}^* + \nu^* &= 0. \end{aligned} \quad (5.5)$$

---

<sup>2</sup>Due to the constraint  $\mathbf{1}^T \mathbf{x} = 1$ , a minimum power constraint introduces an effective maximum power constraint of  $x_i \leq 1 - u \times m$ .

where  $j \in \{1, 2\}$ ,  $\zeta_{1,i}$  is the multiplier associated with  $x_i \geq 0$  and  $\zeta_{2,i}$  the multiplier associated with  $x_i \leq w$ . We consider three cases:  $x_i^* = 0$ ,  $x_i^* = w$  and  $0 < x_i^* < w$ .

- $x_i^* = 0$

In this case,  $\zeta_{2,i}^* = 0$  and thus the final KKT equation of (5.5) gives  $\nu^* \geq 1/\alpha_i$  due to the positivity of  $\zeta_{1,i}^*$ .

- $x_i^* = w$

In this case,  $\zeta_{1,i}^* = 0$  and thus  $\nu^* \leq 1/(\alpha_i + w)$ .

- $0 < x_i^* < w$

In this case, both  $\zeta_{1,i}^* = \zeta_{2,i}^* = 0$ , giving the classical waterfilling relationship  $\nu^* = 1/(\alpha_i + x_i^*)$ .

These three cases lead to the solution:

$$x_i^* = \begin{cases} 0, & \nu^* \geq \frac{1}{\alpha_i} \\ \frac{1}{\nu^*} - \alpha_i, & \frac{1}{\alpha_i + w} < \nu^* < \frac{1}{\alpha_i} \\ w, & \nu^* \leq \frac{1}{\alpha_i + w} \end{cases} . \quad (5.6)$$

This results in a value of  $\nu^*$  as follows:

$$\nu^* = \frac{k}{1 - cw + \sum_{i \in \kappa} \alpha_i}, \quad (5.7)$$

where  $\kappa$  is the set of subchannels where  $\frac{1}{\alpha_i + w} < \nu^* < \frac{1}{\alpha_i}$ ,  $k$  is the number of subchannels in this set and  $c$  is the number of subchannels where  $\nu^* \leq \frac{1}{\alpha_i + w}$ .

### 5.1.3 Dual Constraints and Practical Implementation

We can use both the constraints  $x_i \geq u$  and  $x_i \leq w$  at the same time. Using derivations from Secs. 5.1.1 and 5.1.2 we get the result:

$$x_i^* = \begin{cases} u, & \nu^* \geq \frac{1}{\alpha_i + u} \\ \frac{1}{\nu^*} - \alpha_i, & \frac{1}{\alpha_i + w} < \nu^* < \frac{1}{\alpha_i + u} \\ w, & \nu^* \leq \frac{1}{\alpha_i + w} \end{cases} . \quad (5.8)$$

This gives a value of  $\nu^*$  as follows:

$$\nu^* = \frac{k}{1 - cw + \sum_{i \in \kappa} \alpha_i} \quad (5.9)$$

where  $\kappa$  is the set of subchannels where  $\frac{1}{\alpha_i + w} < \nu^* < \frac{1}{\alpha_i + u}$ ,  $k$  is the number of subchannels in this set and  $c$  is the number of subchannels where  $\nu^* \leq \frac{1}{\alpha_i + w}$ . To implement the dual constraint approach the following algorithm may be used:

---

**Algorithm 5.1** Waterfilling with Dual Constraints  $u, w$

---

- 1:  $c \leftarrow 0$
  - 2: Waterfill across all  $m$  channels with constraint  $x_i \geq u$ .
  - 3: **while**  $\max\{x_i^*\} \geq w$  **do**
  - 4:    $x_{\max}^* \leftarrow w$
  - 5:    $c \leftarrow c + 1$
  - 6:   Recalculate  $\nu^*$  from (5.9).
  - 7:   Waterfill across remaining  $m - c$  channels with constraint  $x_i \geq u$ .
  - 8: **end while**
- 

### 5.1.4 Perturbation and Sensitivity Analysis

In the convex optimization of waterfilling, strong duality<sup>3</sup> holds [54]. Hence, if we view the constraint,  $x_i \geq u$ , as a *perturbation* of the original constraint,  $x_i \geq 0$ , an upper bound can be found to the solution of the modified waterfilling

---

<sup>3</sup>Strong duality means that the solution to the problem is both primal and dual optimal [54].

problem in terms of the the optimal capacity. Using the analysis in [54], we can show that

$$p^*(u) \geq p^*(0) + \sum_{i=1}^m \zeta_i^* u, \quad (5.10)$$

where  $p^*(a)$  is the optimal value of (2.42) with the constraint  $x_i \geq a$ . Hence,  $p^*(0)$  is the solution to the original problem. Converting this into capacity results using (2.41) gives the upper bound:

$$C(u) \leq C_{\text{opt}} - \sum_{i=1}^m \zeta_i^* u, \quad (5.11)$$

where  $C_{\text{opt}}$  is the classic waterfilling solution and  $C(u)$  is the capacity with inequality constraint,  $x_i \geq u$ . Examination of (5.11) leads to two key points:

1. The penalty in the upper bound is proportional to  $u$ . Thus increasing  $u$  will tend to increase the difference between the optimal and modified solutions.
2. The penalty increases with  $\zeta_i^*$ . From the original solution,  $\zeta_i^* \neq 0$  only if  $x_i^* = 0$ . Thus, if a channel has no power in the original system it will cause the modified system be further from optimal.

To find  $\zeta_i^*$ , we set  $x_i^* = 0$  in the 5<sup>th</sup> KKT equation of the waterfilling problem. This gives

$$\zeta_i^* = \nu^* - \frac{1}{\alpha_i}, \quad (5.12)$$

where  $\nu^*$  is calculated from (2.47).

The upper bound in (5.11) using (5.12) is shown in Fig. 5.1 for a large  $n_r = n_t = 12$  ( $12 \times 12$ ) single-user MIMO system with  $\zeta^* = [0, \dots, 0, 0.7734, 2.1782, 3.5453, 4.5983, 4.7447]^T$ . The size of the system chosen for this example is large to ensure that some values of  $\zeta_i^*$  are positive, and it also mimics a broadcast system with large  $t$  or  $K$ . The classical solution to waterfilling is at  $u = 0$  and equal power is at  $u = 1/12 = 0.0833$ . Note that the bound becomes tight for low values of  $u$  which is the interesting case.

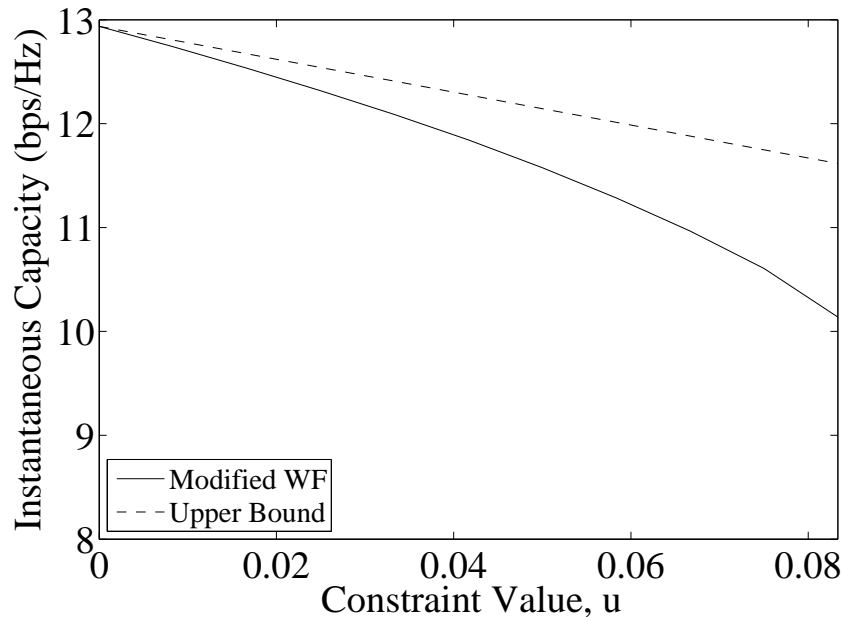


Figure 5.1: Perturbation analysis for a  $12 \times 12$  MIMO system with constraint-modified waterfilling.

## 5.2 Utility Functions

In this section, in order to allow us to be able to adjust certain properties of the waterfilling results, we maximize a modified capacity expression. Note that in (2.42), the waterfilling solution can produce large  $x_i$  values at the expense of some channels where  $x_i = 0$ . To increase fairness,  $x_i$  in (2.42) is replaced with a utility function,  $U(x_i)$ , which has the property of increasing small  $x_i$  values and reducing large  $x_i$  values. This encourages fairness at the expense of suboptimal capacity performance. This approach results in the following optimization problem:

$$\min_{x_i : x_i \geq 0, \sum_{i=1}^m x_i = 1} - \sum_{i=1}^m \log [\alpha_i + U(x_i)] \quad (5.13)$$

for some non-negative function  $U(x_i)$ .<sup>4</sup> This leads to the following KKT conditions for  $i = 1, \dots, m$ :

$$\begin{aligned} x_i^* &\geq 0, & \mathbf{1}^T \mathbf{x}^* &= 1, & \lambda_i^* &\geq 0, \\ \lambda_i^* x_i^* &= 0, & \frac{-U'(x_i^*)}{\alpha_i + U(x_i^*)} - \lambda_i^* + \nu^* &= 0. \end{aligned} \quad (5.14)$$

Evaluating the last two conditions gives us either  $x_i^* = 0$  or, if  $x_i^* > 0$ , the solution:

$$\nu^* = \frac{U'(x_i^*)}{\alpha_i + U(x_i^*)}. \quad (5.15)$$

We can now apply the generalized solution in (5.15) with a variety of utility functions in order to see their effects on both capacity and fairness. The optimization problem in (5.13)-(5.15) results in the power allocations,  $x_1^*, x_2^*, \dots, x_m^*$ . These values are then used in (2.41) to compute the corresponding rate.

### 5.2.1 Nonlinear Utility Functions

In pursuit of utility functions that encourage channel fairness we start with the straightforward case of  $U(x_i) = x_i^s$  for some value of  $s$  which is non-negative.<sup>5</sup>

Using (5.15), we find that

$$\nu^* = \frac{s(x_i^*)^{s-1}}{\alpha_i + (x_i^*)^s}. \quad (5.16)$$

We need to solve Equation (5.16) to find  $x_1^*, x_2^*, \dots, x_m^*$  and hence the resulting suboptimal rate. The solution of (5.16) is split into three cases:  $0 < s < 1$ ,  $s = 1$  and  $s > 1$ .

Case 1:  $s = 1$ : This is the special case of standard waterfilling, where  $\nu^* = \frac{1}{\alpha_i + x_i^*}$ . The solution to this can be found using (2.45).

---

<sup>4</sup>Note that we concentrate on monotonic increasing utility functions.

<sup>5</sup>Negative  $s$  values are ruled out due to the non-concavity of  $\log(\alpha_i + x_i^s)$ .

Case 2:<sup>6</sup>  $s > 1$ : We define  $\gamma = s - 1 > 0$  and rewrite (5.15) as:

$$(x_i^*)^{1+\gamma} - \left( \frac{1+\gamma}{\nu^*} \right) (x_i^*)^\gamma + \alpha_i = 0. \quad (5.17)$$

Rearranging (5.17), we can write

$$(x_i^*)^\gamma \left( x_i^* - \frac{1+\gamma}{\nu^*} \right) = -\alpha_i. \quad (5.18)$$

From (5.18) we see that a real non-zero solution can only be found if

$$-\alpha_i > \min_{x_i^* \in [0, 1]} \left\{ (x_i^*)^{1+\gamma} - \frac{1+\gamma}{\nu^*} (x_i^*)^\gamma \right\}. \quad (5.19)$$

To find the minimum in (5.19), we differentiate (5.18) to give:

$$(1+\gamma)(x_i^*)^\gamma - \frac{\gamma(1+\gamma)}{\nu^*} (x_i^*)^{\gamma-1} = 0. \quad (5.20)$$

Rearranging (5.20), we have

$$(x_i^*)^\gamma (1+\gamma) \left[ 1 - \frac{\gamma}{\nu^*} \frac{1}{x_i^*} \right] = 0, \quad (5.21)$$

which has the solutions  $x_i^* = \frac{\gamma}{\nu^*}$  and  $x_i^* = 0$ . Using  $x_i^* = \frac{\gamma}{\nu^*}$  in (5.19), we find

$$\alpha_i > \frac{\gamma^\gamma}{(\nu^*)^{\gamma+1}}. \quad (5.22)$$

Note that if (5.22) does not hold, from (5.18) we see that  $x_i^* = 0$ , as is the case sometimes in standard waterfilling.

Case 3:  $0 < s < 1$ : We define  $\delta = 1 - s$  ( $s = 1 - \delta$ ) and rewrite (5.15) as:

$$(x_i^*)^{1-\delta} - \frac{1-\delta}{\nu^*} (x_i^*)^{-\delta} + \alpha_i = 0. \quad (5.23)$$

---

<sup>6</sup>For this case,  $\log(\alpha_i + x_i^s)$  is not necessarily concave, and thus the answer is only locally optimal in some cases.

Rearranging (5.23), we write

$$\begin{aligned} x_i^* + \alpha_i(x_i^*)^\delta - \left(\frac{1-\delta}{\nu^*}\right) &= 0 \\ x_i^* + \alpha_i(x_i^*)^\delta &= \left(\frac{1-\delta}{\nu^*}\right). \end{aligned} \quad (5.24)$$

We can now solve Equation (5.24) using nested numerical methods, along with the constraint  $\mathbf{1}^T \mathbf{x}^* = 1$ , to find both  $\nu^*$  and  $\mathbf{x}^*$ . In certain special cases, such as  $\delta = 0.5$ , analytical solutions are also available. Inspection of case 3 leads to Theorem 1.

**Theorem 1.** *For the case where  $U(x_i) = x_i^s$  for  $0 < s < 1$ , the solution is fair, i.e.  $x_i^* \neq 0$  for all  $i$ .*

*Proof.* Take two values from the vector  $\mathbf{x}^*$ ;  $x_i^*$  and  $x_j^*$ , where  $i \neq j$ . Using the fact that the right hand side of (5.24) is constant for all  $i, j$ , we have

$$x_i^* + \alpha_i(x_i^*)^\delta = x_j^* + \alpha_j(x_j^*)^\delta. \quad (5.25)$$

Setting  $x_j^* = 0$  in (5.25), we can write

$$\begin{aligned} x_i^* + \alpha_i(x_i^*)^\delta &= 0 \\ \Rightarrow \alpha_i(x_i^*)^\delta &= -x_i^*. \end{aligned} \quad (5.26)$$

Since, by definition,  $\alpha_i \geq 0$ ,  $x_i^* \geq 0$  and  $0 < \delta < 1$ , (5.26) only holds when  $x_i^* = 0$ . This means that if  $x_j^* = 0$ ,  $x_i^* = 0$  and thus all values of  $\mathbf{x}^*$  are zero. However by the optimization constraint,  $\mathbf{1}^T \mathbf{x}^* = 1$ , this cannot be the case and thus  $x_i^* \neq 0$  for all  $i$ .  $\square$

### 5.2.2 Linear Utility Functions

Another simple subset of viable utility functions are linear functions of the form  $U_i(x_i) = a_i x_i + b_i$ . Note that in its most general form,  $U(x_i)$  need not be the same for all  $i$ . However, not selecting a constant function,  $U_i(x_i) = U(x_i)$ , creates a very complicated solution in all situations except the linear case. Substituting  $U_i(x_i) = a_i x + b$  into (5.15), we find that

$$\begin{aligned} \nu^* &= \frac{a_i}{\alpha_i + a_i x_i^* + b_i} \\ \Rightarrow x_i^* &= \max \left\{ \frac{1}{\nu^*} - \hat{\alpha}_i, 0 \right\}, \end{aligned} \quad (5.27)$$

where  $\hat{\alpha}_i = \frac{\alpha_i - b_i}{a_i}$ . Note the derivation of (5.27) is very similar to that of classical waterfilling and is thus omitted.

A special case of linear utility functions is that where  $b_i = 0$  and  $a_i = a > 1$  for all  $i$  and thus  $\hat{\alpha}_i = \alpha_i/a$ . Since, by definition,  $\alpha_i = 1/\rho\lambda_i$ ,  $a > 1$  produces waterfilling at a higher effective SNR. This is very beneficial to fairness as it is well known that at high SNR, the fairness of waterfilling increases. However, it does come at a detrimental cost to capacity.

### 5.2.3 Utility Function Example

In theorem 1, we showed that  $U(x_i) = x_i^s$  for  $0 < s < 1$  gives a fair allocation of power. However, calculating the resulting capacity for an arbitrary value of  $s$  requires nested numerical methods. For certain values of  $s$  we can remove one level of numerical solution. For example, letting  $s = 0.5$  gives  $U(x_i) = x_i^{1/2}$  and (5.15) becomes:

$$\nu^* = \frac{(1/2)(x_i^*)^{-1/2}}{\alpha_i + (x_i^*)^{1/2}}. \quad (5.28)$$

Rearranging (5.28) and denoting  $y_i = (x_i^*)^{1/2}$  gives:

$$y_i^2 + \alpha_i y_i - \frac{1}{2\nu^*} = 0. \quad (5.29)$$

Taking the positive solution of (5.29) gives:

$$y_i = \frac{-\alpha_i + \sqrt{\alpha_i^2 + \frac{2}{\nu^*}}}{2},$$

$$x_i^* = \left[ \frac{-\alpha_i + \sqrt{\alpha_i^2 + \frac{2}{\nu^*}}}{2} \right]^2. \quad (5.30)$$

The final step is using the optimization constraint,  $\mathbf{1}^T \mathbf{x}^* = 1$ , to calculate the value of  $\nu^*$ . This gives:

$$\sum_{i=1}^m \left[ \frac{-\alpha_i + \sqrt{\alpha_i^2 + \frac{2}{\nu^*}}}{2} \right]^2 = 1. \quad (5.31)$$

We must solve equation (5.31) numerically to find the multiplier  $\nu^*$  and then (5.30) can be used to find  $x_i^*$ .

### 5.2.4 Concavity Preservation

The function  $-\sum_{i=1}^m \log(\alpha_i + x_i)$ , which appears in the original waterfilling problem, is convex by nature. Hence, the special features of convex optimization hold, including the fact that a local minimum is a *global* minimum. For a utility function to give an optimization with the same properties, the function  $\sum_{i=1}^m \log(\alpha_i + U(x_i))$  must be concave.

**Theorem 2.** *The function  $g(x_i) = \log(\alpha_i + U(x_i))$  is concave if*

$$(\alpha_i + U(x_i))U''(x_i) \leq (U'(x_i))^2$$

for all  $x_i \geq 0$ .

*Proof.* The simplest test for concavity is that  $g''(x_i) \leq 0$  for all  $x_i$  within the

domain of the problem ( $\mathbf{dom} x \Rightarrow x_i \geq 0$ ). Differentiating  $g(x_i)$  we find

$$\begin{aligned} g'(x_i) &= \frac{U'(x_i)}{\alpha_i + U(x_i)}, \\ g''(x_i) &= \frac{(\alpha_i + U(x_i))U''(x_i) - (U'(x_i))^2}{(\alpha_i + U(x_i))^2}. \end{aligned} \quad (5.32)$$

Hence for  $g(x_i)$  to be concave requires

$$(\alpha_i + U(x_i))U''(x_i) \leq (U'(x_i))^2, \quad (5.33)$$

for all  $x_i \geq 0$ . □

**Corollary 1.** *If  $U(x_i)$  is real and non-negative for all  $x_i \in \mathbf{dom} x$ , then  $g(x_i)$  is concave if  $U''(x_i) \leq 0$  for all  $x_i \in \mathbf{dom} x$ .*

*Proof.* Since  $U(x_i)$  is real and non-negative,  $(U'(x_i))^2 \geq 0$  for all  $x_i \in \mathbf{dom} x$ . Noting that this also implies  $\alpha_i + U(x_i)$  is real and positive, (5.33) can be contracted to  $U''(x_i) \leq 0$ . □

**Corollary 2.** *If  $U(x_i)$  is real, non-negative and linear for all  $x_i \in \mathbf{dom} x$ ,  $g(x_i)$  is concave.*

*Proof.* Use Corollary 1, noting the fact that since  $U(x_i)$  is linear,  $U''(x_i) = 0$ . □

As an example let  $U(x_i) = x_i^s$ . Now (5.33) gives:

$$\begin{aligned} (\alpha_i + x_i^s)(s(s-1))x_i^{s-2} &\leq s^2x_i^{2s-2} \\ \alpha_i s(s-1)x_i^{s-2} + (s^2 - s)x_i^{2s-2} &\leq s^2x_i^{2s-2} \\ \alpha_i s(s-1)x_i^{s-2} &\leq sx_i^{2s-2}. \end{aligned} \quad (5.34)$$

This can be shown to hold for  $0 \leq s \leq 1$ , never hold for  $s < 0$  and hold only for certain values of  $\alpha_i$  if  $s > 1$ .

Many functions can be proposed as utility functions. However they need to preserve concavity and satisfy  $U(x_i) \geq 0$ , for all  $0 \leq x \leq 1$ . More complicated

functions may not lead to closed form solutions using the KKT conditions and other techniques such as interior-point methods may be required [54]. Note that the solutions found using any methods must be feasible for all  $\alpha_i > 0$ .

## 5.3 Multiuser Applications

Modifications to the waterfilling algorithm have been proposed to promote fairness amongst the subchannels. In a single-user link this has limited application, however in multiuser MIMO systems, fairness is a key issue. Thus it is appropriate to use the modified waterfilling algorithms in the multiuser domain. We consider the ITWF algorithm in [17]. To form a modified-ITWF, we look at Algorithm 2 of [17]. Step 2 of this algorithm uses waterfilling over a “single-user” effective channel  $\mathbf{G}$ . We can replace this step with a modified algorithm from Secs. 5.1 or 5.2.

### 5.3.1 Convergence Analysis

In order to ensure that ITWF works with the new utility function algorithms, they must not affect the convergence properties of ITWF. This leads us to the following theorem.

**Theorem 3.** *Modified waterfilling using a utility function converges if the function  $g(x_i) = \log[\alpha_i + U(x_i)]$  is concave for all  $\alpha_i > 0$ .*

*Proof.* This proof stems from the proofs of Theorems 2 and 3 of [17]. First we note that the utility function modifications only change Step 2 of Algorithm 2. Hence it is sufficient to show that the modified Step 2 has the same properties as those in the original theorems.

Theorem 2 states that Algorithm 1 in [17] converges partly due to the fact that the solution in the maximization in Step 2 has a unique solution. It is straightforward to show that as long as  $g(x_i)$  is concave, the properties

of convex optimization apply, and amongst them is the fact that the solution is globally optimal and unique. Thus, the modified waterfilling algorithm converges if we use Algorithm 1.

The other feature of Algorithm 2 that is different from Algorithm 1 is the averaging step. Theorem 3 of [17] states that Algorithm 2 converges if Algorithm 1 converges, which we have just demonstrated, and if the averaging step is non-decreasing. Noting that the function for optimization,  $f^{\text{exp}}$ , as defined in [17] and (5.35), is identical (only the definition of  $\mathbf{S}$  has changed) the proof in [17] can be used. The one difference between modified waterfilling and the original is the possible non-concavity of the log det function. Thus, for the proof in [17] to hold,  $f^{\text{exp}}$  must be concave. In the modified waterfilling case, we can write  $f^{\text{exp}}$  as:

$$\begin{aligned} f^{\text{exp}} &= \frac{1}{K} \sum_{i=1}^K \log_2 \left| \mathbf{I} + \mathbf{H}_i^\dagger \mathbf{S}_i^{(n)} \mathbf{H}_i + \sum_{j \neq i} \mathbf{H}_j^\dagger \mathbf{Q}_j^{(n-1)} \mathbf{H}_j \right|, \\ &= \frac{1}{K} \sum_{i=1}^K \log_2 \left| \mathbf{I} + \hat{\mathbf{G}}_i^\dagger \mathbf{S}_i^{(n)} \hat{\mathbf{G}}_i \right|, \end{aligned} \quad (5.35)$$

where  $\hat{\mathbf{G}}_i = \mathbf{H}_i (\mathbf{I} + \sum_{j \neq i} \mathbf{H}_j^\dagger \mathbf{Q}_j^{(n-1)} \mathbf{H}_j)^{-1/2}$ . Using (2.40), (2.41) and (5.13) this becomes:

$$f^{\text{exp}} = \frac{1}{K} \sum_{i=1}^{Km} \left\{ \log_2[\hat{\alpha}_i + U(x_i)] + \log_2(\rho \hat{\lambda}_i) \right\}, \quad (5.36)$$

where  $\hat{\alpha}_i = 1/\rho \hat{\lambda}_i$  and  $\hat{\lambda}_i$  is the  $i^{\text{th}}$  eigenvalue of  $\hat{\mathbf{G}}_i$ . From (5.36) it can be seen that  $f^{\text{exp}}$  is concave if  $g(x_i) = \log_2[\hat{\alpha}_i + U(x_i)]$  is concave. Thus the modified version of Algorithm 2 converges since we have chose  $U(x_i)$  to ensure this<sup>7</sup>.  $\square$

Now we again look at waterfilling with modified constraints. For the modifications not to affect ITWF convergence, Step 2 of Algorithm 2 [17] must

---

<sup>7</sup>See Sec. 5.2.4.

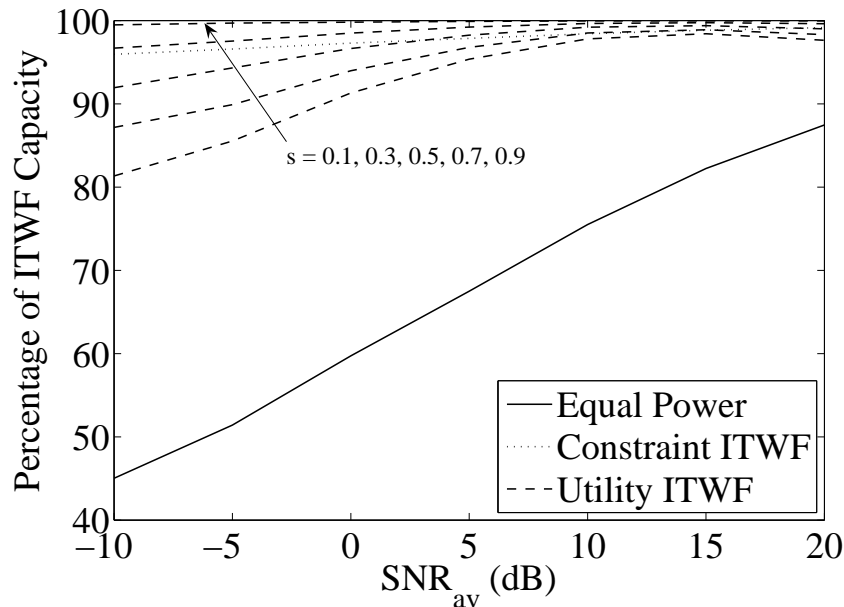


Figure 5.2: Capacity comparisons for a three user (2,4) MIMO-BC system.

result in a unique solution. Since waterfilling with modified constraints does not change the convexity of the optimization problem, a unique solution will exist if a feasible solution exists. Thus, in order for ITWF with modified constraints to converge, the constraints must allow a feasible solution.

## 5.4 Simulation Results

All our simulations were carried out in a shadow fading environment using the model in Sec. 2.12.1. The value,  $A$ , was adjusted to ensure that the mean user SNR was equal to  $\text{SNR}_{\text{av}}$ . We assume each user had the same number of receive antennas, i.e.  $n_{r_i} = n_r = 2$  for  $i = 1, \dots, m$  and  $n_t = 4$  (a (2,4) system). We used the utility function  $U(x_i) = x_i^s$  with varying values of  $s$  as indicated on the figures. We set the constraint value,  $u$ , at 10% of the equal power allocation,  $u = 0.1\rho/Kn_r$ .

Figure 5.2 shows that using waterfilling in any form gives a sizeable gain over equal power especially in the low-SNR region. Note that the results for

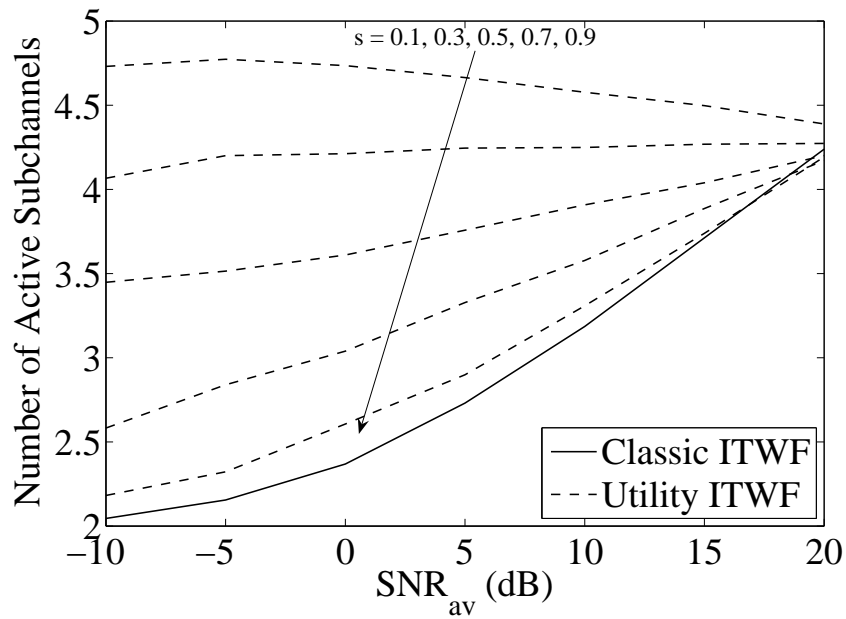


Figure 5.3: Comparison of the number of active subchannels for a three user (2,4) MIMO-BC system.

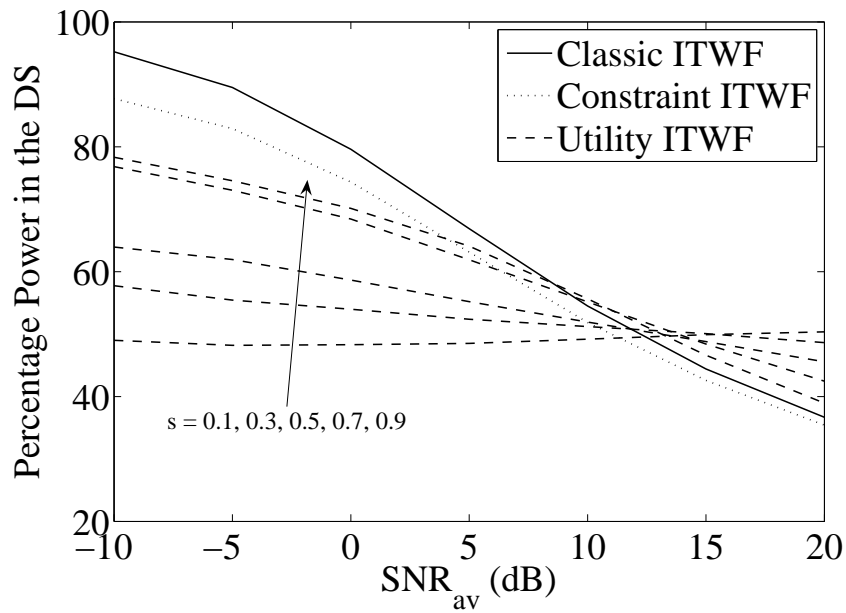


Figure 5.4: Percentage power in the dominant subchannel (DS) for a three user (2,4) MIMO-BC system.

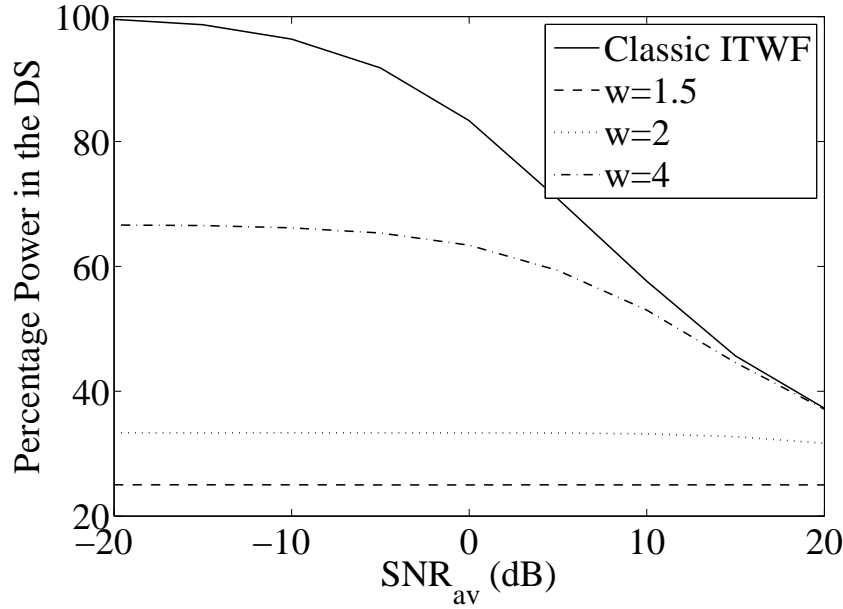


Figure 5.5: Percentage power in the dominant subchannel (DS) for ITWF with a per-channel maximum power constraint for a three user (2,4) MIMO-BC system.

$s \in \{0.7, 0.9\}$  always give higher capacity than the extra constraint approach and achieve more than 95% of ITWF capacity. However, this capacity comes at a cost as seen in Fig. 5.3 which shows the number of active subchannels. Although, by Theorem 1, all subchannels have  $x_i > 0$  for the utility function case,  $x_i$  can still be small. Thus, we define an active subchannel as one with power  $x_i \geq 0.1\rho/Kn_r$  (more than 10% of the equal power allocation). Hence the extra constraint solutions (which are not shown) have all 6 subchannels active. From Figs. 5.2 and 5.3 we can see that decreasing  $s$  allows a considerable increase in fairness with a reasonably small loss in capacity.

Another good measure of system fairness is the power in the dominant subchannel as shown in Fig. 5.4. The utility function approach is less sensitive to SNR and performs well in the low-SNR region. However, at high SNR, classic ITWF and minimum power constraint ITWF become superior.

In Figs. 5.5 and 5.6 we examine ITWF with a maximum per-subchannel power constraint. In the plots,  $w$  is the amount the constraint is above an

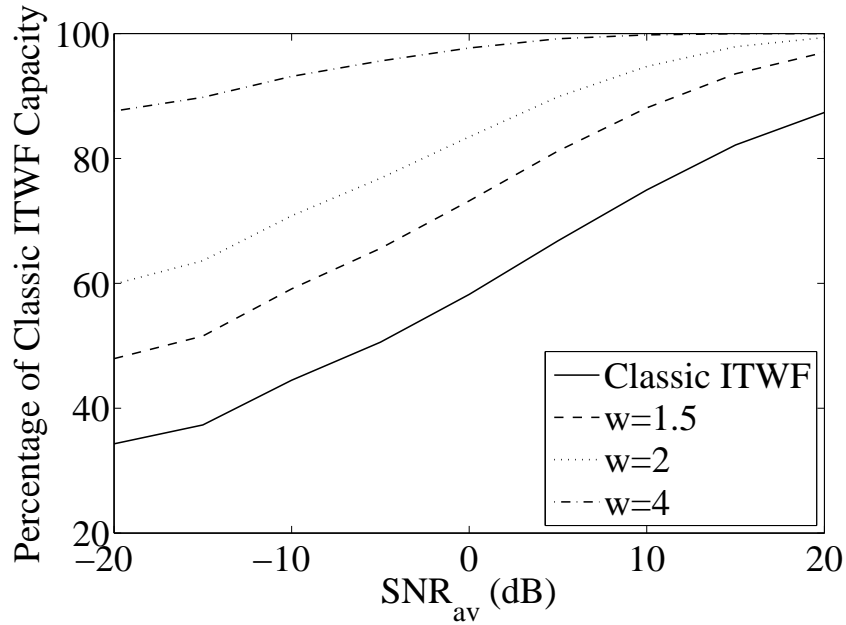


Figure 5.6: Capacity comparisons for ITWF with a per-channel maximum power constraint for a three user (2,4) MIMO-BC system.

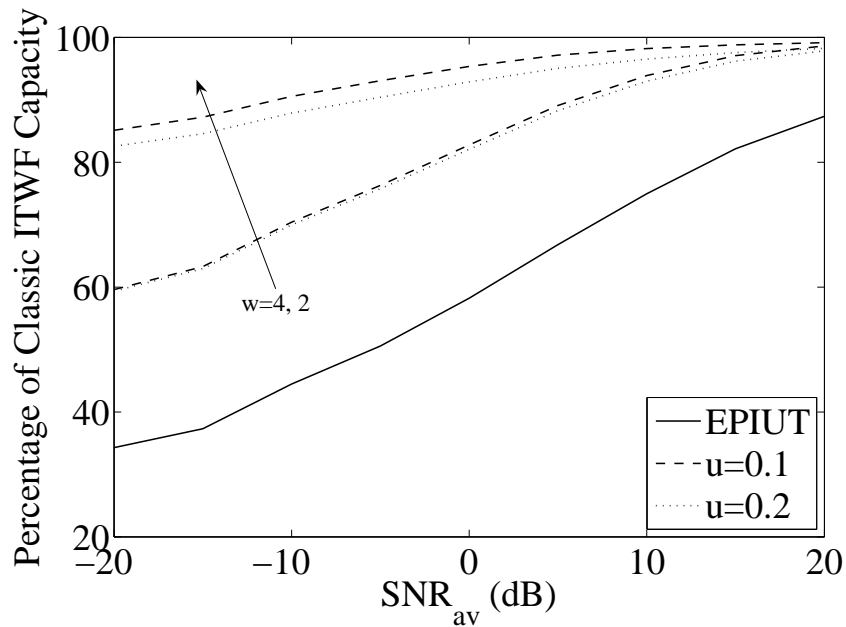


Figure 5.7: Capacity comparisons for ITWF with dual constraints for a three user (2,4) MIMO-BC system.

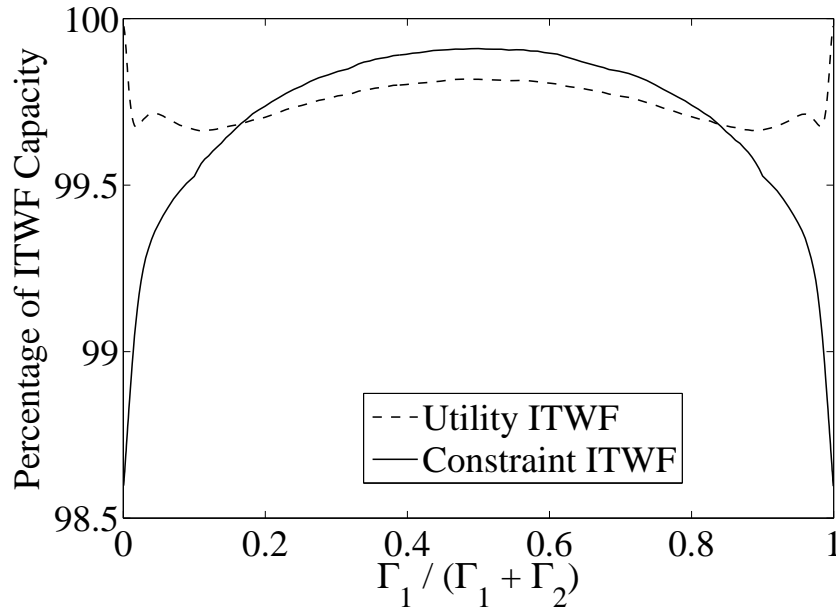


Figure 5.8: Percentage of ITWF capacity achieved in a two user (2,4) MIMO-BC system for varying values of the link gains,  $\Gamma_i$ .

equal power allocation,  $\rho/Kn_r$ , with  $w = 1$  being equal power. In the (2,4) three user system shown,  $w = 6$  is equivalent to having no constraint at all. These figures show that maximum power constraints have an excellent effect on reducing the power in the dominant subchannel but have a detrimental effect on capacity, especially when the constraint is too tight. Figure 5.7 shows the capacity comparison between a few dual constraint systems.<sup>8</sup> It is key to note that the maximum power constraints have a stronger detrimental effect on the capacity than the minimum power constraints.

In Fig. 5.8 we compare the two new algorithms for a two-user MIMO-BC system in a channel with differing link gains. In Fig. 5.8 the value of  $\text{SNR}_{\text{av}}$  is fixed by setting  $\Gamma_1 + \Gamma_2 = 2$  but the relative sizes of  $\Gamma_1$  and  $\Gamma_2$  are varied. The utility function, with  $U(x_i) = x_i^{1/2}$ , performs better than the constraint version for large differences in link gains. At approximately equal link gains the constraint function approach outperforms the utility function.

Figures 5.9 and 5.10 show both the power in the dominant subchannel and

<sup>8</sup>Parameter  $u$  in these plots is also a function of  $\rho/Kn_r$ .

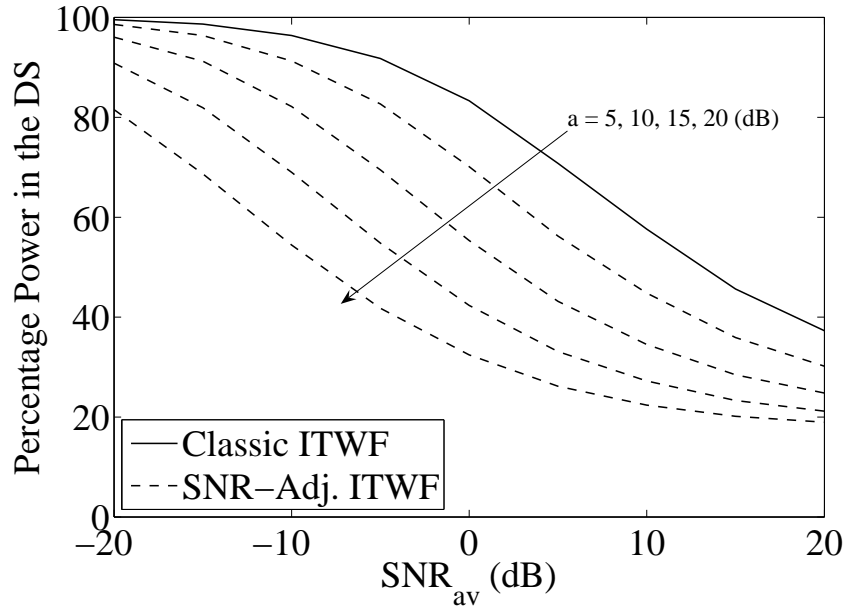


Figure 5.9: Percentage power in the dominant subchannel (DS) for SNR-adjusted ITWF for a three user (2,4) MIMO-BC system.

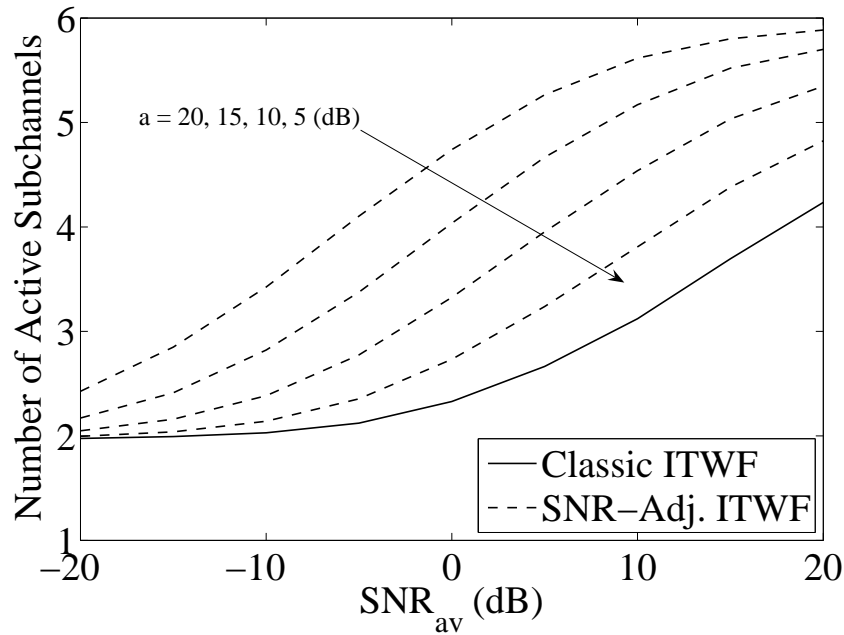


Figure 5.10: Comparison of the number of active subchannels for SNR-adjusted ITWF for a three user (2,4) MIMO-BC system.

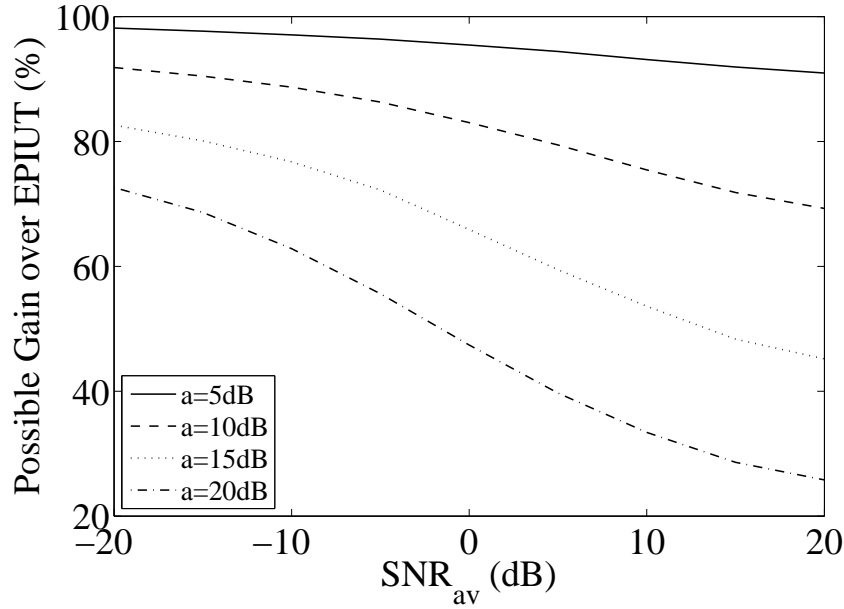


Figure 5.11: Percentage gain over EPIUT for SNR-adjusted ITWF (standard ITWF = 100%) for a three user (2,4) MIMO-BC system.

the number of active channels for SNR-adjusted ITWF. This is the case where a linear utility function is used with the value  $U(x_i) = ax_i$  as discussed in Sec. 5.2.2. From the figures we see that adjusting the value of  $a$  can be viewed as a simple SNR shift of  $a$  (dB) of the original ITWF values and an increase in fairness. However, Fig. 5.11 shows that too large an increase in  $a$  can have a large detrimental effect on capacity, especially at higher SNR values.

## 5.5 Summary

In this chapter we have proposed two modifications to the waterfilling algorithm, based on ‘hard’ and ‘soft’ minimum power allocations. These provide powerful and flexible techniques for increasing multiuser MIMO system fairness without a significant degradation in the overall sum rate. In particular, the novel approach based on a set of utility functions,  $U(x) = x^s$ , can be tuned by the parameter,  $s$ , to trade off sum-rate with fairness. In addition, the utility function  $U(x) = x^{1/2}$  provides a good balance between sum rate, fairness and

complexity.

## Chapter 6

# Collaborative MIMO: Broadcast Channel Capacity

A key application of the MIMO techniques discussed in the previous chapters is in cellular networks. However, in such systems, the intercell co-channel interference becomes a major drawback [24, 26, 27]. Recently, the use of BS collaboration has been proposed to help mitigate this interference [28–31]. Possible collaboration methods include dirty paper coding [28, 84], zero-forcing beamforming [28, 31] and many others. The drawback for most of these techniques is the large amount of feedback required to convey CSI between the cells.

Another technique for reducing interference is transmitter power control. In the downlink this works by adjusting the total output power for each BS in an attempt to mitigate interference, while maintaining a satisfactory intracell link. Examples of this approach for single antenna links are given in [43, 44, 85–87]. However, as for the other techniques, optimal power control still requires BS collaboration and a significant amount of feedback and processing. Despite this, near optimal power control can exist in systems with very limited channel information at the base stations, unlike dirty paper or beamforming techniques. This leads to increased capacity without a large increase in overhead.

In Secs. 6.1 - 6.4, we look at the problem of MIMO multicell power allocation. Firstly, we formulate the sum-rate equation for such a system from results in [24, 25]. Then, building on the work by Badruddin *et. al.* [45], we find a

set of solutions to the power optimization problem. Due to the non-convexity of the aforementioned problem, no one solution is guaranteed to be globally optimal. Thus, to find the global optimum, we need to search amongst all possible cases. In order to reduce the complexity, we propose a more practical algorithm than the brute force approach. This algorithm achieves the optimal rate in the vast majority of scenarios.

The simulation results show that optimal power allocation is almost always the trivial case where a BS is either switched off or transmits at maximum power. Hence, the most important problem, ignoring fairness and scheduling issues, is to select the cells which should remain on. We show that this can be done extremely accurately using only the link gain information so that no CSI is required for the channel matrices. Furthermore, we show that for larger numbers of collaborating cells and higher SNR the scenario where one or more BS is switched off becomes more important.

It is important to note that this is a theoretical upper bound. In a practical system, it is highly unlikely that a cell would be fully turned off for a prolonged time for the benefit of the system at the expense of their own users. Thus, we show via simulations that using a multicell multiple access scheme such as frequency-division multiple access (FDMA) can produce gains over the all on state whilst maintaining quality of service to all users.

On the other hand, in Sec. 6.5 we give an example of full collaboration on a small scale. In Sec. 6.5, we transform adjacent sectorized cells into unsectorized macro-cells using collaboration between adjacent BSs only. We demonstrate that this provides significant gains over an interference-limited system and indicates that full collaboration, even on a small scale, can provide significant gains.

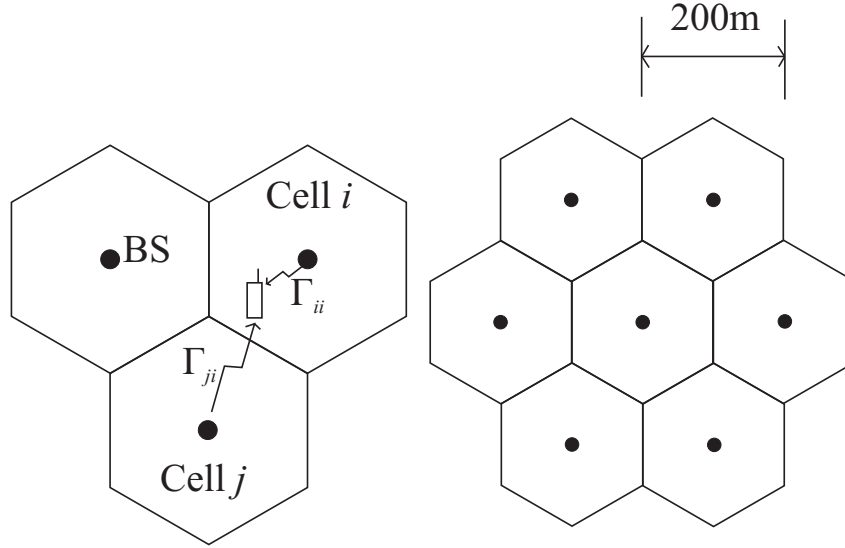


Figure 6.1: Layouts of both 3-cell (left) and 7-cell (right) cellular systems.

## 6.1 System Model and Capacity Results

In this chapter we consider a set of neighbouring cells, specifically focussing on sets of 3 and 7 hexagonal cells as shown in Fig. 6.1. These cells each contain a single-user MIMO link with the BS located at the centre and a mobile station (MS) randomly located in the hexagon.

### 6.1.1 Cell Clusters

We consider a set of  $K$  cells each with a single user MIMO system with  $n_t$  transmit antennas and  $n_r$  receive antennas. The link equation for a single-user MIMO link in a generic cell is given by

$$\mathbf{y} = \mathbf{H}\mathbf{x} + \mathbf{n} + \mathbf{i}, \quad (6.1)$$

where  $\mathbf{i}$  is a  $n_r \times 1$  vector representing interference from all the other cells in the cluster. This multicell MIMO system has capacity,  $C_i$ , for cell  $i$ , where  $C_i$

is given by [25]

$$C_i = \log_2 \frac{|\mathbf{I}_{n_r} + \rho_i \Gamma_i \mathbf{W}_i + \sum_{j=1, j \neq i}^K \rho_j \Gamma_{ji} \mathbf{W}_{ji}|}{|\mathbf{I}_{n_r} + \sum_{j=1, j \neq i}^K \rho_j \Gamma_{ji} \mathbf{W}_{ji}|} \text{ bps/Hz}, \quad (6.2)$$

where  $\mathbf{W}_i = \mathbf{H}_i \mathbf{H}_i^\dagger$  and  $\mathbf{W}_{ji} = \mathbf{H}_{ji} \mathbf{H}_{ji}^\dagger$ . In (6.2),  $\mathbf{H}_i$  is the complex channel matrix for cell  $i$ ,  $\mathbf{H}_{ji}$  is the complex channel matrix between BS  $j$  and MS  $i$ ,  $\Gamma_{ji}$  is the link gain of the link between BS  $j$  and MS  $i$  and  $\rho_i = \frac{P_i}{n_t \sigma^2}$  is a measure of the SNR of cell  $i$  where  $P_i$  is the transmit power of BS  $i$ . Note that this model assumes no CSI at the transmitter.

Whilst (6.2) gives the instantaneous capacity for each cell, we can calculate the mean capacity over the fast (Rayleigh) fading using techniques from [52] (see Sec. 2.9). Given a set of slow-fading parameters, in [52] it is shown that:

$$\mathbb{E}_H\{C_i\} = \mathcal{C}(Kn_t, n_r, \mathbf{D}_1^{(i)}) - \mathcal{C}((K-1)n_t, n_r, \mathbf{D}_2^{(i)}) \quad (6.3)$$

where<sup>1</sup>

$$\mathbf{D}_1^{(i)} = \text{diag}(\rho_{1i} \Gamma_{1i}, \dots, \rho_{ii} \Gamma_{ii}, \dots, \rho_{Ki} \Gamma_{Ki}),$$

$$\mathbf{D}_2^{(i)} = \text{diag}(\rho_{1i} \Gamma_{1i}, \dots, \rho_{Ki} \Gamma_{Ki}).$$

and  $\mathcal{C}(t, r, \Phi)$  is given in Sec. 2.9.

## 6.2 Optimization

In any cluster of cells we wish to maximize the sum-rate whilst only adjusting the power levels at each transmitter. These levels lie within the ranges  $0 \leq P_i \leq P_{\max, i}$ , due to the transmission limitations of each BS. Without loss of generality, we assume that all the transmitters have the same maximum power, that is  $P_{\max, i} = P_{\max}$ . Thus, we define the optimization problem for

---

<sup>1</sup>Note that the diagonal matrix,  $\mathbf{D}_2^{(i)}$ , does not contain the direct link term,  $\rho_{ii} \Gamma_{ii}$ .

the sum-rate as:

$$S^* = \max_{0 \leq P_i \leq P_{\max}, i = 1, \dots, K} S, \quad (6.4)$$

where  $S = \sum_{i=1}^K R_i$  and  $R_i$  is the rate for cell  $i$  which is given by [25]:

$$R_i = \log_2 \frac{|\mathbf{I}_{n_r} + P_i \bar{\Gamma}_i \mathbf{W}_i + \sum_{j=1, j \neq i}^K P_j \bar{\Gamma}_{ji} \mathbf{W}_{ji}|}{|\mathbf{I}_{n_r} + \sum_{j=1, j \neq i}^K P_j \bar{\Gamma}_{ji} \mathbf{W}_{ji}|} \text{ bps/Hz}, \quad (6.5)$$

where  $\bar{\Gamma}_i = \frac{\Gamma_i}{n_i \sigma^2}$ . Defining the Lagrangian for the minimization version of (6.4), noting there is no sum-power constraint, we write

$$L(\mathbf{P}, \boldsymbol{\zeta}) = -S - \sum_{i=1}^K \zeta_{1_i} P_i + \sum_{i=1}^K \zeta_{2_i} (P_i - P_{\max}) \quad (6.6)$$

where  $\mathbf{P} = (P_1, P_2, \dots, P_K)$ ,  $\boldsymbol{\zeta} = (\zeta_{1_1}, \dots, \zeta_{1_K}, \zeta_{2_1}, \dots, \zeta_{2_K})$  and  $\zeta_{1_i}, \zeta_{2_i}$  are the Lagrange multipliers associated with the inequality constraints. The Karush-Kuhn-Tucker (KKT) conditions associated with (6.5) are [54]:

$$\begin{aligned} -P_i^* &\leq 0, & P_i^* - P_{\max}^* &\leq 0, & \zeta_{1_i}^* &\geq 0, & \zeta_{2_i}^* &\geq 0, \\ \zeta_{1_i}^* P_i^* &= 0, & \zeta_{2_i}^* (P_i^* - P_{\max}^*) &= 0, \\ \frac{\partial S^*}{\partial P_i^*} - \zeta_{1_i}^* + \zeta_{2_i}^* &= 0. \end{aligned} \quad (6.7)$$

Taking the final KKT condition in (6.7) and multiplying by  $P_i^*(P_i^* - P_{\max}^*)$ , we have

$$\begin{aligned} P_i^*(P_i^* - P_{\max}^*) \frac{\partial S^*}{\partial P_i^*} - P_i^*(P_i^* - P_{\max}^*) \zeta_{1_i}^* \\ + P_i^*(P_i^* - P_{\max}^*) \zeta_{2_i}^* = 0 \end{aligned} \quad (6.8)$$

Using the 5<sup>th</sup> and 6<sup>th</sup> KKT conditions in (6.7), equation (6.8) gives

$$P_i^*(P_i^* - P_{\max}^*) \frac{\partial S^*}{\partial P_i^*} = 0. \quad (6.9)$$

Equation (6.9) has three sets of solutions:

$$P_i^* = 0, \quad P_i^* = P_{\max}, \quad \frac{\partial S^*}{\partial P_i^*} = 0. \quad (6.10)$$

Whilst the first two solutions given in (6.10) are straightforward, the third solution is harder to find. Setting  $\mathbf{A}_{ji} = \bar{\Gamma}_{ji} \mathbf{W}_{ji}$ , we can rewrite  $S$  as

$$\begin{aligned} S = & \sum_{i=1}^K \log_2 \left| \mathbf{I}_{n_r} + P_i \mathbf{A}_{ii} + \sum_{j=1, j \neq i}^K P_j \mathbf{A}_{ji} \right| \\ & - \sum_{i=1}^K \log_2 \left| \mathbf{I}_{n_r} + \sum_{j=1, j \neq i}^K P_j \mathbf{A}_{ji} \right| \text{ bps/Hz.} \end{aligned} \quad (6.11)$$

Using the property,  $\frac{\partial}{\partial P} \log |P\mathbf{X} + \mathbf{Y}| = \text{Tr}[(P\mathbf{X} + \mathbf{Y})^{-1} \mathbf{X}]$  [88], (6.11) can be differentiated to give

$$\begin{aligned} \frac{\partial S}{\partial P_i} = & \frac{1}{\log 2} \left( \frac{\partial}{\partial P_i} \log_2 \left| \mathbf{I}_{n_r} + P_i \mathbf{A}_{ii} + \sum_{j=1, j \neq i}^K P_j \mathbf{A}_{ji} \right| \right) \\ & - \frac{1}{\log 2} \left( \sum_{j=1, j \neq i}^K \frac{\partial}{\partial P_i} \log_2 \left| \mathbf{I}_{n_r} + P_i \mathbf{A}_{ij} + \sum_{k \neq j, k=1}^K P_k \mathbf{A}_{kj} \right| \right) \\ = & \frac{1}{\log 2} \text{Tr} \left[ \left( \mathbf{I}_{n_r} + P_i \mathbf{A}_{ii} + \sum_{j=1, j \neq i}^K P_j \mathbf{A}_{ji} \right)^{-1} \mathbf{A}_{ii} \right] \\ & - \frac{1}{\log 2} \sum_{j=1, j \neq i}^K \text{Tr} \left[ \left( \mathbf{I}_{n_r} + P_i \mathbf{A}_{ij} + \sum_{k \neq j, k=1}^K P_k \mathbf{A}_{kj} \right)^{-1} \mathbf{A}_{ij} \right]. \end{aligned} \quad (6.12)$$

Setting  $\frac{\partial S^*}{\partial P_i^*} = 0$  and solving (6.12) gives a polynomial of order  $Kn_r - 1$  in  $P_i$ . This can be seen by writing the inverse matrices in (6.12) as  $(P_i \mathbf{F} + \mathbf{G})^{-1} = \text{adj}(P_i \mathbf{F} + \mathbf{G}) |P_i \mathbf{F} + \mathbf{G}|^{-1}$ , where  $\text{adj}(\mathbf{A})$  is the adjugate of the matrix  $\mathbf{A}$ . Multiplying through by the determinants gives a polynomial expression in  $P_i$  which can be identified as having order  $Kn_r - 1$ . Since  $P_i = 0$  and  $P_i = P_{\max}$  are also candidate solutions, there are up to  $Kn_r + 1$  possible feasible values for  $P_i$  and  $K$  powers to be allocated. Furthermore, since (2.32) is non-convex,

it is difficult to find the global maximum value without evaluation of all these possible combinations of solutions.

There are two fundamental problems here: firstly, the overhead in computing all the solutions and secondly, the need for full network CSI (all  $\mathbf{W}_i$  and  $\mathbf{W}_{ji}$  matrices) to compute (6.11) or (6.12). Hence, we consider two trivial simplifications:

- We consider only the  $2^K$  power allocations where  $P_i \in \{0, P_{\max}\}$ ;
- We maximize  $E_H(S)$  rather than  $S$ , so that the  $\mathbf{W}_i$ ,  $\mathbf{W}_{ji}$  matrices are not required.

Furthermore, to avoid the search over the  $2^K$  ON/OFF possibilities, we now derive a the simplified algorithm.

## 6.3 Practical Algorithm

To reduce the optimal search across the  $2^K$  possible ON/OFF solutions we propose a simple, practical algorithm for efficiently finding a near optimal sum rate. Note that the algorithm is ad-hoc in nature but not only approaches the best ON/OFF solution but is also very close to the global optimum where results are available. Our idea is to start with all BSs transmitting at  $P_{\max}$ . Then, one at a time, we switch off an individual BS. If all the sum-rates with  $K - 1$  BSs operational are the less than the original, then our policy is to use all BSs. If some of the sum-rates are higher than the original, then the highest is chosen and our policy is to switch one BS off. Then we repeat the procedure to see if it beneficial to switch off another BS. We repeat this algorithm until no further gains are achieved. Our approach is summarized in Algorithm 6.1 below. This simplified search avoids the tree structure of the optimal method and simplifies the problem from  $O(2^K)$  capacity calculations to  $O(K^2)$ .

---

**Algorithm 6.1** A simplified ON/OFF selection algorithm
 

---

```

1:  $P_i \leftarrow P_{\max}$  for all  $i$ 
2: repeat
3:   Calculate sum rate,  $S$ 
4:   for  $i = 1 \rightarrow K$  do
5:      $P_i \leftarrow 0$ 
6:     Calculate sum rate,  $S_i$ 
7:      $P_i \leftarrow P_{\max}$ 
8:   end for
9:   if  $\max(S_i) > S$  then
10:     $P_i \leftarrow 0$  for  $i$  corresponding to  $\max(S_i)$ 
11:   end if
12: until  $\max(S_i) \leq S$ 

```

---

## 6.4 Power Allocation to One Dominant User

Given any cluster of cells, the maximum sum rate occurs when at least one cell has full power. We use this property later and therefore give the following proof. For any cell,  $i$ , the effect of a small global increase in power can be described by,  $P_i = (1 + \varepsilon)P_i$ . This results in a rate for cell  $i$ ,  $\bar{R}_i$ , given by:

$$\begin{aligned}
\bar{R}_i &= \log_2 |\mathbf{I}_{n_r} + (1 + \varepsilon)P_i \bar{\Gamma}_i \mathbf{W}_i \\
&\quad + \sum_{j=1, j \neq i}^K (1 + \varepsilon)P_j \bar{\Gamma}_{ji} \mathbf{W}_{ji}| \\
&\quad - \log_2 |\mathbf{I}_{n_r} + \sum_{j=1, j \neq i}^K (1 + \varepsilon)P_j \bar{\Gamma}_{ji} \mathbf{W}_{ji}| \text{ bps/Hz.} \tag{6.13}
\end{aligned}$$

Setting  $\mathbf{F} = P_i \bar{\Gamma}_i \mathbf{W}_i$  and  $\mathbf{G} = \sum_{j=1, j \neq i}^K P_j \bar{\Gamma}_{ji} \mathbf{W}_{ji}$ , we can show that  $\bar{R}_i \geq R_i$  or:

$$\log_2 \frac{|\mathbf{I}_{n_r} + (1 + \varepsilon)(\mathbf{F} + \mathbf{G})|}{|\mathbf{I}_{n_r} + (1 + \varepsilon)\mathbf{G}|} \geq \log_2 \frac{|\mathbf{I}_{n_r} + \mathbf{F} + \mathbf{G}|}{|\mathbf{I}_{n_r} + \mathbf{G}|}. \tag{6.14}$$

Rearranging (6.14), we have

$$\begin{aligned} |\mathbf{I}_{n_r} + (1 + \varepsilon)(\mathbf{F} + \mathbf{G})| |\mathbf{I}_{n_r} + \mathbf{G}| &\geq \\ |\mathbf{I}_{n_r} + \mathbf{F} + \mathbf{G}| |\mathbf{I}_{n_r} + (1 + \varepsilon)\mathbf{G}|. \end{aligned} \quad (6.15)$$

Using the determinant property,  $|\mathbf{AB}| = |\mathbf{A}||\mathbf{B}|$ , we finally write

$$\begin{aligned} |\mathbf{I}_{n_r} + \mathbf{G} + (1 + \varepsilon)(\mathbf{F} + \mathbf{G}) + (1 + \varepsilon)(\mathbf{F} + \mathbf{G})\mathbf{G}| &\geq \\ |\mathbf{I}_{n_r} + \mathbf{F} + \mathbf{G} + (1 + \varepsilon)\mathbf{G} + (1 + \varepsilon)(\mathbf{F} + \mathbf{G})\mathbf{G}|, \end{aligned} \quad (6.16)$$

which reduces to

$$|\mathbf{E} + \varepsilon(\mathbf{F} + \mathbf{G})| \geq |\mathbf{E} + \varepsilon\mathbf{G}|, \quad (6.17)$$

where  $\mathbf{E} = \mathbf{I}_{n_r} + \mathbf{F} + 2\mathbf{G} + (1 + \varepsilon)(\mathbf{F} + \mathbf{G})\mathbf{G}$ . Since  $\mathbf{F}$  and  $\mathbf{G}$  are positive semi-definite, (6.17) holds and therefore (6.14) holds. This shows that a small global increase in power will increase each cell's rate and thus the sum rate. This means that the system should increase its power so that at least one BS is capped at  $P_{\max}$ .

## 6.5 Three Cell Collaboration

Now we consider a system of three adjacent cells as in Fig. 6.2(a). We divide each cell evenly into three sectors, each with an even share of directional antennas. This is shown in Fig. 6.2(b). Note that no frequency reuse is required, as interference between the sectors is eliminated using directional antennas. Thus, we assume that the only interfering sectors for the MIMO-BC are those adjacent to the sector in question, but in different cells<sup>2</sup>. Now, we can construct a macro-cell from the three adjacent sectors as shown in Fig. 6.3. This involves collaboration of CSI data between the three BSs, BS<sub>1</sub>, BS<sub>2</sub> and BS<sub>3</sub>, to form an effective collaborative BS (CBS) for the macro-cell. This is only a

---

<sup>2</sup>We assume that interference from further away cells is negligible and is ignored.

very low level of collaboration as each BS would only need partial CSI from its adjacent cells to achieve gains. We give a comparison of the systems with and without collaboration in Fig. 6.4.

To obtain the sum rate of users within the macro-cell, we employ the ITWF algorithm. However, our implementation of ITWF needs to be slightly different due to the diversified nature of the CBS. In the single BS version of ITWF, it is assumed that the cell is not sectorized and the algorithm is free to allocate all its power over a single antenna. However, in the collaborative case, we have an extra power constraint. This is due to the fact that one-third of the power must be allocated across the antennas of each BS<sub>*i*</sub>. Defining  $\Sigma_i$  as the transmit covariance matrix from the CBS to user *i*, the additional constraint can be expressed as

$$\begin{aligned} \sum_{i=1}^{t/3} d_{ii} &\leq P, \\ \sum_{i=t/3+1}^{2t/3} d_{ii} &\leq P, \\ \sum_{i=2t/3+1}^t d_{ii} &\leq P, \end{aligned} \tag{6.18}$$

where the diagonal matrix  $\mathbf{D}$ , with elements  $d_{ii}$ , is defined as

$$\mathbf{D} = \text{diag} \left( \sum_{i=1}^K \Sigma_i \right). \tag{6.19}$$

To acquire the optimal sum rate for this system would require using a modified version of the ITWF algorithm with these extra power constraints included. However, creation of this modified algorithm would be very difficult, due to the fact that ITWF is constructed and performed in the MAC domain and the constraints are in the BC domain. Thus, instead of changes to the ITWF algorithm, we perform scaling on the BC covariance matrices. After we find

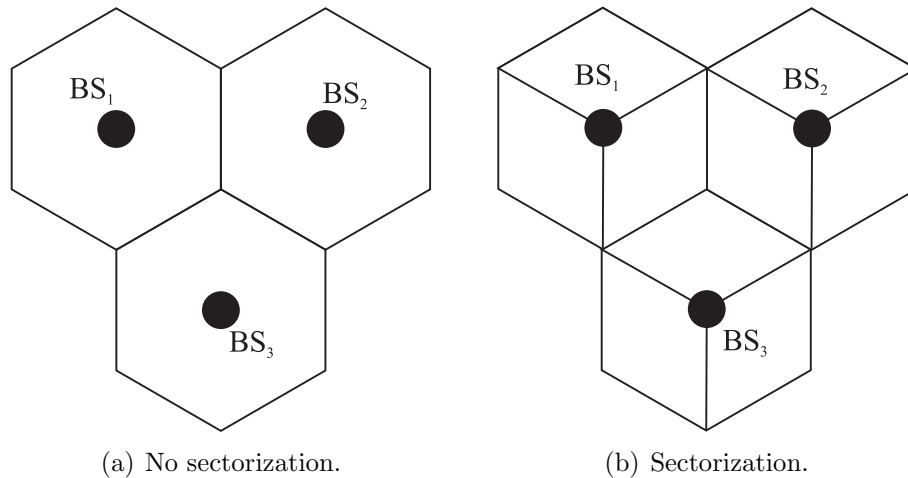


Figure 6.2: Original three cell system.

the optimal solution with ITWF, the resultant MAC covariance matrices are then converted to their BC duals (see Sec. 2.3.3) [19]. We then scale the resulting BC covariance matrices so that the constraints of (6.18) are met in the maximum. This ensures that each BS does not exceed its maximum allowed transmit power whilst still attempting to keep the sum-rate to near optimal levels. Hence, this procedure provides a lower bound on the optimal sum capacity that could be achieved if a modified version of ITWF was employed. The true optimal sum-rate lies between this lower bound and the upper bound of ITWF without these constraints.

## 6.6 Simulation Results

All of our simulations were carried out in a shadow fading environment using the model in Sec. 2.12.1. We adjusted the value,  $A$ , to ensure that the mean SNR of the user at the cell edge ( $r = 100\text{m}$ ) was given by a fixed cell-edge SNR value (see Figs. 6.5-6.8). This mean SNR was averaged over the shadow fading. Note that  $\text{SNR}_{\text{edge}} = \text{SNR}_{\text{av}} - 19.52\text{dB}$ .

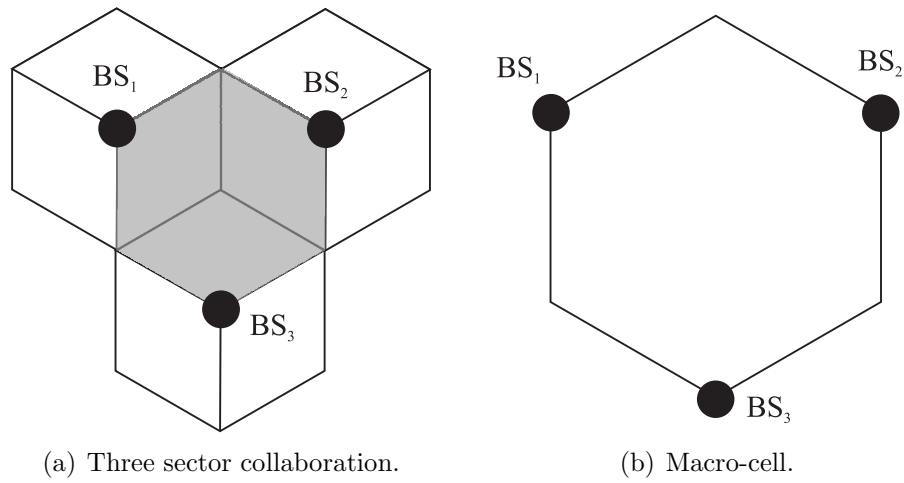


Figure 6.3: Three sector collaboration and equivalent macro-cell.

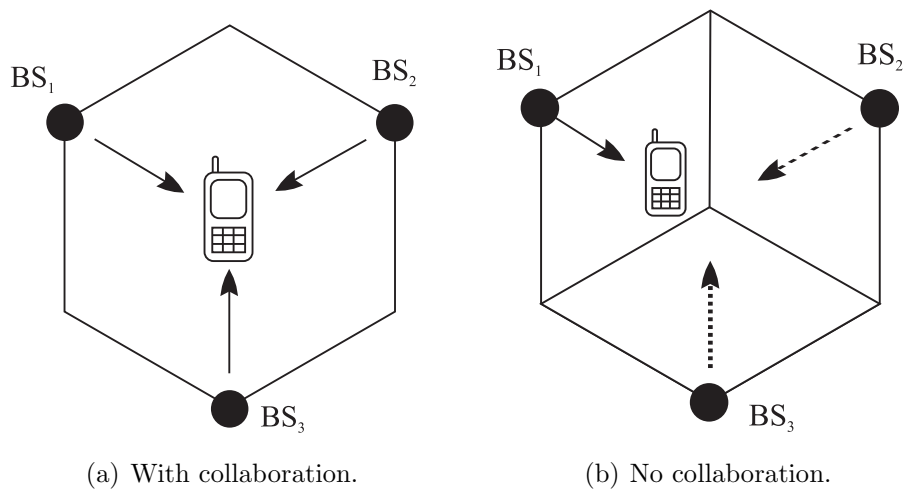


Figure 6.4: Three cell collaboration system comparison (solid lines refer to desired signals and dashed lines refer to interfering signals).

### 6.6.1 Power Control

In each cell we consider a (2,2) MIMO system so that  $n_r = n_t = 2$ . In future work, larger MIMO systems should be considered to see whether any fundamental change in the nature of the results occurs with larger numbers of antennas.

Our first set of simulation results are shown in Table 6.1. Here, we consider a two cell system and it is possible to find the globally optimal power allocation. This is achieved by setting  $P_1 = P_{\max}$ , solving (6.9) for  $P_2$  and then comparing this solution with that obtained by setting  $P_2 = P_{\max}$  and solving (6.9) for  $P_1$ . The largest sum-rate is the optimal power allocation since at least one of the cells must use maximum power (see Sec. 6.4 for a proof). The resulting optimal power allocation gives a sum-rate which is almost identical to the sum-rate given by the simple policy where each BS is either OFF or operating at  $P_{\max}$  as shown in Table 6.1. This motivates our focus in this chapter on power allocation policies which are either ON or OFF. In future work it is desirable to see if this property still holds for larger number of cells.

In Fig. 6.5, we compare the best ON/OFF allocation over all  $2^K$  possibilities with the results of Algorithm 6.1. In these simulation results the rates are computed from (6.5), so the instantaneous channel matrices are used. For both the 3- and 7-cell scenarios the simplified algorithm is virtually optimal.

In Fig. 6.6, three allocation policies are considered. The simplest approach is “All On” where  $P_i = P_{\max}$ , for all  $i = 1, 2, \dots, K$ . The best ON/OFF solution is labeled “Opt(Sim)”. This best sum-rate is achieved by searching all  $2^K$  possibilities using the instantaneous channel matrices. A similar policy computes  $E_H(S)$  for all  $2^K$  possibilities and records the best option. The instantaneous sum-rate for this option is then recorded. Note that this policy, denoted “Opt(Ana)”, uses the analytical mean values of (6.5) using the result in (6.3). Hence, no channel matrices are required.

Figure 6.6 shows two key points. Firstly, it shows that selection based on

Cell-Edge SNR (dB)	-10	0	10	20
Percentage	100	100	99.99	99.99

Table 6.1: Percentage of the Optimal Capacity Achieved by a 2-cell ON/OFF Selection System

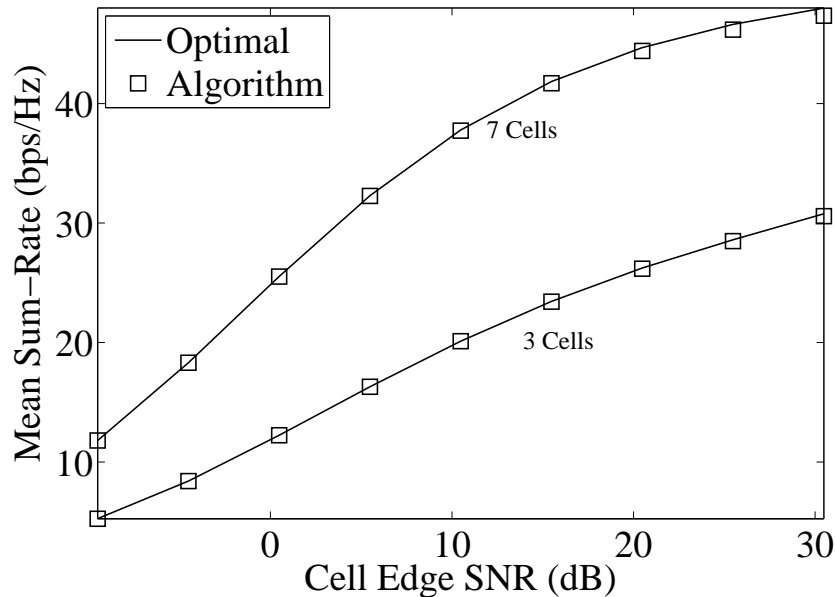


Figure 6.5: Comparison of mean sum-rates for Algorithm 6.1 with the optimal ON/OFF solution.

mean sum-rates (requiring only the  $\Gamma$  values), is approximately equal to the instantaneous capacity selection. This indicates that the link gains and slow fading have a more significant effect on the capacity than the fast Rayleigh fading. Secondly, it shows that power management does provide significant gains over an “All On” approach especially at higher transmit powers and for larger numbers of cells. Also note that as expected, the mean sum-rate for the “All On” approach reaches a ceiling when the gains due to increased power are balanced by increasing interference. Also shown in Fig. 6.6 are the mean sum-rate values (shown by the circles) evaluated using (6.3). These match the simulated means for the “All On” case and provide a check on the analytical results used to select the BSs in the absence of any CSI for the channel matrices.

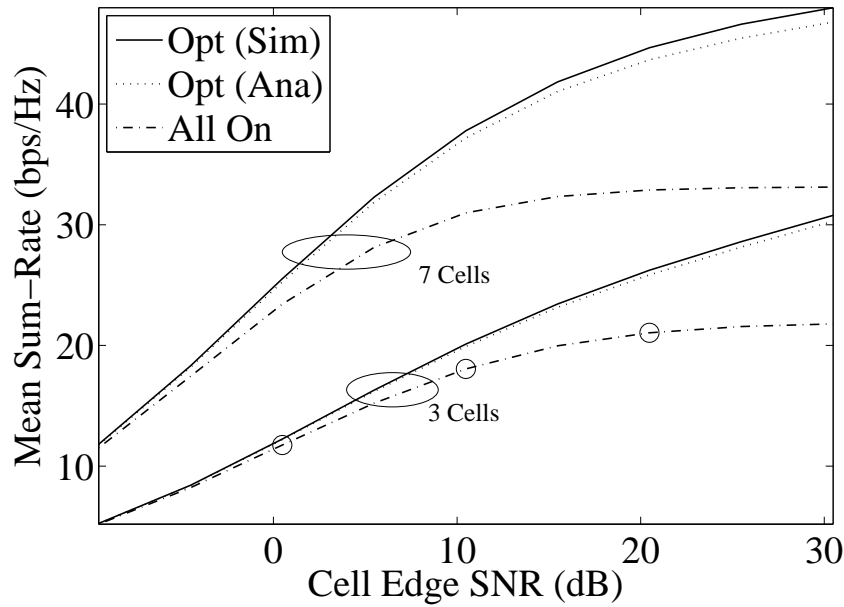


Figure 6.6: Comparison of mean sum-rates for 3-cell and 7-cell systems with various allocation policies.

Figure 6.7 shows the distribution of the number of active cells in the optimum ON/OFF solution versus SNR for a 3-cell system. At lower SNR, when the magnitude of interference is less, using all 3 cells simultaneously is preferred in most cases (approximately 70% of the time the “All On” approach is best at -10dB SNR). However, when the SNR increases, the use of all 3 cells decreases and the use of 2 out of 3 cells starts to dominate.

Thus, with the optimal or suboptimal power allocations some cells will not be active at certain points in time. To address this, a multiple-access scheme such as FDMA can be used to give weighted time/frequency allocations to two sets of cells. Set 1 is operational in frequency slot 1 and set 2 is operational in frequency slot 2. We consider a very simple approach where the set 1 cells operate in a frequency band of  $RF \times BW$  Hz, where  $0 \leq RF \leq 1$  is a reuse factor and  $BW$  is the total bandwidth used by the original system. The set 2 cells then operate in a frequency bin of size  $(1 - RF) \times BW$  Hz. The overall sum rate for comparison is the weighted combination of the individual sum rates for the two sets of cells. The final selection of which cells are in each set

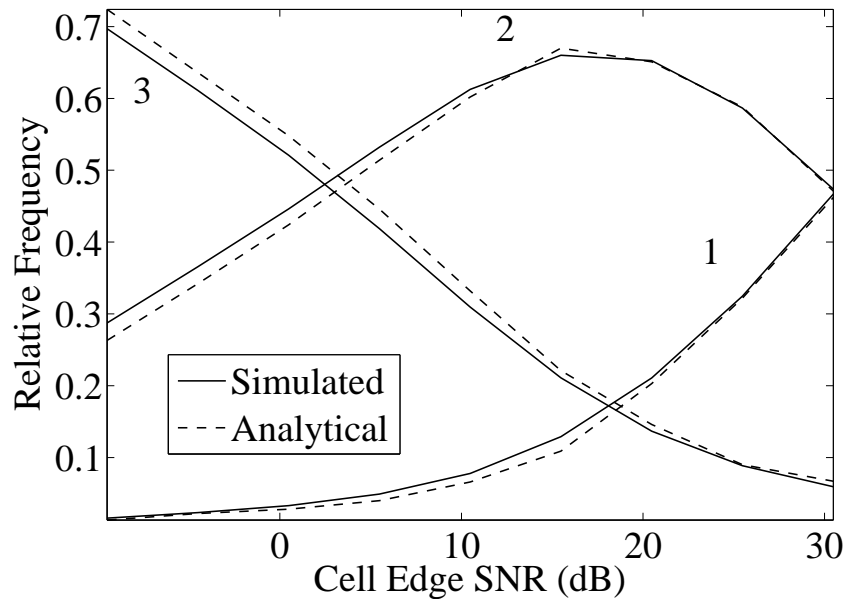


Figure 6.7: Distribution of active cells for a 3-cell system (number of active cells is labeled).

is determined by choosing the maximum of the weighted sum rates.

Figure 6.8 shows such a FDMA scheme with various values of RF. The dynamic allocation strategy (dyn) shown in Fig. 6.8 uses a dynamic reuse factor equal to the number of cells in set 1 divided by the total number of cells. The all on state in Fig. 6.8 has  $RF = 1$ , corresponding to the original system where all cells occupy the full bandwidth. Figure 6.8 shows that sum-rate improvements can be achieved, even when fairness issues are considered. However, with the simple FDMA scheme shown, the advantages of power control are only realized at high SNR. Note that the advantages occur at lower SNR for higher numbers of cells. Hence, with coordination over a larger cluster, say 19 cells, the FDMA scheme may be beneficial at realistic cell-edge SNR values.

### 6.6.2 Three Cell Collaboration

Table 6.2 shows the result of three-cell collaboration for various systems. It shows a number of systems, each with either two or three users per sector (i.e.

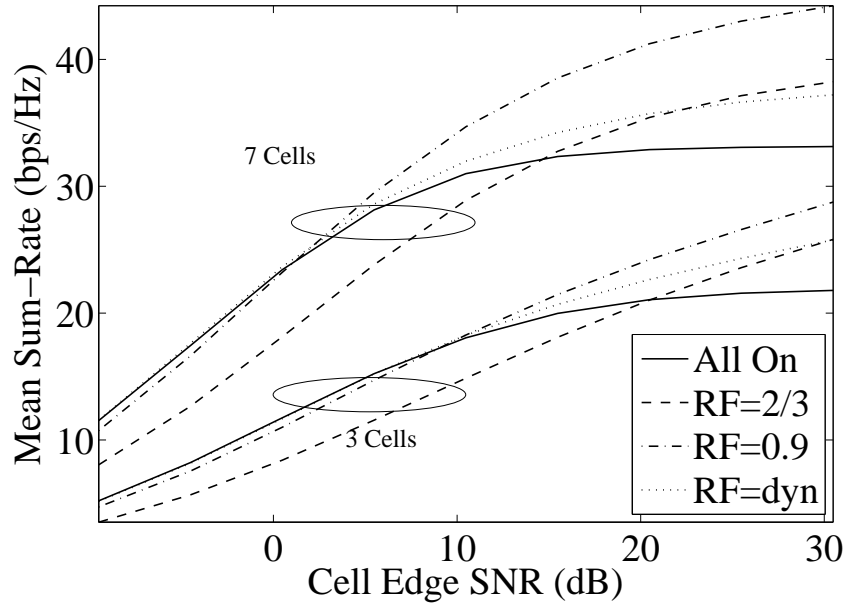


Figure 6.8: Comparison of different FDMA reuse factors.

the CBS has six or nine users). The four different algorithms we employ are as follows:

1. ITWF without the extra power constraints. This is a theoretical upper bound on the collaborative sum rate, as it allows power distributions which exceed the per BS power constraints. This is denoted **ITWF**.
2. ITWF with the extra power constraints applied afterwards. This is denoted **ITWF(P<sub>n</sub>)**. This is a lower bound on the optimal sum-rate. Note that the optimal sum-rate will be between the values given by **ITWF** and **ITWF(P<sub>n</sub>)**.
3. A single three-sector cell ignoring interference from adjacent cells. This is denoted **SingleC**. The available power is allocated using standard sum power ITWF techniques.
4. A single three-sector cell, taking into account interference from neighbouring sectors as noise. Power is also allocated using ITWF. This is denoted **SingleC(w/Int)**.

System	ITWF	ITWF(Pn)	SingleC	SingleC(w/Int)
2 Users $2 \times 2$	11.6	11.0	9.96	6.93
3 Users $2 \times 2$	14.3	13.9	12.7	9.04
2 Users $2 \times 4$	16.5	15.8	14.0	9.83
2 Users $4 \times 4$	23.2	22.2	20.4	14.3
3 Users $2 \times 4$	20.6	19.9	18.3	13.0
3 Users $4 \times 4$	28.4	27.6	25.9	18.5

Table 6.2: Sum-Rates (in bps/Hz) for Different Levels of 3-cell Collaboration ( $\text{SNR}_{\text{av}} = 14.7\text{dB}$ )

Two key points come from Table 6.2. Firstly, the table shows the effects of interference on cellular MIMO systems. In all systems the loss from interference (comparing **SingleC** with **SingleC(w/Int)**) is between 29-30%. This is a significant loss in throughput and provides the motivation for mitigating schemes such as collaboration. Secondly, Table 6.2 shows that, using collaboration, the gains over the interference limited case (comparing **ITWF(Pn)** with **SingleC(w/Int)**) can be from 49% (for the 3 user  $4 \times 4$  system) up to 60% (for the 2 user  $2 \times 4$  system). This indicates that even a very small amount of collaboration, as proposed here, can create very beneficial results.

## 6.7 Summary

In this chapter we have provided analysis and simulation results for cellular MIMO power control. We have also developed a fast, near-optimal algorithm to implement power control. The results show that power control can significantly boost the system throughput, especially at higher SNRs. However, both optimal and suboptimal power allocations often involve switching off one or more BSs. In response to this observation we have also shown that a multiple access policy such as FDMA could be used to improve system capacity whilst still providing some quality-of-service to all cells. Also, we have demonstrated that a small three cell collaboration scheme provides interference mitigation

without large amounts of network CSI at each BS. This shows that BS collaboration has advantages even on a small scale.



## Chapter 7

# Conclusions and Future Work

The main contributions and conclusions of the thesis are discussed below.

### 7.1 Conclusions

In Chapter 3, we studied the problem of antenna selection for single-user MIMO systems. Although the methods we used are not original, our analysis is novel and provides a very simple metric for evaluating the gains from antenna selection. This widely applicable analysis tool is not limited to antenna selection and can be used in a variety of MIMO systems. Our power scaling analysis technique is a convenient and intuitive approach to the rapid assessment of selection techniques in a variety of environments. We also introduced the novel method of PMWF in this chapter, which provides increased gains in the low-SNR regions at very little complexity.

In Chapter 4 we provided an in depth study of the broadcast channel. This highlighted many key points about this channel and its capacity, especially in a shadow fading environment. Firstly, we showed that user fairness cannot be taken for granted in highly variable channels. Although, capacity can be straightforwardly optimized, the resulting systems can lack user fairness, which may be key in providing quality service to all users within the system. Secondly, our work reinforces the fact that differing suboptimal methods favour different scenarios. For example, the equal power approach, EPIUT, is very

successful in the Rayleigh fading case, when users have equal link gains. However, when the link gains vary, such as in the case of shadowing, the EPIUT approach deteriorates and simple antenna selection and beamforming techniques become very close to optimal. Since, in the shadowing case, certain antenna selection techniques approach ITWF capacity, these can be used as a lower bound for ITWF with the possibility of closed-form analysis. Finally, we also show that various suboptimal methods can be modelled simply and effectively using an equivalent SNR metric derived from the work in Chapter 3.

Next, in Chapter 5 we looked at modifications to the highly powerful ITWF algorithm to increase system fairness without significant losses in sum capacity. This is based on modifying the underlying waterfilling algorithm. Firstly, when we apply simple constraints to the waterfilling algorithm, we ensure channel (and thus user) fairness. This is a very important point as it can also be used to provide minimum rates in some circumstances. Our analysis of these methods indicated that the losses in capacity due to increasing user fairness were dependent on both the gains in fairness and the fairness of the system before constraints were added. Thus, if the system encounters shadowing, the original system fairness will be low and the losses in capacity will be higher. Secondly, we have proposed a novel approach of using a utility function with the waterfilling algorithm providing a powerful and flexible way to ensure fairness without a large drop in overall capacity.

Finally, in Chapter 6 we studied the issues related to taking MIMO into the cellular environment. Whilst previous work has covered the areas of full collaboration between base stations and used techniques such as dirty paper coding to maximise network capacity, these methods required a large amount of CSI. We showed that gains could be made with only limited CSI knowledge by using transmitter power control in an attempt to mitigate intercell interference. We also showed that this power control can be approximated by a method with two simple states per cell yielding very little loss in overall sum rate. Finally, we gave an example of more intense collaboration that provided gains, where

a three-cell system can collaborate using methods discussed in Chapter 4.

## 7.2 Suggestions for Future Work

The key metric used throughout this thesis has been the sum capacity which is relevant when the MIMO link is used for multiplexing gain. However, the MIMO link can also be used for diversity gains, which are mostly measured using the bit error rate (BER). Algorithms aimed at optimizing multiplexing gain in general do not optimize diversity gains. A good example is the use of OSA in Chapter 3. In this thesis, optimal antenna selection is based on maximizing the link capacity. However a brief investigation of antenna selection to optimize BER has resulted in selections which can be quite different from the capacity selections. This also applies to NSA, which we have shown approaches optimality with regard to link capacity but does not necessarily approach optimality when applied to optimizing BER. Future research is needed to find simple selection methods which can optimize diversity gains or even optimize both multiplexing and diversity gains simultaneously. The same philosophy applies to the work in Chapter 4. In this chapter, all our calculations and derivations of suboptimal algorithms are based on maximizing multiplexing gains. Future work is needed to find suboptimal algorithms which can achieve high diversity gains in a variety of shadowing and shadowing-free environments.

The majority of this thesis is based upon the assumption of a flat-fading time-invariant Rayleigh channel. Although, we have done some work on Ricean and correlated Rayleigh channels in this thesis, it is an open area of research to apply the methods developed to other channel models. Also, time variation may have some part to play in fairness issues and needs to be looked at. Of more importance, due to fact that we have shown that slow fading can have more importance than fast fading, is the development of a model to map changes in slow fading over time. This would be due to movements in the

mobile users through a region containing shadowing objects. A study of the variations in slow fading would need to cover fairness effects as it is the link gain which primarily governs whether a user is on or off. Such studies would be able to statistically determine how long a user could be without a signal.

One key conclusion from Chapter 4 was that sub-optimal algorithms behave differently in different environments. An area of future work would be to adapt the type of suboptimal algorithm to the current channel environment. This would increase the sum rate effectively in all environments.

In Chapter 5 we provided a novel modification to the waterfilling algorithm by using utility functions. Whilst some utility functions were suggested, a large set of functions can be suitable for adjusting the algorithm to account for various properties such as fairness. Future work is needed to investigate such functions and see their effect on the waterfilling algorithm. Another area of future work springs up from Chapter 5. Whilst our work has been focused on MIMO capacity, waterfilling can be used in other areas of communication. One such area is the allocation of power across subchannels in an orthogonal frequency division multiplexing (OFDM) system. Many OFDM systems do not employ waterfilling in its general form, as the solutions increase certain channels to such an extent that the peak to average power ratio (PAPR) becomes too high. Use of a modified waterfilling algorithm applying maximum channel power constraints as discussed in Chapter 5 could be investigated to increase OFDM capacity without having too much of a negative effect on PAPR levels.

The majority of the work in this thesis is based on information theory. Thus, a key point of future work would be to implement these results in practical systems. Whilst the work in Chapter 3 would be relatively easy to implement, the work in Chapter 5 would be much more difficult to implement. However, the work in Chapter 6 would also be relatively simple to apply to a current MIMO cellular system with base station collaboration. Unfortunately, such systems are rare at this time, and thus this technology is a good candidate for future generation base stations.

## Appendix A

# Finding the Cumulative Distribution Function of the Ratio of Two Shadow Fading Link Gains

In this appendix, we derive an expression for the CDF of the ratio of two shadow-faded and distance-attenuated link gains. This ratio is defined as follows:

$$Z = \frac{\Gamma_1}{\Gamma_2} = \frac{\exp(X_1)r_1^{-\gamma}}{\exp(X_2)r_2^{-\gamma}}, \quad (\text{A.1})$$

where  $\exp(X_1)$  and  $\exp(X_2)$  are lognormal variables representing the shadow fading to user 1 and user 2 respectively and  $r_1$  and  $r_2$  are the distances between MS 1 and the BS and MS 2 and the BS. For the case of uniform location of users in the annulus with inner radius,  $R_0$ , and outer radius,  $R$ , we can easily find the PDF of the distance as:

$$f(r) = \frac{2r}{R^2 - R_0^2} = ar, \quad (\text{A.2})$$

where  $a = 2/(R^2 - R_0^2)$  and  $R_0 < r < R$ . Defining the variables  $u = r_1/r_2$  and  $v = r_2$ , gives  $r_1 = uv$  and  $r_2 = v$ . Note that  $R_0 < uv < R$  and  $R_0 < v < R$ .

The joint PDF of the variables  $u$  and  $v$  is given by

$$f(u, v) = (auv)(av) \begin{vmatrix} v & u \\ 0 & 1 \end{vmatrix} = a^2 uv^3, \quad (\text{A.3})$$

in the region  $R_0 < uv < R$ ,  $R_0 < v < R$ . Integrating over  $v$  gives:

$$\begin{aligned} f(u) &= a^2 u \int_{\max(R_0, R_0/u)}^{\min(R, R/u)} v^3 dv \\ &= \frac{a^2 u}{4} [\min(R, R/u)^4 - \max(R_0, R_0/u)^4] \\ &= \begin{cases} \frac{a^2 u}{4} \left( R^4 - \frac{R_0^4}{u^4} \right), & u < 1 \\ \frac{a^2 u}{4} \left( \frac{R^4}{u^4} - R_0^4 \right), & u \geq 1 \end{cases}. \end{aligned} \quad (\text{A.4})$$

From (A.4) we can compute the CDF for the two different cases  $u < 1$  and  $u \geq 1$ . For the case  $u < 1$ :

$$\begin{aligned} F(u) &= \int_{R_0/R}^u f(t) dt \\ &= \frac{a^2}{4} \int_{R_0/R}^u R^4 t - R_0^4 t^{-3} dt \\ &= \frac{a^2}{8} \left[ R^4 t^2 + \frac{R_0^4}{t^2} \right]_{R_0/R}^u \\ &= \frac{a^2}{8} \left[ \left( R^4 u^2 + \frac{R_0^4}{u^2} \right) - \left( R^2 R_0^2 + R^2 R_0^2 \right) \right] \\ &= \frac{a^2}{8} \left( R^4 u^2 + \frac{R_0^4}{u^2} - 2R^2 R_0^2 \right). \end{aligned} \quad (\text{A.5})$$

For the case  $u \geq 1$ :

$$\begin{aligned}
F(u) &= \frac{a^2}{8}(R^4 + R_0^4 - 2R^2R_0^2) + \int_1^u \frac{a^2}{4} (R^4 t^{-3} - R_0^4 t) dt \\
&= \frac{1}{2} + \frac{a^2}{8} \left[ -\frac{R^4}{t^2} - R_0^4 t^2 \right]_1^u \\
&= \frac{1}{2} + \frac{a^2}{8} \left[ \left( -\frac{R^4}{u^2} - R_0^4 u^2 \right) - (-R_4 - R_0^4) \right] \\
&= \frac{1}{2} + \frac{a^2}{8} \left( R_4 + R_0^4 - \frac{R^4}{u^2} - R_0^4 u^2 \right). \tag{A.6}
\end{aligned}$$

Now, including the shadow fading gives the CDF for  $Z$ , we can write

$$\begin{aligned}
F_Z(x) &= \text{P} \left( \exp(X) \left( \frac{r_1}{r_2} \right)^{-\gamma} < Z \right) \\
&= \text{P} \left( \exp(X) u^{-\gamma} < Z \right) \\
&= \text{P} \left( u > Z^{-1/\gamma} \exp(X/\gamma) \right) \\
&= 1 - \text{E} \left\{ F_u \left[ Z^{-1/\gamma} \exp(X/\gamma) \right] \right\}, \tag{A.7}
\end{aligned}$$

where  $X = X_1 - X_2$ . Letting  $c = Z^{-1/\gamma}$ , the CDF of  $u$ ,  $F_u$ , is as follows. For  $u < 1$  ( $c \exp(X/\gamma) < 1$ ), we have

$$F_u[c \exp(X/\gamma)] = \frac{a^2}{8} \left[ R^4 c^2 \exp(2X/\gamma) + \frac{R_0^4}{c^2} \exp(-2X/\gamma) - 2R^2 R_0^2 \right]. \tag{A.8}$$

For  $u \geq 1$  ( $c \exp(X/\gamma) \geq 1$ ),

$$F_u[c \exp(X/\gamma)] = \frac{1}{2} + \frac{a^2}{8} \left[ R^4 + R_0^4 - R_0^4 c^2 \exp(2X/\gamma) - \frac{R^4}{c^2} \exp(-2X/\gamma) \right]. \tag{A.9}$$

Since  $X$  is a normal variable, we can perform the expectation in (A.7) using the dummy normal variable  $w$ . Doing this, we find

$$\begin{aligned}
F_Z(w) &= 1 - E_w \{ F_u [Z^{-1/\gamma} \exp(w/\gamma)] \} \\
&= 1 - \int_{-\infty}^{\infty} F_u [c \exp(w/\gamma)] f_w(w) dw \\
&= 1 - \int_{-\infty}^{w_0} F_u(\cdot) f_w(w) dw - \int_{w_0}^{w_1} F_u(\cdot) f_w(w) dw \\
&\quad - \int_{w_1}^{w_2} F_u(\cdot) f_w(w) dw - \int_{w_2}^{\infty} F_u(\cdot) f_w(w) dw, \tag{A.10}
\end{aligned}$$

where  $w_0$ ,  $w_1$  and  $w_2$  represent the limits  $u = \frac{R_0}{R}$ ,  $u = 1$  and  $u = \frac{R}{R_0}$  respectively. To find  $w_0$ , we set  $u = \frac{R_0}{R}$ , yielding

$$\begin{aligned}
\frac{R_0}{R} &= c \exp(w_0/\gamma) \\
\frac{R_0}{cR} &= \exp(w_0/\gamma) \\
w_0 &= \gamma \log \left( \frac{R_0}{cR} \right). \tag{A.11}
\end{aligned}$$

Then to find  $w_1$ , we set  $u = 1$ :

$$\begin{aligned}
1 &= c \exp(w_1/\gamma) \\
w_1 &= \gamma \log \left( \frac{1}{c} \right). \tag{A.12}
\end{aligned}$$

Finally to find  $w_2$ , we set  $u = \frac{R}{R_0}$ :

$$\begin{aligned}
\frac{R}{R_0} &= c \exp(w_2/\gamma) \\
\frac{R}{cR_0} &= \exp(w_2/\gamma) \\
w_2 &= \gamma \log \left( \frac{R}{cR_0} \right). \tag{A.13}
\end{aligned}$$

Note that  $F_u(\cdot) = 0$  for  $w < w_0$  and  $F_u(\cdot) = 1$  for  $w > w_2$ . Taking the individual parts of (A.10), we can write

$$\begin{aligned}
& \int_{w_0}^{w_1} F_u(c \exp(w/\gamma)) f_w(w) dw \\
&= \int_{w_0}^{w_1} \frac{a^2}{8} \left( R^4 c^2 \exp(2w/\gamma) + \frac{R_0^4}{c^2} \exp(-2w/\gamma) - 2R^2 R_0^2 \right) f_w(w) dw \\
&= \frac{a^2}{8} \left[ R^4 c^2 \int_{w_0}^{w_1} \exp(2w/\gamma) f_w(w) dw + \frac{R_0^4}{c^2} \int_{w_0}^{w_1} \exp(-2w/\gamma) f_w(w) dw \right. \\
&\quad \left. - 2R^2 R_0^2 \int_{w_0}^{w_1} f_w(w) dw \right]. \tag{A.14}
\end{aligned}$$

In the same way, we have

$$\begin{aligned}
& \int_{w_1}^{w_2} F_u[\exp(w/\gamma)] f_w(w) dw = \frac{1}{2} \int_{w_1}^{w_2} f_w(w) dw + \\
& \frac{a^2}{8} \left[ (R^4 + R_0^4) \int_{w_1}^{w_2} f_w(w) dw - R_0^4 c^2 \int_{w_1}^{w_2} \exp(2w/\gamma) f_w(w) dw + \right. \\
& \quad \left. \frac{R^4}{c^2} \int_{w_1}^{w_2} \exp(-2w/\gamma) f_w(w) dw \right], \tag{A.15}
\end{aligned}$$

where

$$f_w(w) = \frac{1}{\sqrt{2\pi\sigma^2}} \exp\left(-\frac{(w-\mu)^2}{\sigma^2}\right),$$

and  $\int_a^b f_w(w)dw = F_w(b) - F_w(a)$ . Calculating the integrals in (A.14) and (A.15) requires the following general integral:

$$\begin{aligned}
& \int_a^b \exp(\pm 2w/\gamma) f_w(w) dw \\
&= \int \exp(\pm 2w/\gamma) \frac{1}{\sqrt{2\pi\sigma^2}} \exp\left(-\frac{(w-\mu)^2}{\sigma^2}\right) dw \\
&= \frac{1}{\sqrt{2\pi\sigma^2}} \int_a^b \exp\left(\frac{\pm 4w\sigma^2/\gamma - (w-\mu)^2}{\sigma^2}\right) dw \\
&= \frac{1}{\sqrt{2\pi\sigma^2}} \int_a^b \exp\left(-\frac{(w - (\mu \pm 2\sigma^2/\gamma))^2 - 4\sigma^4/\gamma^2 \mp 4\sigma^2\mu/\gamma}{2\sigma^2}\right) dw \\
&= \frac{\exp(4\sigma^2/\gamma^2 \pm 4\mu/\gamma)}{\sqrt{2\pi\sigma^2}} \int_a^b \exp\left(\frac{-(w - (\mu \pm 2\sigma^2/\gamma))^2}{2\sigma^2}\right) dw \\
&= \frac{\exp(4\sigma^2/\gamma^2 \pm 2\mu/\gamma)}{\sqrt{2\pi\sigma^2}} P(a \leq N \leq b) \\
&= \frac{\exp(4\sigma^2/\gamma^2 \pm 2\mu/\gamma)}{\sqrt{2\pi\sigma^2}} P\left(\frac{a - \mu \mp 2\sigma^2/\gamma}{\sigma} \leq Z \leq \frac{b - \mu \mp 2\sigma^2/\gamma}{\sigma}\right) \\
&= \frac{\exp(4\sigma^2/\gamma^2 \pm 2\mu/\gamma)}{\sqrt{2\pi\sigma^2}} \left[ \Phi\left(\frac{b - \mu \mp 2\sigma^2/\gamma}{\sigma}\right) - \Phi\left(\frac{a - \mu \mp 2\sigma^2/\gamma}{\sigma}\right) \right],
\end{aligned} \tag{A.16}$$

where  $\Phi(x) = P(\mathbb{N}(0,1) < x)$ . Substituting (A.16), (A.14) and (A.15) into (A.10) and also using the fact  $\int_{w_2}^{\infty} F_u(\cdot) f_w(w) dw = (1 - F_w(w_2))$ , we finally

have

$$\begin{aligned}
F(Z) = & \frac{a^2 R^2 R_0^2}{4} \left[ \Phi \left( \frac{w_1 - \mu}{\sigma} \right) - \Phi \left( \frac{w_0 - \mu}{\sigma} \right) \right] \\
& - \left( \frac{1}{2} + \frac{a^2 (R^4 + R_0^4)}{8} \right) \left[ \Phi \left( \frac{w_2 - \mu}{\sigma} \right) - \Phi \left( \frac{w_1 - \mu}{\sigma} \right) \right] \\
& - \frac{a^2 R^4 c^2}{8} \exp[2/\gamma(\sigma^2/\gamma + \mu)] \left[ \Phi \left( \frac{w_1 - \mu - 2\sigma^2/\gamma}{\sigma} \right) - \Phi \left( \frac{w_0 - \mu - 2\sigma^2/\gamma}{\sigma} \right) \right] \\
& - \frac{a^2 R_0^4}{8c^2} \exp[2/\gamma(\sigma^2/\gamma - \mu)] \left[ \Phi \left( \frac{w_1 - \mu + 2\sigma^2/\gamma}{\sigma} \right) - \Phi \left( \frac{w_0 - \mu + 2\sigma^2/\gamma}{\sigma} \right) \right] \\
& + \frac{a^2 R_0^4 c^2}{8} \exp[2/\gamma(\sigma^2/\gamma + \mu)] \left[ \Phi \left( \frac{w_2 - \mu - 2\sigma^2/\gamma}{\sigma} \right) - \Phi \left( \frac{w_1 - \mu - 2\sigma^2/\gamma}{\sigma} \right) \right] \\
& + \frac{a^2 R^4}{8c^2} \exp[2/\gamma(\sigma^2/\gamma - \mu)] \left[ \Phi \left( \frac{w_2 - \mu + 2\sigma^2/\gamma}{\sigma} \right) - \Phi \left( \frac{w_1 - \mu + 2\sigma^2/\gamma}{\sigma} \right) \right] \\
& + \Phi \left( \frac{w_2 - \mu}{\sigma} \right). \tag{A.17}
\end{aligned}$$



## Appendix B

# Isotropic Analysis of Largest Column Density

Consider the  $m \times n$  matrix  $\mathbf{H}$  in the i.i.d. Rayleigh case. We define an arbitrary column of  $\mathbf{H}$  by  $\mathbf{X} = [X_1, X_2, \dots, X_m]^T$  and its norm by  $R = \sum_{i=1}^m |X_i|^2$ . In NSA we choose this column for inclusion in  $\mathbf{S}$  if it has one of the  $t$  largest column norms. Hence, the distribution of  $\mathbf{S}$  is affected by the selection of the “largest” columns and is no longer i.i.d. complex Gaussian. We derive The distribution of the column with the  $k$ -th largest norm as follows

$$f_{\mathbf{X}}(\mathbf{x}|k) = \int_0^\infty f_{\mathbf{X}}(\mathbf{x}|R=r) f_{P_k}(r) dr \quad (\text{B.1})$$

where conditioning on  $k$  implies the  $k$ -th largest norm,  $\mathbf{x} = [x_1, x_2, \dots, x_m]^T$ , and  $P_k$  is the  $k$ -th largest norm as before. Using Bayes rule, we can simplify the conditional density in (B.1) as

$$f_{\mathbf{X}}(\mathbf{x}|R=r) = \frac{f_R(r|\mathbf{x}) f_{\mathbf{X}}(\mathbf{x})}{f_R(r)}. \quad (\text{B.2})$$

Now, conditioned on  $\mathbf{x}$ ,  $R$  has a degenerate distribution and  $f_{\mathbf{X}}(\mathbf{x})$  is simply the joint density of  $m$  independent complex Gaussians. Hence, we have

$$f_{\mathbf{X}}(\mathbf{x}|R=r) = \frac{\delta(r - \sum_{i=1}^m |x_i|^2) \exp(-\sum_{i=1}^m |x_i|^2)}{\pi^m f_R(r)}. \quad (\text{B.3})$$

Substituting (B.3) into (B.1) we finally write

$$\begin{aligned}
f_{\mathbf{X}}(\mathbf{x}|k) &= \int_0^\infty \frac{\delta(r - \sum_{i=1}^m |x_i|^2) \exp(-\sum_{i=1}^m |x_i|^2)}{\pi^m f_R(r)} \\
&\quad \times \frac{n!}{(n-k)!(k-1)!} F_R(r)^{k-1} [1 - F_R(r)]^{n-k} f_R(r) dr \\
&= \frac{n!}{\pi^m (n-k)!(k-1)!} \exp\left(-\sum_{i=1}^m |x_i|^2\right) \\
&\quad \times F_R\left(\sum_{i=1}^m |x_i|^2\right)^{k-1} \left[1 - F_R\left(\sum_{i=1}^m |x_i|^2\right)\right]^{n-k} \quad (\text{B.4})
\end{aligned}$$

and so the joint density of the  $k$ -th largest column remains isotropic as it is solely a function of  $\sum_{i=1}^m |x_i|^2$ .

# Bibliography

- [1] A. Paulraj, R. Nabar, and D. Gore, *Introduction to Space-Time Wireless Communications*. Cambridge, UK: Cambridge University Press, 2003.
- [2] “Introduction to MIMO systems,” Application Note 1MA102, Rohde and Schwarz, June 2006.
- [3] C. E. Shannon, “A mathematical theory of communication,” *Bell Labs. Tech. J.*, vol. 27, no. 1, pp. 379–423, 2006.
- [4] A. J. Paulraj and C. B. Papadias, “Space-time processing for wireless communications,” *IEEE Signal Processing Mag.*, vol. 14, no. 6, pp. 49–82, Nov. 1997.
- [5] A. Lozano, F. R. Farrokhi, and R. A. Valenzuela, “Lifting the limits on high-speed wireless data access using antenna arrays,” *IEEE Commun. Mag.*, pp. 156–162, Sept. 2001.
- [6] S. D. Blostein and H. Leib, “Multiple antenna systems: Their role and impact in future wireless access,” *IEEE Commun. Mag.*, vol. 41, pp. 94–101, July 2003.
- [7] D. Tse, P. Viswanath, and L. Zheng, “Diversity-multiplexing tradeoff in multiple-access channels,” *IEEE Trans. Inform. Theory*, vol. 50, no. 9, pp. 1859–1874, Sept. 2004.

- [8] I. Berenguer and Z. Wang, "Space-time coding and signal processing for MIMO communications," *J. Comput. Sci. Tech.*, vol. 18, no. 6, pp. 689–702, 2003.
- [9] V. Tarokh, N. Seshadri, and A. R. Calderbank, "Space-time codes for high data rate wireless communication: Performance criterion and code construction," *IEEE Trans. Inform. Theory*, vol. 44, pp. 744–765, Mar. 1998.
- [10] S. M. Alamouti, "A simple transmit diversity technique for wireless communications," *IEEE J. Select. Areas Commun.*, vol. 16, pp. 1451–1458, Oct. 1998.
- [11] G. J. Foschini, "Layered space-time architecture for wireless communication in a fading environment when using multi-element antennas," *Bell Labs. Tech. J.*, vol. 1, no. 2, pp. 41–59, 1996.
- [12] J. H. Winters, "On the capacity of radio communication systems with diversity in a Rayleigh fading environment," *IEEE J. Select. Areas Commun.*, vol. 5, no. 5, pp. 871–878, June 1987.
- [13] G. J. Foschini and M. J. Gans, "On limits of wireless communication in a fading environment when using multiple antennas," *Wireless Personal Commun.*, vol. 6, no. 3, pp. 311–335, Mar. 1998.
- [14] I. E. Telatar, "Capacity of multi-antenna Gaussian channels," *European Trans. on Telecomm. Related Technol.*, vol. 10, pp. 585–595, Nov.-Dec. 1999.
- [15] D. Gesbert, M. Shafi, D.-S. Shiu, P. J. Smith, and A. Naguib, "From theory to practice: An overview of MIMO spacetime coded wireless systems," *IEEE J. Select. Areas Commun.*, vol. 21, no. 3, pp. 281–302, Apr. 2003.

- [16] W. Yu, W. Rhee, S. Boyd, S. A. Jafar, and J. M. Cioffi, "Iterative water-filling for Gaussian vector multiple-access channels," *IEEE Trans. Inform. Theory*, vol. 50, no. 1, pp. 145–152, Jan. 2004.
- [17] N. Jindal, W. Rhee, S. Vishwanath, S. A. Jafar, and A. Goldsmith, "Sum power iterative water-filling for multi-antenna Gaussian broadcast channels," *IEEE Trans. Inform. Theory*, vol. 51, no. 4, pp. 1570–1580, Apr. 2005.
- [18] A. Goldsmith, S. Vishwanath, S. A. Jafar, and N. Jindal, "Capacity limits of MIMO channels," *IEEE J. Select. Areas Commun.*, vol. 29, no. 5, pp. 684–702, June 2003.
- [19] S. Vishwanath, N. Jindal, and A. Goldsmith, "Duality achievable rates and sum rate capacity of MIMO Gaussian broadcast channels," *IEEE Trans. Inform. Theory*, vol. 49, no. 10, pp. 2658–2668, Oct. 2003.
- [20] S. Vishwanath, S. Jafar, and A. Goldsmith, "On the capacity of multiple input multiple output broadcast channels," in *Proc. IEEE Int'l. Conf. on Communications*, New York City, USA, 28 Apr-2 May 2002, pp. 1444–1450.
- [21] W. Yu and J. M. Cioffi, "Sum capacity of Gaussian vector broadcast channels," *IEEE Trans. Inform. Theory*, vol. 50, no. 9, pp. 1875–1892, Sept. 2004.
- [22] G. Caire and S. Shamai, "On the achievable throughput of a multiple antenna Gaussian broadcast channel," *IEEE Trans. Inform. Theory*, vol. 49, no. 7, pp. 1691–1706, July 2003.
- [23] J. G. Andrews, W. Choi, and R. W. Heath Jr., "Overcoming interference in spatial multiplexing MIMO cellular networks," *IEEE Wireless Commun. Mag.*, vol. 14, pp. 95–104, Dec. 2007.

- [24] R. S. Blum, "MIMO capacity with interference," *IEEE J. Select. Areas Commun.*, vol. 21, no. 5, pp. 793–801, June 2003.
- [25] M. Chiani, M. Z. Win, and H. Shin, "Capacity of MIMO systems in the presence of interference," in *Proc. IEEE Global Telecommunications Conf.*, San Francisco, CA, USA, Nov 27 - Dec 1, 2006, pp. 1–6.
- [26] S. Catreux, P. Driessen, and L. Greenstein, "Attainable throughput of an interference-limited multiple-input multiple-output (MIMO) cellular system," *IEEE Trans. Commun.*, vol. 49, no. 8, pp. 1307–1311, Aug. 2001.
- [27] R. S. Blum, J. H. Winters, and N. R. Sollenberger, "On the capacity of cellular systems with MIMO," *IEEE Commun. Lett.*, vol. 6, no. 6, pp. 242–244, June 2002.
- [28] G. Foschini, H. Huang, K. Karakayali, R. Valenzuela, and S. Venkatesan, "The value of coherent base station coordination," in *Conference on Information Sciences and Systems*, The John Hopkins University, USA, Mar 16-18 2005.
- [29] H. Zhang and H. Dai, "Cochannel interference mitigation and cooperative processing in downlink multicell multiuser MIMO networks," *EURASIP Journal on Wireless Communications and Networking*, no. 2, pp. 222–235, 2004.
- [30] H. Huang, A. Hottinen, M. Shafi, P. J. Smith, M. Trivellato, and R. Valenzuela, "Increasing downlink cellular throughput with limited network MIMO coordination," accepted to *IEEE Trans. Wireless Comm.*, 2009.
- [31] M. Karakayali, R. A. Valenzuela, and G. J. Foschini, "Network coordination for spectrally efficient communication in cellular systems," *IEEE Wireless Commun. Mag.*, vol. 13, no. 4, pp. 56–61, Aug. 2006.

- [32] J. Cheng and T. Berger, "Capacity and performance analysis for hybrid selection/maximal-ratio combining in Nakagami fading with unequal fading parameters and branch powers," in *Proc. IEEE Int'l. Conf. on Communications*, Anchorage, USA, May 11-15, 2003, pp. 3031–3035.
- [33] A. Molisch, M. Win, and J. Winters, "Capacity of MIMO systems with antenna selection," in *Proc. IEEE Int'l. Conf. on Communications*, Helsinki, Finland, June 11-14, 2001, pp. 570–574.
- [34] M. Z. Win and J. H. Winters, "Virtual branch analysis of symbol error probability for hybrid selection/maximal-ratio combining in Rayleigh fading," *IEEE Trans. Commun.*, vol. 49, no. 11, pp. 1926–1934, Nov. 2001.
- [35] S. Sanayei and A. Nosratinia, "Antenna selection in MIMO systems," *IEEE Commun. Mag.*, vol. 42, no. 10, pp. 68–73, Oct. 2004.
- [36] R. S. Blum and J. H. Winters, "On optimum MIMO with antenna selection," *IEEE Commun. Lett.*, vol. 6, no. 8, pp. 322–324, Aug. 2002.
- [37] Z. Zhou, Y. Dong, X. Zhang, W. Wang, and Y. Zhang, "A novel antenna selection scheme in MIMO systems," in *Proc. Int'l. Conf. on Communications, Circuits and Systems*, Chengdu, China, June 27-29, 2004, pp. 190–194.
- [38] A. Ghrayeb, "A survey on antenna selection for MIMO communication systems," in *Proc. 2nd IEEE Int'l. Conf. on Information and Communication Technologies*, vol. 2, Damascus, Syria, April 24-28, 2006, pp. 2104–2109.
- [39] G. Caire and S. Shamai (Shitz), "On the achievable throughput of a multiantenna Gaussian broadcast channel," *IEEE Trans. Inform. Theory*, vol. 49, no. 7, pp. 1691–1706, July 2003.

- [40] J. Lee and N. Jindal, “Symmetric capacity of MIMO downlink channels,” in *Proc. 2006 IEEE Int’l Symp. on Inform. Theory*, Seattle, USA, July 9-14, 2006, pp. 1031–1035.
- [41] Z. Motamedi and M. R. Soleymani, “For better or worse: The impact of shadow fading on the capacity of large MIMO networks,” in *Proc. IEEE Global Telecommunications Conf.*, Washington D.C., USA, Nov 27-30, 2007, pp. 3200–3204.
- [42] L. Yang, “On the capacity of MIMO Rayleigh fading channels with log-normal shadowing,” in *Congress on Image and Signal Processing*, Sanya, Hainan, China, May 27-30, 2008, pp. 479–482.
- [43] R. Yates, “A framework for uplink power control in cellular radio systems,” *IEEE J. Select. Areas Commun.*, vol. 13, no. 7, pp. 1341–1347, Sept. 1995.
- [44] S. Ulukus and R. Yates, “Stochastic power control for cellular radio systems,” *IEEE Trans. Commun.*, vol. 46, no. 6, pp. 784–798, June 1998.
- [45] N. Badruddin, J. Evans, and S. Hanly, “Maximizing sum rate for two interfering wireless links,” in *Australian Communications Theory Workshop*, Christchurch, NZ, Jan 30-Feb 1 2008, pp. 75–81.
- [46] T. Ozugur, M. Naghshineh, P. Kermani, and J. Copeland, “Fair media access for wireless lans,” in *Proc. IEEE Global Telecommunications Conf.*, Rio de Janeiro, Brazil, December 5-9 1999, pp. 570–579.
- [47] C. Li and X. Wang, “Adaptive opportunistic fair scheduling over multiuser spatial channels,” *IEEE Trans. Commun.*, no. 10, pp. 1708–1717, Oct. 2005.
- [48] M. Kang and M.-S. Alouini, “On the capacity of MIMO Rician channels,” in *Proc. 40th Allerton Conf. on Communications, Control, and Computing*, Monticello, IL, USA, Oct. 2002, pp. 936–945.

- [49] D.-S. Shiu, G. J. Foschini, M. J. Gans, and J. M. Kahn, “Fading correlation and its effect on the capacity of multielement antenna systems,” *IEEE Trans. Commun.*, no. 3, pp. 502–513, Mar. 2000.
- [50] M. Gans, “The effect of Gaussian error in maximal ratio combiners,” *IEEE Trans. Commun.*, vol. 19, no. 4, pp. 492–500, Aug. 1971.
- [51] W. C. Jakes, *Microwave Mobile Communications*. New York: Wiley, 1974.
- [52] M. Chiani, M. Z. Win, and H. Shin, “MIMO networks: the effects of interference,” submitted to *IEEE Trans. Inform. Theory*, 2008.
- [53] H. David and H. Nagaraja, Eds., *Order Statistics*. Hoboken, NJ, USA: John Wiley and Sons Inc., 2003.
- [54] S. Boyd and L. Vandenberghe, *Convex Optimization*, 1st ed. Cambridge, UK: Cambridge University Press, 2004.
- [55] W. Karush, “Minima of functions of several variables with inequalities as side constraints,” M. Sc. Dissertation, University of Chicago, Chicago, Illinois, USA, 1939.
- [56] H. Kuhn and A. Tucker, “Nonlinear programming,” in *Proc. 2nd Berkeley Symposium*, Berkeley, USA, 1951, pp. 481–492.
- [57] H. Huang and R. Valenzuela, “Fundamental simulated performance of downlink fixed wireless cellular networks with multiple antennas,” in *Proc. IEEE Int’l. Symp. on Personal and Mobile Radio Communications*, Berlin, Germany, Sept. 11-14, 2005, pp. 161–165.
- [58] R. Heath and A. Paulraj, “Antenna selection for spatial multiplexing systems based on minimum error rate,” in *Proc. IEEE Int’l. Conf. on Communications*, Helsinki, Finland, June 11-14, 2001, pp. 2276–2280.

- [59] Z. Chen, B. Vucetic, and J. Yuan, “Space-time trellis codes with transmit antenna selection,” *IEE Electronics Letters*, vol. 39, pp. 854–855, May 2003.
- [60] A. Molisch, M. Win, and J. Winters, “Capacity of MIMO systems with antenna selection,” in *Proc. IEEE Int’l. Conf. on Communications*, Helsinki, Finland, June 11-14, 2001, pp. 570–574.
- [61] M. Gharavi-Alkhansari and A. B. Gershman, “Fast antenna subset selection in MIMO systems,” *IEEE Trans. Signal Processing*, vol. 52, no. 2, pp. 339–347, Feb. 2004.
- [62] L. Dai, S. Sfar, and K. Letaief, “Optimal antenna selection based on capacity maximization for MIMO systems in correlated channels,” *IEEE Trans. Commun.*, vol. 54, no. 3, pp. 563–573, Mar. 2006.
- [63] A. Molisch and X. Zhang, “FFT-based hybrid antenna selection schemes for spatially correlated MIMO channels,” *IEEE Commun. Lett.*, vol. 8, no. 1, pp. 36–38, Jan. 2004.
- [64] P. J. Smith, S. Roy, and M. Shafi, “Capacity of MIMO systems with semicorrelated flat fading,” *IEEE Trans. Inform. Theory*, vol. 49, no. 10, pp. 2781–2788, Oct. 2003.
- [65] N. L. Johnson and S. Kotz, Eds., *Continuous Univariate Distributions-1*. Hoboken, NJ, USA: John Wiley and Sons Inc., 1970.
- [66] B. C. Arnold, N. Balakrishnan, and H. N. Nagaraja, Eds., *A First Course in Order Statistics*. Hoboken, NJ, USA: John Wiley and Sons Inc., 1992.
- [67] N. L. Johnson and S. Kotz, Eds., *Continuous Univariate Distributions-2*. Hoboken, NJ, USA: John Wiley and Sons Inc., 1970.

- [68] S. Loyka, “Channel capacity of MIMO architecture using the exponential correlation matrix,” *IEEE Commun. Lett.*, vol. 5, no. 9, pp. 369–371, Sept. 2001.
- [69] K. Alam and K. T. Wallenius, “Distribution of a sum of order statistics,” *Scand. J. Stat., Theory Appl.*, vol. 6, pp. 123–126, 1979.
- [70] J. Rice, *Mathematical Statistics and Data Analysis*, 2nd ed. Belmont, CA, USA: Duxbury Press, 1994.
- [71] S. Sanayei and A. Nosratinia, “Capacity of MIMO channels with antenna selection,” *IEEE Trans. Inform. Theory*, vol. 53, pp. 4356–4362, Nov. 2007.
- [72] A. Goldsmith, *Wireless Communications*. New York, USA: Cambridge University Press, 2005.
- [73] S. H. Choi, P. Smith, B. Allen, W. Q. Malik, and M. Shafi, “Severely fading MIMO channels: Models and mutual information,” in *Proc. IEEE Int’l. Conf. on Communications*, Glasgow, Scotland, June 24-28 2007, pp. 4628–4633.
- [74] P. J. Smith, S. Roy, and M. Shafi, “Capacity of MIMO systems with semicorrelated flat fading,” *IEEE Trans. Inform. Theory*, vol. 49, no. 10, pp. 2781–2788, Oct. 2003.
- [75] D. P. Palomar and J. R. Fonollosa, “Practical algorithms for a family of waterfilling solutions,” *IEEE Trans. Signal Processing*, vol. 53, no. 2, pp. 686–695, Feb. 2005.
- [76] T. M. Cover and J. A. Thomas, *Elements of Information Theory*. New York, USA: Wiley, 2003.
- [77] D. P. Palomar, J. M. Cioffi, and M. A. Lagunas, “Joint Tx-Rx beamforming design for multicarrier MIMO channels: A unified framework for

- convex optimization,” *IEEE Trans. Signal Processing*, vol. 51, no. 9, pp. 2381–2401, Sept. 2003.
- [78] K. H. Lee and D. P. Petersen, “Optimal linear coding for vector channels,” *IEEE Trans. Commun.*, vol. 24, no. 12, pp. 1283–1290, Dec. 1976.
- [79] J. Yang and S. Roy, “On joint transmitter and receiver optimization for multiple-input multiple-output (MIMO) transmission systems,” *IEEE Trans. Commun.*, vol. 42, no. 12, pp. 3221–3231, Dec. 1994.
- [80] H. Sampath, P. Stoica, and A. Paulraj, “Generalized linear precoder and decoder design for MIMO channels using the weighted MMSE criterion,” *IEEE Trans. Commun.*, vol. 49, no. 12, pp. 2198–2206, Dec. 2001.
- [81] E. N. Onggosanusi, A. M. Sayeed, and B. D. Van Veen, “Efficient signaling schemes for wideband space-time wireless channels using channel state information,” *IEEE Trans. Veh. Technol.*, vol. 52, no. 1, pp. 1–13, Jan. 2003.
- [82] N. Jindal and A. Goldsmith, “Capacity and optimal power allocation for fading broadcast channels with minimum rates,” *IEEE Trans. Inform. Theory*, vol. 49, no. 11, pp. 2895–2909, Nov. 2003.
- [83] A. Bayesteh, M. A. Sadrabadi, and A. K. Khandani, “Throughput and fairness maximization in wireless networks,” in *10th Canadian Workshop on Information Theory*, Edmonton, Alberta, Canada, June 6-8, 2007.
- [84] M. Costa, “Writing on dirty paper,” *IEEE Trans. Inform. Theory*, vol. 29, no. 3, pp. 439–441, May 1983.
- [85] A. Gjøndemsjø, D. Gesbert, G. E. Oien, and S. G. Kiani, “Optimal power allocation and scheduling for two-cell capacity maximization,” in *Proc. 4th Int’l. Symp. on Modeling and Optimization in Mobile, Ad Hoc and Wireless Networks*, Boston, USA, Apr. 2006, p. 16.

- [86] A. Gjendemsjo, D. Gesbert, and G. E. Oien, “Binary power control for multi-cell capacity maximization,” in *Proc. Signal Processing Advances in Wireless Communications*, Helsinki, Finland, June 17-20 2007, pp. 1–5.
- [87] M. Ebrahimi, M. A. Maddah-Ali, and A. K. Khandani, “Power allocation and asymptotic achievable sum-rates in single-hop wireless networks,” in *Proc. 40th Annual Conf. on Information Sciences and Systems*, Princeton, NJ, USA, Mar. 2006, p. 498503.
- [88] K. B. Petersen and M. S. Pedersen, *The Matrix Cookbook*, 2008. [Online]. Available: <http://matrixcookbook.com>